Nuclear Heat Transfer and Passive Cooling

Volume 3: **Natural Convection and Passive Cooling**

FRAZER-NASH CONSULTANCY

Introduction to the Technical Volumes and Case Studies

Convection, Radiation and Conjugate Heat Transfer

Natural Convection and Passive Cooling

Confidence and Uncertainty

Liquid Metal Thermal Hydraulics

Molten Salt Thermal Hydraulics

Liquid Metal CFD Modelling of the TALL-3D Test Facility

Fuel Assembly CFD and UQ for a Molten Salt Reactor

Reactor Scale CFD for Decay Heat Removal in a Lead-cooled Fast Reactor

System Code and CFD Analysis for a Light Water Small Modular Reactor

Authors:	Tim Houghton	Frazer-Nash Consultancy
	Dean Wilson	The University of Manchester
Contributors:	Adam Owens	Moltex Energy
	Akash Dhandhukia	Terrestrial Energy
	David Cuming	DBD International
	Graham Macpherson	Frazer-Nash Consultancy
	Hector Iacovides	The University of Manchester
	Janne Wallenius	LeadCold
	Ji Soo Ahn	Imperial College London
	Milorad Dzodzo	Westinghouse Electric Company
	Paolo Ferroni	Westinghouse Electric Company
	Richard Underhill	Frazer-Nash Consultancy
	Steven Moor	Rolls-Royce
Technical Volumes Lead:	Tim Houghton	Frazer-Nash Consultancy
Approver:	Brian Gribben	Frazer-Nash Consultancy

Document Number: FNC 60148/49310R

Issue and Date: Issue 1, December 2021

Legal Statement

Preface

Nuclear thermal hydraulics is the application of thermofluid mechanics within the nuclear industry. Thermal hydraulic analysis is an important tool in addressing the global challenge to reduce the cost of advanced nuclear technologies. An improved predictive capability and understanding supports the development, optimisation and safety substantiation of nuclear power plants.

This document is part of *Nuclear Heat Transfer and Passive Cooling: Technical Volumes and Case Studies*, a set of six technical volumes and four case studies providing information and guidance on aspects of nuclear thermal hydraulic analysis. This document set has been delivered by Frazer-Nash Consultancy, with support from a number of academic and industrial partners, as part of the UK Government *Nuclear Innovation Programme: Advanced Reactor Design*, funded by the Department for Business, Energy and Industrial Strategy (BEIS).

Each technical volume outlines the technical challenges, latest analysis methods and future direction for a specific area of nuclear thermal hydraulics. The case studies illustrate the use of a subset of these methods in representative nuclear industry examples. The document set is designed for technical users with some prior knowledge of thermofluid mechanics, who wish to know more about nuclear thermal hydraulics.

The work promotes a consistent methodology for thermal hydraulic analysis of single-phase heat transfer and passive cooling, to inform the link between academic research and end-user needs, and to provide a high-quality, peer-reviewed document set suitable for use across the nuclear industry.

The document set is not intended to be exhaustive or provide a set of standard engineering ‘guidelines’ and it is strongly recommended that nuclear thermal hydraulic analyses are undertaken by Suitably Qualified and Experienced Personnel.

The first edition of this document set has been authored by Frazer-Nash Consultancy, with the support of the individuals and organisations noted in each. Please acknowledge these documents in any work where they are used:

> Frazer-Nash Consultancy (2021) Nuclear Heat Transfer and Passive Cooling,
> Volume 3: Natural Convection and Passive Cooling.

Contents

1 Introduction 1
- 1.1 Passive and Active Cooling Systems . . . 1
- 1.2 Natural, Forced and Mixed Convection and Circulation . . . 3
- 1.3 Passive Cooling Applications . . . 4

2 Technical Context 7
- 2.1 Flow Phenomena . . . 7
  - 2.1.1 Plumes . . . 7
  - 2.1.2 Stratification . . . 9
  - 2.1.3 Surface Effects . . . 11
- 2.2 Theory . . . 12
  - 2.2.1 Natural, Forced and Mixed Convection . . . 12
  - 2.2.2 Buoyancy, Mixing and Pressure Loss . . . 15
  - 2.2.3 Turbulence and Transition . . . 17
  - 2.2.4 Buoyancy Affected Flows and CFD . . . 20
- 2.3 Fluid Material Properties . . . 28
  - 2.3.1 Sources of Property Data . . . 29
  - 2.3.2 Implementing Property Data . . . 30
- 2.4 Modelling Challenges . . . 32

3 Methodology 35
- 3.1 System and Subchannel Analysis . . . 36
  - 3.1.1 System Analysis . . . 37
  - 3.1.2 Subchannel Analysis . . . 41
- 3.2 CFD Analysis . . . 43
  - 3.2.1 Introductory Remarks . . . 43
  - 3.2.2 CFD Approaches . . . 44
  - 3.2.3 Mesh Generation . . . 45
  - 3.2.4 Case Definition . . . 47
  - 3.2.5 LES Aspects . . . 49
  - 3.2.6 RANS Aspects . . . 51
  - 3.2.7 Hybrid Approaches . . . 59
  - 3.2.8 Convergence . . . 60
- 3.3 Experimental Methods . . . 62
  - 3.3.1 Scaling . . . 62
  - 3.3.2 Integral Measurements . . . 63
  - 3.3.3 Detailed Flow Field Measurements . . . 65
  - 3.3.4 Geometry, Boundary and Operating Conditions . . . 68
  - 3.3.5 Post-Processing . . . 68

4 Future Developments 69

4.1 Natural Circulation 69
4.2 Hybrid methods 70
4.3 Turbulent Heat Transfer Models 71

5 References 72

6 Nomenclature 87

7 Abbreviations 89

1 Introduction

This technical volume considers fluid flow and heat transfer in passive cooling systems, focusing primarily on flows driven by buoyancy. Such flows are of particular relevance to passive cooling systems in the nuclear industry and present particular technical challenges.

This volume is part of a set of technical volumes, and it is recommended that Volume 1 (Introduction to the Technical Volumes and Case Studies) and Volume 2 (Convection, Radiation and Conjugate Heat Transfer) are reviewed for context. This introduction defines and contrasts the characteristics of passive cooling systems with active cooling systems, introduces natural, forced and mixed convection and presents typical applications of passive cooling systems.

1.1 Passive and Active Cooling Systems

IAEA (1991) defines a passive safety system as: *Either a system which is composed entirely of passive components and structures or a system which uses active components in a very limited way to initiate subsequent passive operation*. Therefore, passive safety systems are designed to reduce or remove the need for active intervention by an operator or control system to bring and maintain a reactor to a safe shut-down state, in the event of a particular scenario occurring.

Passive cooling systems therefore transfer heat without needing external inputs (at least after system operation is initiated), and typically take advantage of natural forces or phenomena such as gravity, buoyancy, pressure differences, conduction, thermal radiation or natural heat convection to accomplish safety functions without requiring an active power source (IAEA, 2009a).

Active Cooling Systems: Most of the cooling systems in current Nuclear Power Plants (NPPs) are closed loop active systems, and they are often numerous, partly because indirect cooling using chains of systems connected to each other is common. These systems, their support systems[1] and all the associated components must be designed and integrated within the whole NPP, manufactured in a supply chain, installed, commissioned and maintained through life. As such, while designing and testing these systems may appear relatively straightforward from a technical perspective, they may be expensive and present risks during construction and operational life.

Passive Cooling Systems: By contrast, passive cooling systems do not contain components such as pumps and fans, and may use simpler cooling chains or no cooling chains at all. Therefore, new reactor designs are making more extensive use of passive safety features because they are intended to achieve the same or higher reliability using fewer systems/components (less complexity), thus reducing capital and Operation and Maintenance

[1] Such as electrical, control and instrumentation, motor cooling, other cooling systems and all their support systems.

(O&M) costs associated with the installation and maintenance of mechanical, control and instrumentation support systems. For example, a reactor design developed by NuScale[2] uses natural circulation of the reactor coolant flow around the primary circuit (e.g. without main coolant pumps) under normal operation and loss of power conditions. Examples of passive cooling systems include core cooling, containment cooling, safety injection and decay heat removal systems.

Overall, IAEA (2002b) notes that using passive safety systems is a desirable method of increasing simplification and potentially reliability, and that passive systems should be used where appropriate. However, the nature of the flows, complex coupling between the flow and temperature field, and weak or unstable driving forces associated with passive cooling systems (e.g. natural circulation) can make justification of the plant's operation and safety performance more challenging:

- Can result in physically larger system components, because the flow velocities associated with passive cooling systems are normally lower than active cooling systems.
- Might require more detailed analytical modelling, experimental work and testing to design, substantiate performance and confirm reliability, particularly where a graded approach indicates a high level of scrutiny is appropriate (Volume 1, Section 2.2.5), because:
  - The cooling flow rate and heat transfer performance are coupled (although a benefit of this is that the cooling flow rate may increase as heat is transferred to the flow).
  - Actuation may not be as instantaneous as switching on an active system, so more time may be needed to reach full cooling performance.
  - Thermal mass may be more significant than would be the case for active systems.
  - Natural or mixed convection flow fields are likely to occur, and these are often spatially complex and intrinsically unsteady.
  - System flows are more likely to be at transitional Reynolds numbers, due to the lower driving forces associated with natural circulation.

IAEA (1991) also recognises that passive cooling systems may require modest control functions to enable operation. Some guidance on categorising the 'passivity' of passive systems from Category A (more passive) to Category D (less passive) is provided, and discussed further in IAEA (2002b). This considers aspects such as the level of control functionality needed and the importance of moving parts or fluids. For example, a static wall used to segregate systems from one another might be Category A, a system with moving fluids but no moving parts, control functions or support systems might be Category B, and a system with active initiation followed by passive execution (e.g. that opens valves to connect a natural circulation loop, see Section 1.2) might be Category D. This illustrates that the overall robustness of a passive cooling system may not begin and end with thermal hydraulics. The wider system must be appropriately designed as a whole to provide the overall robustness or reliability required.

As noted above, achieving the potential benefits of passive cooling may involve more sophisticated technical design work than might be needed for active cooling systems. A motivation for this technical volume is to help develop understanding of how sophisticated this work might need to be and how it might be approached.

[2] www.nuscalepower.com

1.2 Natural, Forced and Mixed Convection and Circulation

Convection: The terms natural, forced and mixed convection describe mechanisms of convective heat transfer, rather than overall system behaviour:

- Natural convection[3]: Local heat transfer arising from flow driven by local buoyancy effects.
- Forced convection: Local heat transfer arising from flow driven by work input.
- Mixed convection: Local heat transfer arising from aspects of both natural convection and forced convection.

Flows that may result from natural, forced and mixed convection are illustrated in Figure 1.1.

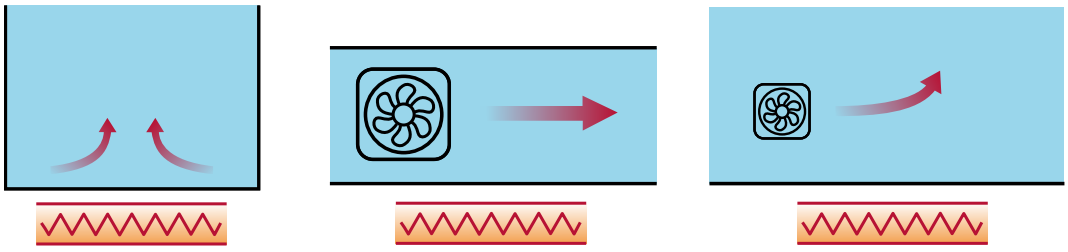

(a) Natural Convection (b) Forced Convection (c) Mixed Convection

Figure 1.1: Typical flows associated with natural, forced and mixed **convection**.

Circulation: The terms natural, forced and mixed circulation describe what is driving the flow from the perspective of the *overall system*:

- Natural circulation: Flow in the system as a whole driven by buoyancy.
- Forced circulation: Flow in the system driven by mechanical equipment like a pump or fan, as seen in most active cooling systems.
- Mixed circulation: Flow in the system driven by both buoyancy and mechanical equipment (which may be aiding or opposing each other).

Illustrations of natural, forced and mixed circulation are shown in Figure 1.2.

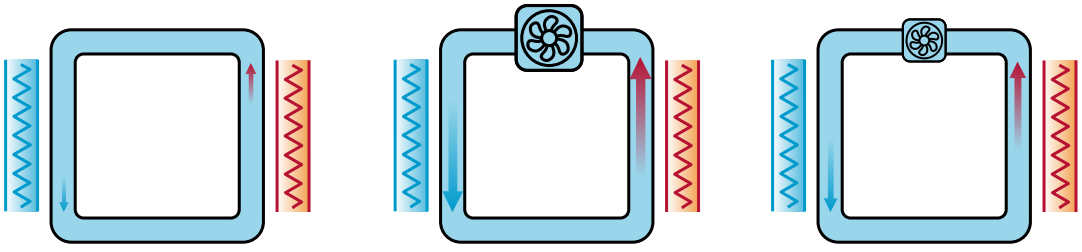

(a) Natural Circulation (b) Forced Circulation (c) Mixed Circulation

Figure 1.2: Example systems containing natural, forced and mixed **circulation**.

[3] The term 'free convection' is sometimes used to describe natural convection. The term 'free' normally refers to flows that are away from walls, and as these can inhibit natural convection this term may be appropriate (e.g. in pools). However, to avoid confusion with other 'free' flow features, the term 'free convection' is not used in this volume for clarity.

For a system operating using forced *circulation*, such as a pumped primary circuit or auxiliary cooling system under normal operation or faults where the pumps are running, most of the flow fields in the circuit, pipework, valves and pumps are likely to be forced convection. However, mixed convection could be encountered if there are locations where relatively low forced flow velocities occur near strong thermal gradients. In addition, natural convection may occur in areas where the forced flow is quiescent (such as inside 'dead', or isolated, pipework spurs).

Mixed circulation is unusual, but could be encountered where both mechanical components and temperature gradients are significant in driving the flow. For example, a heavy pump slowly decelerating to a stop in a system containing large temperature gradients (as might occur in a primary circuit if the main coolant pump electrical supply is interrupted).

For natural circulation, natural convection is likely to be encountered where there are strong thermal gradients (such as at the start of a transient or in a pool, where flow is likely to be quiescent). However, where natural circulation is well established in a piped system, the flow in the vicinity of these thermal gradients may more closely resemble mixed convection as a result of the momentum of the flow in the system, even though this flow is entirely driven by buoyancy effects. The flow in parts of the system where thermal gradients are low (such as pipework) may resemble flow fields associated with forced convection, but unlike in forced circulation the overall flow rate and heat transfer performance are coupled, and flow velocities are likely to be lower.

Passive cooling systems are likely to make use of natural circulation. However, as noted above, the resulting flow fields inside the system may resemble natural, mixed or forced convection. Natural, forced and mixed convection flows are considered in more detail in Section 2.2.

1.3 Passive Cooling Applications

Passive cooling systems are widely used in a range of applications. In NPPs, typical uses for passive cooling systems include:

- Cooling the primary circuit, particularly for decay heat removal in accident scenarios, to maintain the integrity of the fuel and/or primary circuit (typically the first and second barriers that confine nuclear material within the power plant).
- Cooling containment buildings internally or externally, to manage internal pressure in the event of a primary circuit breach and maintain the integrity of the building (which is typically the third barrier).
- Cooling spent nuclear fuel (again to preserve the integrity of confining barriers).
- Cooling the air in buildings to manage internal temperatures (supporting the continued operation of systems and access by operators).

Passive cooling systems must be carefully designed in a holistic manner to ensure that the overall performance of the NPP is appropriate, and generally adopt one of the following arrangements:

1. Volumes of cold water that can be fed directly into the NPP's cooling systems. Such systems are generally driven by gas pressure in accumulators or gravity feed from elevated tanks, and provide a finite amount of cooling (the cooling stops when there is no more water left).

2. Volumes of initially cold water that can be used as a heat sink (rather than being injected into the NPP's cooling systems), again providing a finite amount of cooling. Heat is typically transferred into this volume from the plant using natural circulation in pipework, or thermal radiation in high-temperature reactors.
3. Cooling chimneys that are used as a heat sink by a natural circulation loop that removes heat from the plant. This provides a long term source of cooling, providing the chimney and cooling loop are designed to remain effective in the prevailing weather conditions.
4. Ducts or louvres that exhaust heated air from rooms within buildings and allow cool air to enter, transferring heat by natural circulation.

Some Advanced Nuclear Technologies (ANTs) are designed to use the same cooling systems for normal operation and safety scenarios within their design basis (and to minimise changes in operating states) although additional systems may also be included (e.g. to manage design extension conditions). Natural circulation is often proposed to cool the reactor vessel, reactor pits and the containment, either directly or indirectly through a closed cooling loop. Passive coolers may also be immersed into the primary pool and connected to a closed cooling loop. High temperature reactors are likely to make more use of thermal radiation for cooling than is normal in Light Water Reactor (LWR) designs due to their higher operating temperatures (particularly in safety scenarios), and these designs often use ambient air as the ultimate heat sink for passive cooling systems. In designs where fuel is incorporated into the coolant, melting plugs may be used to drain the fuel into cooling chambers. These aspects are discussed in more detail in Volume 5 (Liquid Metal Thermal Hydraulics) and Volume 6 (Molten Salt Thermal Hydraulics).

Details on the application of passive cooling systems to LWRs are provided in IAEA (2009a), which provides a high-level overview of the passive systems typically employed (the annexes describe how around 20 designs, including integral designs, incorporate passive safety systems). Further discussion on the incorporation of passive cooling systems into LWRs is presented in IAEA (2002b). A number of papers considering various aspects of passive cooling system design are presented in IAEA (1996) and detailed case studies on three reactor designs are presented in IAEA (2013c). An example of the passive cooling systems in an operating NPP is shown in Figure 1.3.

Passive ventilation systems are also used, particularly for cooling plant buildings and facilities for storing spent fuel. IAEA (2018) and Appendix 3 of IAEA (2005) contain a brief discussion on passive ventilation systems specifically. From a technical perspective, the physical phenomena relevant to Heating, Ventilation, and Air Conditioning (HVAC) systems are similar to those for mechanical cooling systems (illustrated by the example in Section 2.2.2). However, HVAC systems are likely to have lower temperature gradients, different types of requirements (e.g. confinement of radioactivity within the plant using filters, managing humidity and pressure levels in rooms etc.) and different components (using ducts, dampers, fans and chillers instead of pipes, valves, pumps and heat exchangers). Open loop passive cooling using natural convection within an HVAC system is generally called natural ventilation. Further detail on aspects of HVAC design are included in Haines and Myers (2010) and ASHRAE (2017).

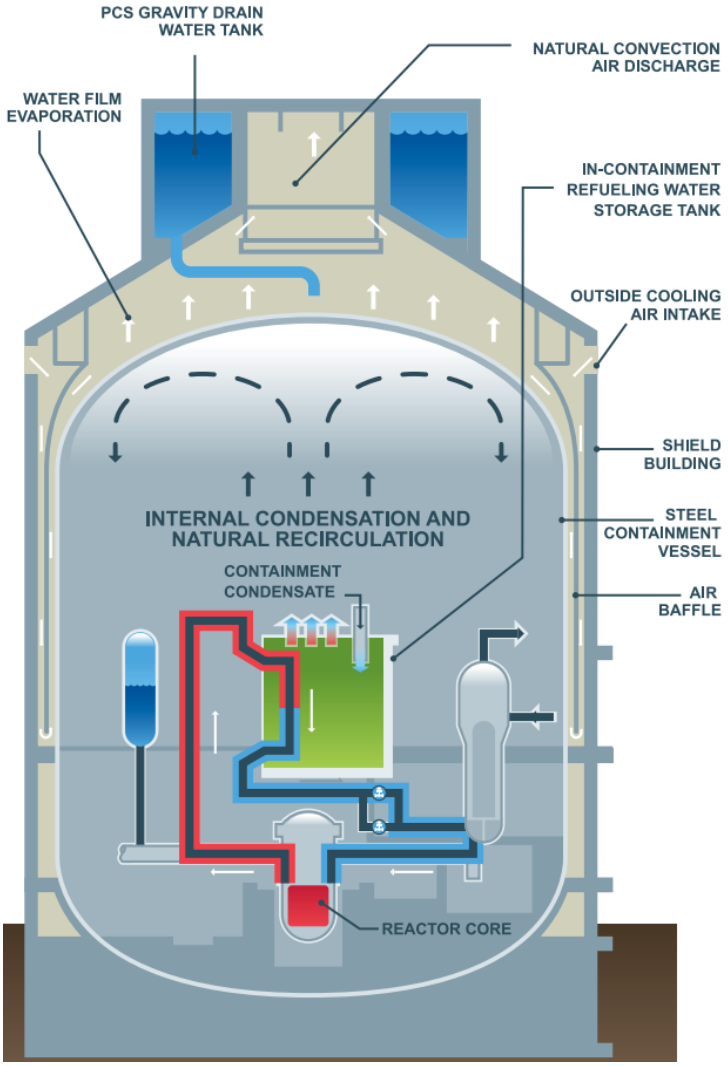

Figure 1.3: An illustration of passive cooling features employed by the Westinghouse AP1000 Nuclear Power Plant. Further detail is available at www.westinghousenuclear.com/new-plants/ap1000-pwr/safety.

2 Technical Context

This section introduces some of the key technical aspects of the buoyancy affected flows that may occur in passive cooling systems. The key flow phenomena and theory are presented, fluid material properties are discussed and key modelling challenges are considered.

This section does not consider all the phenomena that might be relevant to the design of a whole system[1], but guidance in this area is developed through a series of three reports developed by an International Atomic Energy Agency (IAEA) Coordinated Research Project (CRP), (IAEA, 2005, 2009a and 2012), which in turn build on a number of Organisation for Economic Co-operation and Development (OECD) Nuclear Energy Agency (NEA) reports on passive safety systems. Heat transfer by phase change[2] is also not considered in detail, as described in Volume 1.

2.1 Flow Phenomena

Key relevant flow phenomena such as plumes, stratification and surface effects are introduced below. In many practical engineering applications, different flow phenomena may interact with each other within a system[3] or with external ambient conditions (especially for open loop systems). These interactions may be simple and intuitive, but may also be very complex and their behaviour counter-intuitive even to skilled engineers. Analysis may be needed to identify and understand such interactions and may also enable them to be avoided or simplified by design if they have an undesirable impact (Section 3).

2.1.1 Plumes

When the density of a volume of fluid is reduced relative to fluid surrounding it, buoyancy forces act to push the less dense volume of fluid upwards. This results in the less dense fluid accelerating upward in a buoyant plume and more dense fluid being drawn in beneath to replace it. In natural convection, this reduced density is generally caused by increased fluid temperature, which may result from contact with a heated surface or heated fluid entering a cold volume from elsewhere.

Figure 2.1 shows illustrative diagrams of free and bounded plumes, which are considered separately below, and Figure 2.2 shows these plumes in a flow loop. In this volume, plumes are generally described as if they are of low density (e.g. hot); high density (e.g. cold) plumes generally show the same behaviours in the opposite sense. Plumes caused by fluid species with different densities may show similar behaviours to the thermal plumes discussed below (Woods, 2010).

[1] Such as might be considered for Phenomena Identification and Ranking Table (PIRT) analysis, described in Volume 1.
[2] Such as evaporation from free surfaces, or boiling and condensation in pools, heat exchangers, steam generators, boilers or heat pipes (Rohsenow *et al.*, 1998; Reay *et al.*, 2014).
[3] Examples include interactions between plumes (IAEA, 2005), between plumes and stratification, and between plumes, stratification and wall boundary layers.

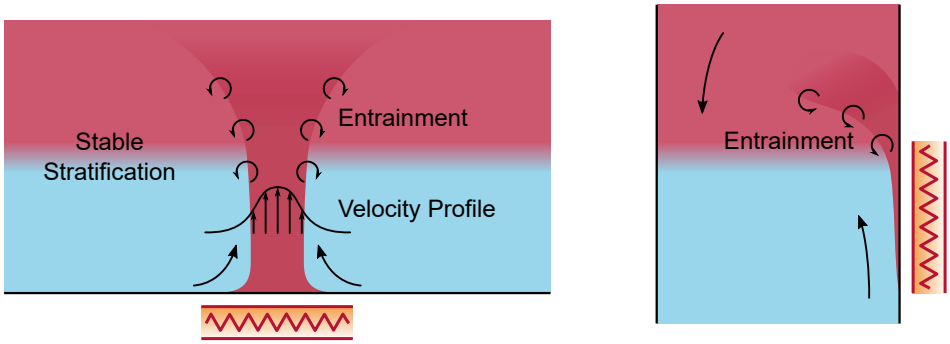

(a) Free Plume (b) Wall Bounded Plume

Figure 2.1: Illustrations showing free and wall bounded plumes with stratification.

Free Plumes (Pools and Plena): For a 'free plume' rising through fluid away from walls and surrounded by a more dense fluid (e.g. in pools or large plena), the core of the plume will continue to accelerate until the buoyancy forces acting on it are counteracted by energy dissipation associated with its motion (Section 2.2.2). As the plume rises, this mixing with the cooler surrounding fluid will cause entrainment of surrounding flow into the plume, resulting in an increasing mass of rising fluid, but a cooling and hence decelerating plume core.

If there is a large height of cool surrounding fluid, the plume will eventually dissipate (or 'mix out') into the surrounding fluid, losing all of its momentum and transferring all of its excess thermal energy to the surrounding fluid. If the plume encounters other plumes, flow features, walls or free surfaces, it will also interact with these, resulting in complex flow features and further mixing. If the temperature of the surrounding fluid rises, the buoyancy forces driving the plume will reduce and a vertical plume will therefore tend to decelerate and widen. Plume behaviour is discussed further in Gebhart *et al.* (1988), Rodi (1982) and Turner (1973). Rising temperature with height is often a result of stratification; as well as modifying plume behaviour, stratification can also decouple flows above and below an abrupt temperature gradient (Section 2.1.2).

Where jets from pipework discharge into a large volume, the initial flow is likely to be driven by momentum effects. However, the momentum of the jet will decrease through mixing as it moves through the volume. If the density of the jet is different to the surrounding fluid (e.g. because it is hot), buoyancy effects are likely to become dominant as the jet develops and, given enough distance, the jet is likely to develop into a free plume (Gebhart *et al.*, 1988).

Bounded Plumes (Loops and Channels): For a 'bounded plume' rising through fluid near adjacent walls within a system (e.g. in pipes within loops or channels within a reactor core), the initial flow phenomena are likely to be similar to a free plume with the addition of dissipation caused by wall-bounded flow phenomena like momentum and thermal boundary layers (Section 2.2.2). However, once the plume displaces a significant amount of fluid, wider system effects become important. If the wider system is slow to react[4], the flow adjacent to the plume may flow strongly in the opposite direction to the plume as a result of mass continuity, causing local mixing and slowing the development of the plume itself. Once plumes become able to rise up through the system, the

[4] This is likely, because the low driving forces in passive systems tends to lead to large reactors and components being used to reduce power density and flow pressure losses, both of which increase the mass of fluid in the system

forcing effect of the heated flow on the system as a whole is likely to depend on the instantaneous (i.e. time-varying) balance between:

1. What density variation is generated over what height (i.e. the magnitude of the overall hydrostatic pressures driving the flow).
2. The momentum of the heated flow (i.e. the mass of flow moving and its velocity, resulting from the acceleration due to the driving force).
3. The energy dissipation due to viscous effects around the whole flow.
4. The flow behaviour in the wider system, which may or may not be strongly coupled.

An example of free and bounded plumes occurring in a flow loop is shown in Figure 2.2. In a closed loop system containing a heater and cooler, complex and coupled behaviour may occur at every length scale, from detailed local flow interactions to whole-system flow oscillations (or even reversal, see IAEA, 2012 and Section 2.4). This flow behaviour may be coupled with additional phenomena, such as geometry distortions or phase changes.

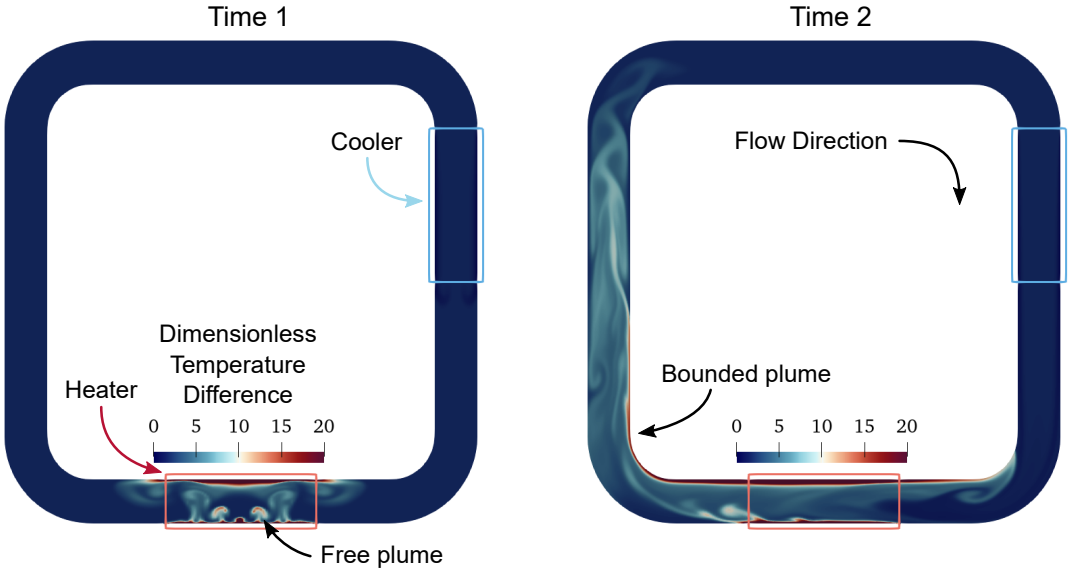

Figure 2.2: Free and bounded plumes occurring in a simple (two-dimensional, laminar) flow loop containing heated and cooled walls.

2.1.2 Stratification

Stratified flows are often described as stable or unstable (Figure 2.3):

- In stable stratification, a warmer (less dense) fluid sits stably above cooler (more dense) fluid. In this situation, slow molecular conduction is often the only mechanism to transfer heat from the warmer fluid into the cooler fluid below (in the absence of thermal radiation effects). As a result, heated fluid may collect under the free surface, sitting above the cooler fluid in the pool and preventing the fluid from circulating.
- In unstable stratification, a cooler fluid is above a warmer fluid, leading to the development of buoyancy-driven flows. An example is Rayleigh-Bénard cells, a particular flow phenomenon with plumes arranged in a cell-like structure.

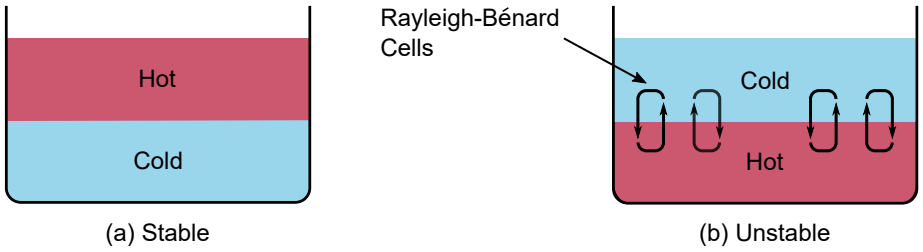

Figure 2.3: Stable and unstable stratification.

Stratification is a particular feature of pools or volumes of fluid within systems, and can also be important in pipework. Some examples of scenarios where stratification in volumes or pipes may influence NPP design are illustrated in Figure 2.4:

1. In systems where a cold tank of water is used as a heat sink, stratification can cause the capacity of this heat sink to reduce. This is because the tank effectively 'fills down' with warm fluid from the top, so cooling is likely to reduce once the interface between warm and cool fluid descends to the level of the heat exchanger transferring heat into the pool (IAEA, 2013c).
2. Stratification can cause sharp temperature gradients in large volumes (such as vessels in a primary circuit). If this interface moves around (e.g. due to flow unsteadiness caused by natural convection), components or walls that cross this interface will suffer repeated temperature fluctuations (thermal striping) that may cause thermal fatigue (IAEA, 2014 and Section 2.1.3).
3. Stratification within system components can also cause the development of sharp temperature fluctuations in the downstream flow (referred to as thermal 'fronts' or 'slugs'), which may cause thermal fatigue or shock in downstream components (IAEA, 2012 and Section 2.1.3).
4. Where a cold fluid enters a pipe full of slow moving hot fluid via a T-junction (such as safety injection into a Pressurised Water Reactor (PWR) primary circuit under natural circulation), the cold fluid may not mix with the hot fluid, but form a layer at the bottom of the pipe. This forms two regions of fluid, which can move in different directions with different velocities. The cold fluid may flow some distance down the pipe and cause Pressurised Thermal Shock (PTS), where components (such as parts of the Reactor Pressure Vessel (RPV) in a PWR) are exposed to high thermal stress (IAEA, 2012, IAEA, 2005 and CSNI, 2015a).
5. In a spur of pipework or a pipe connected to a cooler containing stagnant flow, the heat transfer from the pipe may cause natural circulation within the pipe itself, with outgoing hot fluid forming a layer above the returning cold fluid (sometimes called a 'thermosyphon'). This situation can cause large bending moments in pipework, problems associated with condensation of steam, and transport of hot fluid over long distances (which can cause an 'induced steam generator break' in a PWR primary circuit in two-phase conditions, CSNI, 2015a). If the pipe contains thermocouples these may be immersed in different areas of a complex flow field, making the readings difficult to understand (particularly for complex pipe routes).
6. Where a region of pipework contains a low-point, this can trap cold fluid that has entered the system. The cold fluid may then remain in this 'cold trap' and resist or stagnate the natural circulation of hot fluid in the system (IAEA, 2005, Annex 15). It is necessary to understand

situations in which a passive cooling system might become ineffective, in order to set the Limits and Conditions for Operations (LCOs) for the NPP.

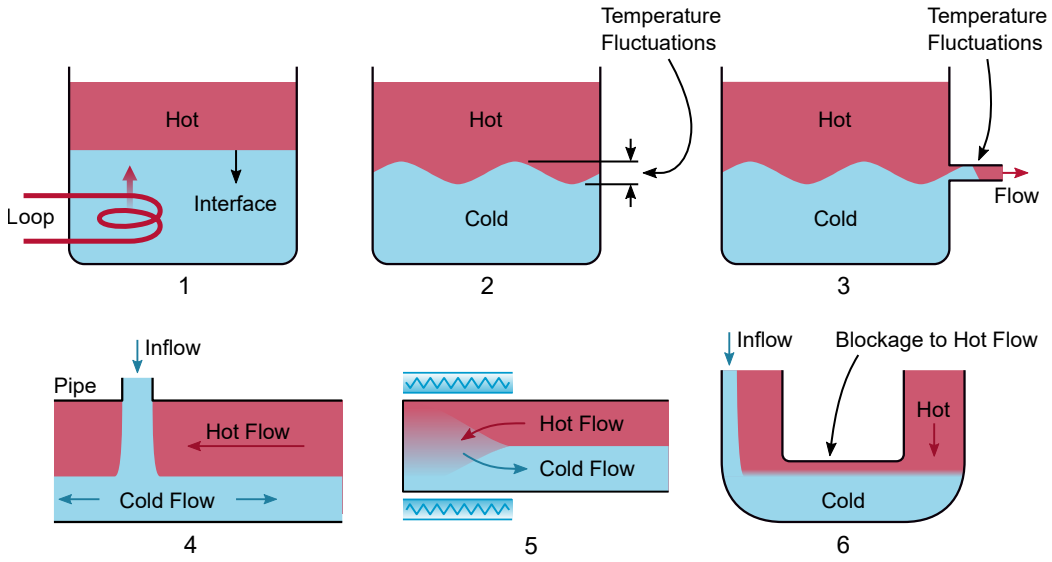

Figure 2.4: Example phenomena associated with stratification in volumes and pipes.

Where there is a large, abrupt and stable density gradient (or 'stratification interface') the flows on either side of this gradient may become effectively decoupled, so that plumes or other flow features on one side may have a negligible impact on the flow on the other side (as in the cold trap example above). Where the density gradient is more modest, a warm plume or other flow feature may still be able to rise through the gradient, but the driving buoyancy forces will reduce, typically causing marked changes in the development of the flow field (Section 2.1.1, Woodcock and Dzodzo, 2000). The Atwood number, At (Section 2.2.1) may be useful in characterising the stability of such stratified flows.

2.1.3 Surface Effects

Walls: Heat transfer between solids and adjacent fluids, and the potential for thermal stresses to occur within the solid, is considered in detail in Volume 2 (Convection, Radiation and Conjugate Heat Transfer). The following aspects are characteristic of buoyancy driven flows:

- These flows are often unsteady and poorly mixed (i.e. containing regions of relatively hot and cold fluid adjacent to each other). If such a flow is adjacent to a component or wall, this may suffer repeated temperature fluctuations that may cause thermal fatigue (often referred to as 'thermal striping').
- As noted in Section 2.1.2, stratification interfaces (whether stable or unstable) can cause temperature fluctuations that may cause thermal fatigue, or changes in temperatures within components that may cause high stresses.
- Buoyancy effects can cause dramatic changes to local heat transfer because they can modify the production of turbulence close to the wall (discussed further in Section 2.2.1).

Free Surfaces: This set of technical volumes focuses on single-phase flow (see Volume 1) and free surfaces are therefore not considered in detail. However, the following phenomena are characteristic of buoyancy driven flows:

- There is often a sharp temperature gradient across free surfaces. Similar to stratification (discussed in Section 2.1.2), if this free surface level fluctuates (e.g. due to flow unsteadiness caused by natural convection) components or walls crossing the free surface may suffer repeated temperature fluctuations that may cause thermal fatigue. This is a particular issue for pool-type reactors with metal coolants.
- Surface evaporation can cause significant heat transfer from heated pools (e.g. spent fuel pools) and this can alter the flow fields within the pool and in the gas or air above it. This heat transfer is therefore likely to depend on the detailed three-dimensional flow field in both the pool and the gas or air above it.
- Aside from evaporation, heat transfer can vary significantly across free surfaces as a result of the sub-surface natural convection flow field (CSNI, 1994) and sharp gradients and fluctuating levels may lead to deposits forming on wetted structures (surface deposition is considered further in Volume 2, Section 2.2.2).

2.2 Theory

This section provides a brief overview of the theory relevant to passive cooling systems, considering heat transfer by natural, forced and mixed convection; buoyancy, mixing and pressure loss effects associated with buoyancy affected flow fields; turbulence and transition; and key aspects of Computational Fluid Dynamics (CFD) theory relevant to buoyancy affected flows.

2.2.1 Natural, Forced and Mixed Convection

Key Dimensionless Groups: Similarity analysis of the Navier-Stokes and energy equations gives three key non-dimensional groups that indicate the overall nature of convection flow fields[5]:

1. Reynolds number (Re), a ratio of momentum forces to viscous forces.
2. Grashof number (Gr), a ratio of buoyancy forces to viscous forces.
3. Prandtl number (Pr), a ratio of momentum diffusivity to thermal diffusivity.

For forced convection, the key dimensionless groups are Re and Pr (which can be combined to form the Péclet number, $Pe = RePr$). For natural convection, the key dimensionless groups are Gr and Pr (which can be combined to form the Rayleigh number, $Ra = GrPr$). For mixed convection, Gr, Pr and Re are all relevant. The Atwood number, At (a non-dimensional density difference) is also used to characterise the stability of flows featuring density effects like stratification.

It is possible to introduce large uncertainties in analysis work by using information that is inappropriate to the flow field under study. Identifying the significance of buoyancy and inertial effects

[5] Other groups may be important in different scenarios, such as the Froude number (Fr), Kutateladze number (Ku) or Eckert number (Ec) where there are free surfaces, two-phase or high speed flow respectively. Mass transfer equivalents also exist where buoyancy forces are generated by different species instead of thermal effects. For further information see Rogers and Mayhew (1992), Incropera *et al.* (2011), Rohsenow *et al.* (1998), Kakaç *et al.* (1987), Schlichting and Gersten (2017) and Zohuri and Fathi (2015).

(i.e. whether flow in a particular part of a system should be considered as natural, forced or mixed convection and laminar or turbulent flow) is therefore important, for example to understand:

- What surface heat transfer correlations should be used in a system model.
- What flow phenomena might be expected in a CFD model, and how the mesh should be constructed to capture the resulting gradients of flow variables.

The significance of buoyancy effects can be difficult to understand without analysis, so scoping calculations may be needed in addition to the methods discussed in this section.

Convective surface heat transfer is important for many passive cooling systems, and is introduced in some detail in Volume 2 (Section 2.1.2) alongside another key non-dimensional group:

- Nusselt number (Nu), a ratio of convective to conductive heat transfer in a fluid at a boundary.

Nu may be defined locally or as an area-average for a given surface ($\overline{Nu}$), and can be used to calculate local or area-averaged Heat Transfer Coefficients (HTCs), h or $\overline{h}$ respectively (as discussed in Volume 2). Correlations for Nu (and $\overline{Nu}$) are normally based on the non-dimensional numbers discussed above, so different correlations are likely to be appropriate for natural, forced and mixed convection.

Forced and Natural Convection: Nusselt numbers for pure forced and natural convection are often denoted Nu_F and Nu_N respectively. A number of correlations for Nu are available for different geometries in research papers and books, such as Rogers and Mayhew (1992), Incropera *et al.* (2011) and Rohsenow *et al.* (1998). As with any correlation, care must be taken to ensure that the correlation is valid for the flow and fluid that is being assessed. Particular issues for buoyancy affected flows include:

- The range of non-dimensional numbers the correlation is valid for, and how similar the geometry is to the geometry assumed in the correlation.
- Whether the surface is heating or cooling the flow and whether a uniform heat flux or uniform temperature is assumed.
- How similar the flow field is to the flow assumed in the correlation (normally uniform, steady, fully developed flow is assumed).

It is also important that the characteristic length scales, temperatures and fluid properties used in the correlation are appropriate, and these aspects are discussed in Volume 2. Aspects specific to liquid metal and molten salt are considered in Volume 5 and Volume 6. In particular, it is noted that the effect of buoyancy on heat transfer for low Pr fluids (like sodium and lead) can be quite different to conventional fluids (Jackson, 1983, Jackson *et al.*, 1994).

Mixed Convection: A range of flow regimes are often possible even for a simple geometry like a vertical tube, and correlations are likely to depend on Re and Ra (or Gr). From this perspective, pure forced and natural convection (complex as they may be) could be viewed as relatively straightforward special cases. One way of aiding clarity is to use a flow regime map, which plots the significance of momentum (Re) against the significance of buoyancy (Ra or Gr). Lines showing boundaries for application of correlations for forced, natural and mixed convection and laminar or

turbulent flow can then be plotted, based on where mixed convection heat transfer does not deviate by more than, say, 5%-10% from pure forced or free convection (see Figure 2.5).

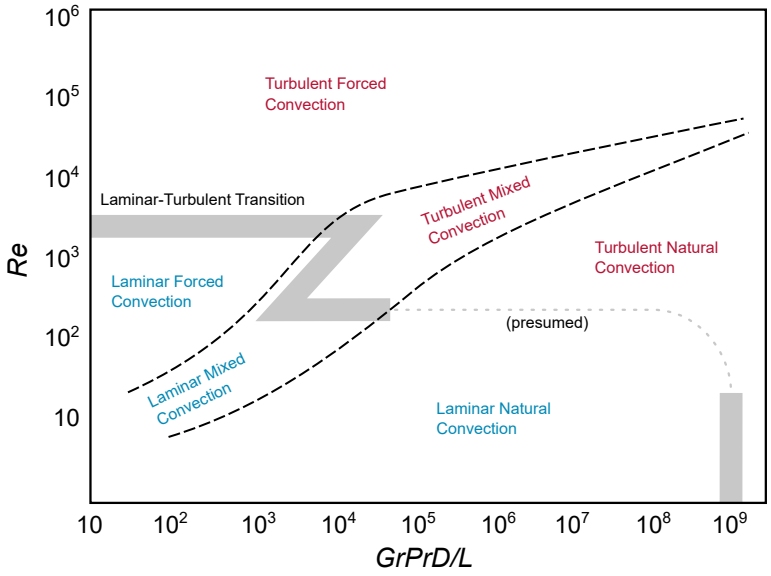

Figure 2.5: Illustrative flow regime map (based on a vertical tube, after Metais and Eckert, 1964).

Different flow regime maps are needed for different geometries (in particular, external and internal flows are treated differently). Situations where buoyancy effects are assisting (same direction to the forced flow), resisting (opposite direction to the forced flow) or transverse (perpendicular to the forced flow) are generally also treated separately. The impact of increasing buoyancy on forced convection heat transfer can also be very different for laminar or turbulent flows. Guidance on these aspects is provided in Rohsenow *et al.* (1998) and Kakaç *et al.* (1987). A number of correlations are presented in Runchal (2020), Gebhart *et al.* (1988) and Martynenko and Khramtsov (2005).

Aside from graphical methods, the dimensionless group below may be helpful in determining whether flow should be considered as forced, natural or mixed convection:

$$\frac{Gr}{Re^n}, \text{ a ratio of buoyancy forces to momentum forces}$$

Forced convection is then expected to dominate as $Gr/Re^n \rightarrow 0$ and natural convection as $Gr/Re^n \rightarrow \infty$. Dimensional arguments indicate that $n = 2$, and this group (Gr/Re^2) is often referred to as the Richardson number, Ri (particularly used in environmental fluid mechanics, Turner, 1973). However, other values of n have been correlated with experimental results for different geometries, inclinations, boundary conditions and fluids, and other dimensionless groups including Ra and Pr have also been proposed. A review of relevant literature (such as Gebhart *et al.*, 1988, Kakaç *et al.*, 1987, Jackson *et al.*, 1989, Rohsenow *et al.*, 1998) is likely to be helpful before using these groups to provide anything more than a rough indication.

Mixed convection in turbulent flows can be especially complex, as differing levels of buoyancy force can cause marked reductions or increases in heat transfer (principally due to significant modification of turbulence production in the turbulent portion of the boundary layer). This situation in vertical pipes has received significant study (partly as a result of the application to boiler design)

and a review is presented in Jackson *et al.* (1989). This work has been extended to passive cooling systems (IAEA, 2002b, Annex Part 2) and an overview is provided in Jackson (2018).

In general (at the time of writing), detailed mixed convection guidance tends to be contained in text books written some time ago (like the references above) or in papers in the literature tailored to specific systems (for which general applicability may be unclear). Careful review of the literature may therefore be needed to identify guidance relevant to a specific situation under study.

2.2.2 Buoyancy, Mixing and Pressure Loss

Buoyancy provides the driving force for natural convection (Section 2.1.1). It is a 'body force' resulting from gravity acting on volumes of fluid with different densities. The hydrostatic pressure differences it generates are proportional to the product of the difference in density ($\Delta\rho$) and the height over which this difference is maintained. Accurate material properties are therefore important in assessing the impact of buoyancy (Section 2.3).

The motion driven by buoyancy effects is counteracted by energy dissipation, or pressure losses (essentially entropy generation). These result from viscous effects associated with the mixing of the flow across gradients, in situations like plume boundaries, near walls, and between different flow features. This mixing is often dominated by complex turbulence phenomena (Section 2.2.3). Assessing these effects is a challenge across the whole field of thermofluid mechanics, of which Nuclear Thermal Hydraulics (NTH) is a part (Denton, 1993 provides internal aerodynamics context). Natural convection flow fields in particular are driven by temperature gradients that are highly dependent on the mixing between different areas of fluid or the distribution of heat sources and sinks. How this mixing is treated will depend on the scenario under study.

Pools and Plena: For free plumes rising through a quiescent fluid (such as in a pool), correlations may be used to predict the development of plumes (for example Turner, 1973; Shabbir and George, 1994; Gebhart *et al.*, 1988; Woods, 2010). These correlations effectively predict the balance between the driving buoyancy effects and energy dissipation associated with mixing at the plume boundaries, and are often based on experimental observations in idealised situations.

However, the situation in pools and plena in a cooling system may differ significantly from the idealised situation used to develop these correlations, particularly if there are interactions between different flow phenomena or between the flow and structures. As a result, the flows in pools and plena are often investigated using experiments or CFD (Section 3) to gain detailed information and understanding of the flow field. In some situations (e.g. for a specific plena), experiments or CFD may be used to develop application-specific correlations.

Loops and Channels: Open or closed loop systems are often assessed using a system analysis (Section 3.1), where coefficients are used to predict the stagnation pressure loss over a part of the system. The two most generally useful coefficients are the 'stagnation pressure loss coefficient' or 'loss coefficient' (K) and the related 'flow resistance' (ζ):

$$\Delta P_T = K\tfrac{1}{2}\rho U^2 = \zeta\frac{W^2}{\rho} \quad \text{where} \quad \zeta = \frac{K}{2A_{cs}^2}$$

The loss coefficient (K) is dimensionless. K is widely used because for low-speed turbulent flows (i.e. the majority of flows of interest to engineers) the stagnation pressure losses (and associated energy dissipation and entropy generation) scale with $\frac{1}{2}\rho U^2$, the 'dynamic pressure', which is the kinetic energy per unit volume of the flow. Loss coefficients are generally based on experimental observations in idealised scenarios, and are available for flow through a wide variety of components (Miller, 2009; Idelčik and Ginevskiĭ, 2007; IAEA, 2001).

The flow resistance (ζ) is not dimensionless (it has units m^{-4}). However, ζ is easier to work with in a systems analysis, because it can be summed directly to calculate an overall pressure loss through a number of components, using a common mass flow rate (W). This mass flow rate is generally of interest in a system analysis because it is conserved through continuity. As a result, calculating pressure losses from K involves continually using some characteristic area (A_{cs}) for each component to calculate an appropriate local velocity (generally a superficial velocity, Volume 2, Section 2.1.2), which is inconvenient and causes a risk of incorrect/inconsistent areas being used.

A number of other coefficients may also be encountered for calculating pressure losses:

- For lengths of pipework or ductwork, K is normally calculated from the pipe (or 'Darcy', or 'Moody') friction coefficient (f, introduced in Volume 2, Section 3.4.2.5), using the length to diameter ratio of the pipe (i.e. $K = fL/D$). The 'hydraulic diameter' is useful for non-circular geometries (i.e. $D_h = 4A_{cs}/p_{cs}$, where p_{cs} is the perimeter of the cross-section).
- For nozzles and orifices, a 'discharge coefficient' (C_d) is sometimes used, which is the ratio of the actual discharge to the theoretical discharge. This can normally be converted using $K = 1/C_d^2$ if K and C_d are based on the nozzle/orifice area or $K = (A_1/A_2C_d)^2$ if K is based on the upstream pipe area (A_1) and C_d is based on the nozzle/orifice area (A_2).
- For valves, a number of dimensional 'flow coefficients' are in use (typically C_v, imperial, and K_v, metric). A number of other coefficients may be used to provide additional corrections for compressible flows such as for pressure relief valves. Pressure loss data and guidance for using this is normally available from manufacturers, but care must be taken to ensure that these are used appropriately (additional detail on this topic is available in Miller, 2009).

Correlations for K are often based on uniform inflows, perfectly mixed outflows, isothermal and incompressible flow and are normally only valid for specific ranges of Re and Pr (although corrections may be available to extend their use, Miller, 2009). As such, for complex flows (like natural or mixed convection) their applicability may be uncertain, and a correlation may not be available for complex geometry in part of a system. In parts of a system where these aspects are a concern, experiments or CFD may be used to investigate the flow in more detail and provide comparative data, or develop application-specific correlations (NSC, 2018).

Example: To illustrate balancing buoyancy and pressure loss in an air chimney, consider a Reactor Vessel Auxiliary Cooling System (RVACS) driven by a hydrostatic pressure difference between the heat addition from a reactor (at height h_1) and the top of the chimney (at height h_2). The air in the outer annulus is assumed to be at a cold ambient temperature, while the air in the inner annulus is heated so that the difference in density between the air at the inlet and outlet of the RVACS is $\Delta\rho = \rho_1 - \rho_2$ (Figure 2.6). In this simplified example, the driving buoyancy is assumed

to be balanced by the total pressure loss for the flow through the inner and outer annuli ΔP_T, so that:

$$\Delta\rho g(h_2 - h_1) = \Delta P_{T,1} + \Delta P_{T,2} = K_1 \tfrac{1}{2}\rho_1 U_1^2 + K_2 \tfrac{1}{2}\rho_2 U_2^2 = \left(\frac{K_1}{2A_1^2}\frac{1}{\rho_1} + \frac{K_2}{2A_2^2}\frac{1}{\rho_2}\right) W^2$$

Where g is acceleration due to gravity and U is the flow velocity through each annulus (calculated from the flow rate and cross-sectional area), but writing the equation in terms of a common W shows that there is only a single flow rate variable that needs to be calculated.

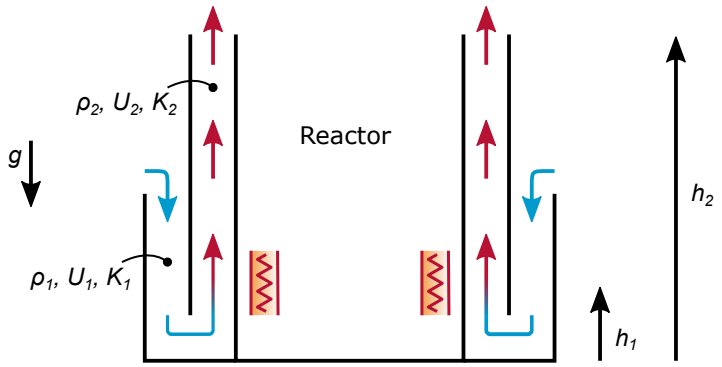

Figure 2.6: Passive ventilation (natural circulation) in a simple RVACS.

2.2.3 Turbulence and Transition

Turbulence and transition can have a significant impact on the flow in passive cooling systems, particularly where surface heat transfer occurs. The nature of turbulence and the transition between laminar and turbulent flows is a large and complex topic that has been a subject of international research for many decades. This section therefore provides an overview of the aspects of turbulence and transition most relevant to natural convection.

Turbulence: Turbulence is a flow phenomenon characterised by apparently chaotic and irregular variations in flow velocity and pressure. From a physical perspective, a flow will transition from laminar to turbulent when its kinetic energy exceeds a level where viscosity can no longer damp out small perturbations arising in the flow. These perturbations can then grow, causing eddies over a wide range of temporal and spatial scales (Figure 2.7).

In a buoyant free plume, the initially laminar flow may quickly become turbulent, with eddying motion at the plume boundaries causing significant entrainment (or mixing) of external fluid into the plume, increasing the mass of fluid moving in the plume but reducing its temperature and hence the driving body force (Section 2.1.1). Turbulence enhances the mixing of momentum and thermal energy (across velocity and temperature gradients respectively) thereby exerting a strong influence on the behaviour of flows near walls, particularly in boundary layers, wall-bounded shear layers, or separations. This can affect surface heat transfer (Section 2.1.3), flow pressure losses and mass flow rates (Section 2.2.2). This is a significant topic in its own right, and a detailed discussion on boundary layer flows is provided by Schlichting and Gersten (2017). In a turbulent mixed convection flow, existing shear-driven (i.e. non-buoyant) turbulence may quickly mix out warmer fluid from the near-wall regions before plume flow structures can form.

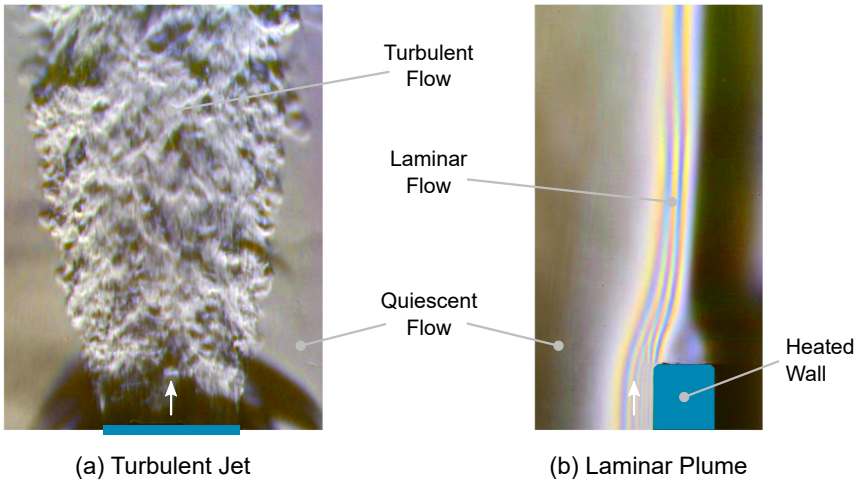

Figure 2.7: False colour Schlieren pictures showing density variations in turbulent and laminar flows.

At the largest scales, turbulent eddies can be of the same order as the flow geometry. At the smallest scales, the kinetic energy of the turbulent eddies is dissipated as heat by viscosity. As *Re* increases, a widening inertial sub-range occurs between these scales (Figure 2.8). From a mathematical perspective, it is the non-linear nature of the momentum terms in the Navier-Stokes equations which gives rise to turbulence (turbulence theory is discussed in detail in Pope, 2000).

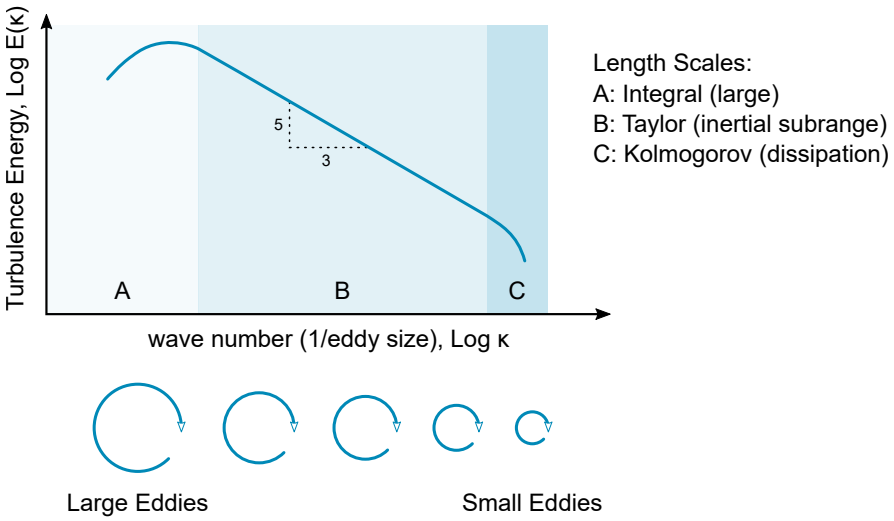

Figure 2.8: The kinetic energy spectrum of turbulence.

Turbulence is prevalent in most engineering flows, and often has a significant impact on processes important to NTH analysis. One of its impacts is increased mixing of advected quantities (such as energy, momentum or species concentration). Once a flow becomes turbulent, the turbulence (and its associated mixing) typically becomes the dominating feature and will often play a crucial role in determining many other important engineering parameters, such as:

- Heat transfer from surfaces.
- Mixing of momentum and energy.
- Pressure drops and mass flow rates.

- Forces acting on immersed bodies and surfaces.
- Existence and development of secondary flows or stratification.
- Solid deposition and transport.

Because the nature of laminar and turbulent flow is very different, it is important to understand whether flow in a particular part of a system should be considered as laminar, turbulent or transitional (in a similar way to identifying whether a flow should be considered as natural, forced or mixed convection). While general engineering flows are often turbulent, the low velocities characteristic of natural circulation make laminar or transitional flows more common than would be normal for forced circulation.

The treatment of turbulence in modelling work varies with the approach employed. For a system-level analysis (Section 3.1), this is likely to include understanding whether the flow is likely to be laminar or turbulent, steady-state or time-dependent, developing or fully developed[6], so that heat transfer correlations can be used appropriately (Section 2.1.3). For CFD analysis (Section 3.2) this is rather more involved, and is discussed in Section 2.2.4.

Transition: Since key parameters like surface heat transfer and pressure loss coefficients vary significantly between laminar and turbulent flows (Volume 2, Incropera *et al.*, 2011), transition is of interest for passive cooling systems. There are a number of different laminar to turbulent transition mechanisms, which tend to occur in different situations (Schlichting and Gersten, 2017).

- *Natural* transition results from the amplification of hydrodynamic instabilities in a stable laminar flow.
- *Bypass* transition often occurs in turbomachinery, and results from disturbances caused by high upstream turbulence levels causing 'spots' of turbulence that trip boundary layers ('bypassing' natural transition).
- *Separated* transition results from separation of laminar boundary layers under adverse pressure gradients causing a free-shear layer that may (or may not) reattach as a turbulent boundary layer.

Depending on the type of flow, it may be possible to identify approximate conditions around which transition might be expected to occur:

- For *forced convection* where buoyancy forces are negligible, Re is the key non-dimensional group. Transition is expected at around $Re \approx 2{,}300$ for steady and fully developed flow in pipes and around $Re \approx 500{,}000$ for steady flow over flat plates at zero incidence (Schlichting and Gersten, 2017). It is important that Re is based on appropriate fluid properties (Section 2.3) and an appropriate characteristic length (e.g. internal diameter for fully developed internal pipe flow or length from the leading edge for external flow over a plate). Real plant geometries and flows may differ substantially from uniform flow in pipes or over flat plates, and this may increase or decrease the Re at transition. Increased surface roughness or upstream turbulence can substantially reduce the Re at which transition occurs.
- For *natural convection*, Gr and Ra are the key non-dimensional groups. Gebhart *et al.* (1988) provides specific non-dimensional groups based on Gr for predicting the start and end of

[6] Although the correlations used in system codes may well be for developed flow only.

transition (Gr is also considered more useful than Ra for predicting transition in fluids where Pr is not close to unity such as metals, Dzodzo, 2018). However, as a rough indication in common fluids like air and water, transition is expected at around $Ra \approx 10^9$ for a vertical plate (Incropera *et al.*, 2011). As noted above, it is important that non-dimensional groups are based on appropriate fluid properties and characteristic length (e.g. the height of the plate). Complex geometry and surface roughness may change transition behaviour significantly (similar to forced convection).

- For *mixed convection*, Re and Gr are important and the situation is much more complex, even for a simple geometry. Flow regime maps may be helpful and are discussed in Section 2.2.1, and a review is presented in Runchal (2020).

It is noted that these are typical values, the actual values of Re and Gr at transition may vary. In particular, the exact onset of transition from laminar to turbulent flow is affected by factors such as local geometry, surface finish, upstream turbulence, buoyancy effects and vibration. Complex geometries with non-uniform flows, rough surfaces and high upstream turbulence are likely to cause transition at lower Re, and vice-versa. Also, even at high bulk Gr values, regions with stagnant fluid, laminar circulation, transitional and fully turbulent regions may exist in complex geometries.

In buoyancy driven flows, laminar, transitional and fully turbulent regions can often be present simultaneously, as a result of the relatively low driving forces. For example, in a simple differentially heated square cavity, significant amounts of turbulence are generated close to the vertical walls (where temperature gradients are large), which is convected around the cavity by the convection cell that develops (driven by the mean buoyancy force). However, in the centre of the cavity the flow may remain relatively quiescent and therefore be laminar (Hanjalić, 2002).

2.2.4 Buoyancy Affected Flows and CFD

Buoyancy affected flows present particular challenges for CFD modelling, particularly if they are turbulent. The heat transfer (whether by natural, forced or mixed convection), buoyancy effects, mixing and pressure losses discussed in the previous sections can all be coupled within a flow field, and their detailed impacts on this flow field can be strongly affected by turbulence. As such, the prediction of heat transfer, buoyancy, mixing and pressure losses is strongly linked with the approach taken to predict turbulence, one of the key challenges for CFD modelling work.

The common approaches for predicting turbulence are introduced in Volume 1 (Section 4.5.3). The practical aspects of using CFD to model buoyant flows are discussed in Section 3.2. By contrast, this section presents an overview of selected theory on Large Eddy Simulation (LES) and Reynolds-Averaged Navier-Stokes (RANS), the most commonly used CFD approaches, with a focus on heat transfer and buoyant flows.

2.2.4.1 LES

In LES, the larger length scales are resolved and the effects of the unresolved smaller motions are modelled using a Sub-Grid-Scale (SGS) model (Runchal, 2020, Ciofalo, 1994). Early SGS models were developed with the principle that turbulence is more isotropic at the smaller scales (Pope, 2000), meaning that these were much simpler than their RANS counterparts. However, as with

RANS turbulence modelling, a number of higher-order models have also been developed. Some of the more commonly available models include:

Smagorinsky: First introduced by Smagorinsky (1963), this expresses the eddy-viscosity as a function of a length scale (the effective grid size, usually computed as $\Delta = V_{cell}^{1/3}$) and a velocity scale (the filtered strain-rate). A coefficient, termed the Smagorinsky constant (or coefficient), is defined by assuming local equilibrium between sub-grid turbulent kinetic energy production and dissipation. The model does not therefore properly account for non-equilibrium effects (such as may occur in buoyancy driven flows). The Smagorinsky constant is normally set by the user across the whole solution, so cannot be tailored for local flow regimes. Modifications are required to make the model valid for near-wall regions. Buoyancy extensions have been proposed by Eidson (1985).

Dynamic Smagorinsky: One key issue with the Smagorinsky model is that the appropriate value for the Smagorinsky constant is different in different flow regimes (Pope, 2000). The Dynamic Smagorinsky model provides a means for determining an appropriate local value for the constant (or coefficient), as discussed in Lilly (1992) and Germano *et al.* (1991).

WALE: The Wall-Adapting Local Eddy-Viscosity (WALE) model extends the Smagorinsky model by relating the turbulent viscosity to the local rotation rate, in addition to the local strain rate (Nicoud and Ducros, 1999). It is designed to return the correct near-wall behaviour for wall bounded flows and is thus generally recommended over the Dynamic Smagorinsky model.

Whether or not buoyant extensions to the above SGS models are required will depend on both how dominant the buoyant effects are in a particular flow, and how fine the LES mesh is. With coarser meshes, the contribution of the unresolved scales to the solution increases and thus the choice of SGS model can be more important.

For heated flows, a term representing unresolved temperature variations appears in the filtered energy equation and is usually referred to as the SGS heat flux. As with RANS (Section 2.2.4.4), models for the SGS heat flux are less mature with most approaches using a turbulent (or eddy) diffusivity approach along with a fixed turbulent Prandtl number.

2.2.4.2 RANS Context

In RANS, the mean (Reynolds-averaged) flow is resolved, and the effects of turbulence on this mean flow is modelled using a turbulence model. For flows where buoyancy or heat transfer play a dominant role, such models must account for both the turbulent transfer of momentum (using turbulence models to predict the Reynolds stresses) and the turbulent transfer of heat (using turbulent heat transfer models to predict the turbulent heat fluxes). For natural convection flow fields in particular, these are closely coupled and reliable predictions of both are generally important. While a large number of models are available for turbulent momentum transfer, far fewer are available for the turbulent transfer of heat or other scalars (Hanjalić, 2002).

Challenges associated with buoyancy and the turbulent heat fluxes are introduced below. Sections 2.2.4.3 and 2.2.4.4 then provide an overview of the turbulence and turbulent heat transfer models typically available in commercial CFD codes, considering their limitations and application to passive cooling flows. It is noted that turbulence modelling is a large and active research topic and comprehensive coverage is not possible in this document (more information is available in, for

example, Durbin, 2018, Runchal, 2020, Gatski and Rumsey, 2002 and Wilcox, 2006). Near-wall modelling is considered in Section 3.2.6.

Buoyancy: Buoyancy driven flows are difficult for turbulence models because of the following challenges (which are not normally present in non-buoyant flows):

1. Anisotropy: Buoyancy only directly affects momentum in the direction of gravity, and has a similarly anisotropic effect on the Reynolds stresses and turbulent heat fluxes. The most commonly used turbulence models, linear Eddy Viscosity Models (EVMs), cannot directly account for this anisotropy.
2. Generation and suppression of turbulence: Buoyancy forces can either generate or suppress turbulence depending on the alignment between gravity and the density (temperature) gradients. Even in geometrically simple systems, this can result in a multitude of regimes (laminar, turbulent and transitional) coexisting, which is challenging (Hanjalić, 2002).
3. Coupling: The close two-way coupling buoyancy imposes between the mean velocity and temperature fields also applies to the turbulence fields, so the Reynolds stresses appear in equations and models for the turbulent heat fluxes and vice versa. This complicates modelling and can increase the numerical stiffness of the resulting models.
4. Multiple timescales: The presence of velocity and temperature fields gives two associated timescales in the flow, causing concurrent effects on both fields that also influences the turbulence.

Accounting for buoyancy in RANS turbulence models typically involves Reynolds-averaging the buoyancy force terms and including them in the derivation of the model's transport equations. The main modelling effort is predicting the turbulent heat fluxes (see below). Additional effects arise through the influence of buoyancy on the fluctuating pressure, which can be accounted for in Reynolds Stress Models (RSMs) with modifications to the so-called pressure-strain term (Section 2.2.4.3).

Turbulent Heat Transfer: Turbulent heat transfer arises due to the significantly increased mixing that occurs once a flow becomes turbulent. In a RANS approach, the impact of this on the mean temperature field is captured by the turbulent heat flux. This arises from Reynolds-averaging the energy equation, and represents the averaged product of the velocity and temperature fluctuations. It describes the effect of turbulence on the transport of mean energy within the flow, and therefore affects the mean temperature in a similar manner to how the Reynolds stresses affect mean momentum.

2.2.4.3 RANS Turbulence Models

This section considers the theory associated with the main turbulence models, which are illustrated in Figure 2.9 (selecting models is considered in Section 3.2.6).

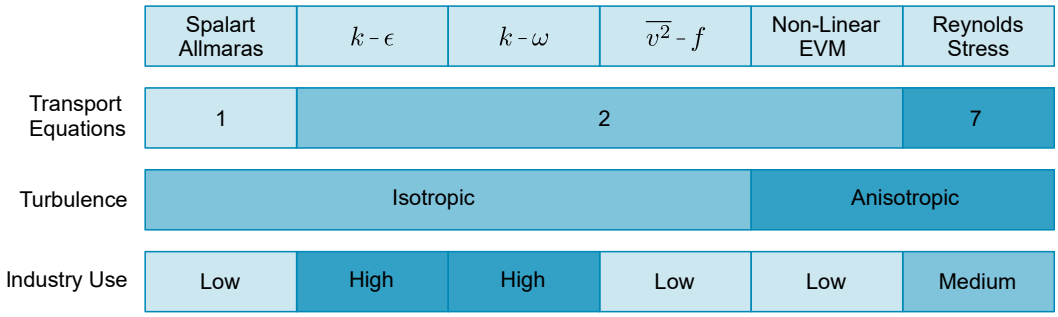

Figure 2.9: Summary of the main RANS turbulence models.

Linear EVMs, General Remarks: These use a simple linear algebraic relationship to relate the Reynolds stresses to the mean strains via a turbulent (or eddy) viscosity (μ_t)[7]. They are generally categorised into zero-equation, one-equation, or two-equation models (depending on how many transport equations they include). The two-equation k - ε and k - ω family of models and one-equation Spalart-Allmaras model are popular linear EVMs and are discussed in following sections.

As a result of the linear algebraic stress-strain relationship, linear EVMs cannot predict the highly anisotropic impact of buoyancy forces on the Reynolds stresses (or interaction between the Reynolds stresses and turbulent heat fluxes). These models are therefore challenged by natural or mixed convection flows where the direct influences of buoyancy on shear stresses are significant. They are also challenged by complex flows that may occur in natural convection (such as impingement, streamline curvature, rotation, strong unsteadiness, turbulence-driven secondary flows) because the linear relationship is unable to fully capture interactions between the mean strain field and anisotropic Reynolds stresses. While the aggregate effect of these influences may appear in the turbulent kinetic energy equation, it will not normally capture the full effects on the Reynolds stresses. Ad-hoc corrections to address these aspects are ultimately empirical and will likely only be of benefit within the intended range of applicability.

Despite the above well-known weaknesses, linear EVMs may perform surprisingly well in buoyancy affected flows, since they are capable of responding sufficiently to changes in mean-strain caused by the action of buoyancy forces (rather than the direct impact of buoyancy on the turbulence itself). However, their performance may well be poor where the direct influence of buoyancy on turbulence is a dominant feature (Section 2.2.1), or where buoyancy (or other) forces lead to strongly anisotropic strain fields.

The inclusion of buoyancy effects in linear EVMs varies, but generally involves using terms to represent the generation or dissipation of turbulent energy due to the direct action of buoyancy. For models which solve a transport equation for the turbulent kinetic energy (k), a buoyant generation term is usually added to the equation. This is exact, but based on the predicted turbulent heat fluxes. Whilst this represents the direct effects of buoyancy on the turbulent kinetic energy, the effects of buoyancy on the anisotropy of the turbulence cannot be included. For two-equation models which solve a length scale determining transport equation (e.g. ε or ω), an equivalent term can

[7] The terms μ_t and ν_t are both used in this context and may both be referred to as the turbulent (or eddy) viscosity. However, since ν is the kinematic viscosity, ν_t is often referred to as the kinematic eddy viscosity.

be added, but may not be, since the direct effect of buoyancy here is less well understood. CFD software may include this by default, or include an option to, and the constants used may vary.

Linear EVMs, Zero Equation Models: These use very simple algebraic relations to predict the turbulent viscosity, mostly using constants input by users or simple measures such as wall distance. Examples include Prandtl mixing length, Cebeci-Smith and Baldwin-Lomax model. Increased computer power and availability of more advanced models mean these models are rarely used.

Linear EVMs, Spalart-Allmaras Model: Proposed by Spalart and Allmaras (1992) for flows over wings, this is a one-equation model that solves a transport equation for the turbulent viscosity directly. This model has been shown to give good results for boundary layers in external aerodynamics, but has not been calibrated for general industrial flows and there are few examples of application to buoyancy driven flows in research literature. As such, for passive cooling applications, its use is likely to be limited to starting up more complex calculations with stability problems.

Linear EVMs, k-ε Models: Proposed by Jones and Launder (1972), this is one of the best-known and most widely used linear EVM. This two-equation model solves transport equations for the turbulent kinetic energy, k, and the dissipation rate of that energy, ε. The original model did not account for viscous effects found in the near-wall region (the flow was assumed to be fully turbulent everywhere) but a number of low-Re variants have been proposed which do include terms to allow the model to be applied in such regions[8] (Chien, 1982; Launder and Sharma, 1974; Yang and Shih, 1993). The original model did not include direct buoyancy effects, but this can be included as noted in the general remarks above. Many model variants exist, but two are most common[9]:

1. Realizable k-ε model includes an alternative formulation for the turbulent viscosity (using a variable c_μ) and a modified transport equation for ε (Shih *et al.*, 1995). While realisability appears desirable, turbulent stresses are not really generated in the way an EVM supposes, limiting its efficacy (Hanjalić and Launder, 2011).
2. RNG k-ε model applies a statistical technique called Re-Normalisation Group (RNG) theory to the Navier-Stokes equations (Yakhot *et al.*, 1992). The resulting model has the same form as standard k-ε but has coefficients arising from the procedure and an additional term in the ε equation designed to improve sensitivity in flows with strong straining. It is argued that this should improve performance over the standard k-ε for a wide range of flows.

One of the weaknesses of the k-ε family of models is a tendency for large turbulent length scales to arise in strong adverse pressure gradients, linked to modelling of diffusion processes within the ε equation[10]. However, this is addressed by the Yap correction (Yap, 1987; Craft *et al.*, 2000), which can significantly improve velocity profile predictions in buoyancy-driven turbulent flows in vertical pipes (Ince and Launder, 1989) and should be considered if available.

[8] Often references within literature refer to a 'standard' k-ε model; this typically refers to the high-Re version of Jones and Launder (1972), but many studies incorrectly associate the term 'standard' with later variants. This is important because many deficiencies of the 'standard' model have been addressed in later variants.

[9] As published, these do not include wall-damping terms and thus must be used with wall functions, but some CFD developers may include modifications to enable such models to be used with a low-Re near-wall approach, so software documentation should be checked.

[10] For impinging jets this was shown to result in overly excessive heat transfer rates (Craft *et al.*, 1993) and termed the turbulent/round jet anomaly.

Linear EVMs, k-ω Models: Proposed by Wilcox (1988), this is another widely used family of linear EVMs. This two-equation model solves an equation for k and ω (instead of ε) and can solve right up to the wall without further modifications (i.e. without introducing viscous damping terms, as must be done for the ε equation). As for k-ε, direct buoyancy effects can be included as noted in the general remarks above. The original model displayed strong sensitivity to free-stream conditions (Menter, 1994), but this has been addressed in later variants:

1. Baseline (BSL), Menter (1994) effectively blends a k-ω formulation in the near-wall region with a k-ε model in the far field, as this does not demonstrate such free stream sensitivity.
2. Shear Stress Transport (SST), Menter (1994) further developed the BSL model by introducing a limiter into the turbulent viscosity formulation, effectively causing the model to respond more like a shear-stress transport equation.
3. Generalized k-ω (GEKO) model, Menter *et al.* (2020) replaces the relatively inflexible calibrated coefficients used by most models with a set of user-definable parameters. This allows the model to be adjusted in specific areas without invalidating the base calibration, and attempts to provide greater flexibility within one model to cover a wider range of applications.

At time of writing, k-ω models have been less well used for buoyancy driven flows than k-ε models, and the implementation of buoyancy effects in commercial CFD software has been inconsistent. For some ascending mixed convection flows in particular (Keshmiri *et al.*, 2012), the k-ω SST model has struggled to capture the impairment in heat transfer experienced as the influence of buoyancy was increased. Although interesting, GEKO is relatively new and there are therefore few published examples of its application, especially relating to buoyancy affected flows.

Other Linear EVMs: A range of other linear EVMs have been developed, of which a number are based on the elliptic relaxation concept introduced by Durbin (1991) and one of the more popular is the v^2-f model. In addition to k and ε, this solves transport equations[11] for $\overline{v^2}$ and f, which come from the solution of an elliptic equation. This has been extended to account for buoyancy effects (Kenjereš *et al.*, 2005) and has demonstrated improvements over other linear EVMs in a number of flows involving turbulent heat transfer, including mixed convection vertical channel flow (Keshmiri *et al.*, 2012), impinging jets (Behnia *et al.*, 1999) and ribbed walls (Manceau *et al.*, 2000).

Non-Linear EVMs: Non-linear EVMs have also been developed to link the mean strains and Reynolds stresses more reliably than linear EVMs, whilst retaining the same convenient modelling framework. Most schemes extend the linear Boussinesq stress-strain relation to include non-linear (i.e. quadratic or cubic) combinations of mean strain terms. The main advantage of this is that the impact of flow curvature, rotation, or buoyancy on Reynolds stresses can be accounted for at least qualitatively, with little impact on computational cost.

Improvements over linear EVMs have been demonstrated in flows with curvature, separation, transition, impinging jets and anisotropy-driven secondary flows (Craft *et al.*, 2000, Jaramillo *et al.*, 2008). Anisotropy-driven secondary flows can alter heat transfer and increase mixing in fuel bundle channels (Ninokata *et al.*, 2009; EPRI, 2014). Non-linear EVMs were therefore selected by some participants in a CFD benchmark of the NESTOR and OMEGA 5x5 fuel bundle experiment (EPRI,

[11] $\overline{v^2}$ is a surrogate scalar which is the wall-normal stress component in a turbulent boundary layer, but in an elliptic relaxation EVM it provides an additional velocity scale (Hanjalić and Launder, 2011).

2014), and were recommended as robust and computational efficient (Kang and Hassan, 2016). As such, while non-linear EVMs are not extensively used for buoyancy driven flows in industry, they may provide improvements in future.

Reynolds Stress Models: Unlike EVMs, RSMs[12] solve transport equations for each of the Reynolds stresses directly, without making use of the Boussinesq eddy-viscosity hypothesis. This enables anisotropic turbulence effects (which may be significant in buoyant or near-wall flows, Omranian *et al.*, 2014) to be modelled directly. This enables better prediction of the different rates at which individual stresses are generated, convected, diffused and dissipated (Hanjalić and Launder, 2011). The performance of more advanced turbulence heat flux models are also likely to improve, since many of these models are reliant on accurate values of the Reynolds stresses being available (Section 2.2.4.4). RSMs therefore have a much wider range of applicability than EVMs.

The direct effects of buoyancy are included via a generation term, which is exact, but (as with EVMs) requires accurate values of the turbulent heat flux. Most modelling effort is focused on the pressure-strain term, which represents a physical process absent from models using a transport equation for k, and CFD tools may distinguish RSMs by how this term is treated. Notable models include:

1. The Launder-Reece-Rodi (LRR) (Launder *et al.*, 1975) and Speziale-Sarkar-Gatski (SSG) (Speziale *et al.*, 1991) RSM models use linear and quadratic relations for the pressure-strain correlation respectively. While initially developed as high-Re models (like k-ε), low-Re extensions are available (Shima, 1998; Hanjalić and Jakirlić, 1998).
2. Elliptic-Blending RSM (EBRSM) (Manceau and Hanjalić, 2002) was developed based on an elliptic relaxation concept (Durbin, 1991) and uses a different approach to modelling the pressure-strain contribution. This has been successful in a number of complex flows (Billard *et al.*, 2012), including those affected strongly by buoyancy (Dehoux *et al.*, 2017).
3. Two-Component Limit (TCL) (Craft, 1998) is a low-Re form of LRR developed to satisfy the so-called TCL, a highly anisotropic state where one of the normal stress components becomes very small compared to the other two.[13] This has demonstrated superiority in a number of buoyancy related flows (Craft *et al.*, 1996; Omranian *et al.*, 2014).

In addition to solving equations for each Reynolds stress, RSMs also need to solve a length scale determining equation. Typically either ε or ω is used, inheriting the deficiencies present in those equations. From a physical perspective, RSMs are particularly appropriate for modelling flows with strong buoyancy influences, especially in unfamiliar situations. A detailed assessment of RSMs can be found in Hanjalić and Launder (2011).

[12] Also known as 'stress transport models' or 'second-moment closures'.
[13] While appearing academic, flow in the very near-wall region may well approach this limit, as may a strongly stable buoyancy affected flow.

2.2.4.4 RANS Turbulent Heat Transfer Models

Modelling turbulent heat transport has received much less attention than turbulent momentum transport, and while a number of approaches exist, options in most CFD tools are limited. As for turbulence models, there is a hierarchy of models (Figure 2.10) ranging from simple turbulent (or eddy) diffusivity approaches (relating turbulent heat fluxes to mean temperature gradients, analogous to the turbulent viscosity concept) to full differential transport approaches (solving separate equations for each component of the turbulent heat flux vector). The choice of turbulent heat transfer model is an area of active research (Section 4), and is related to the choice of turbulence model (Section 3.2.6).

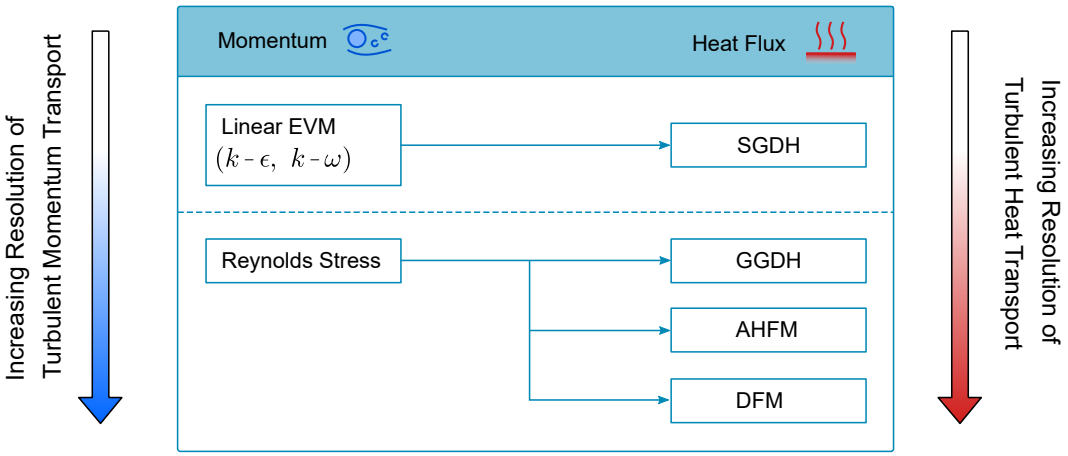

Figure 2.10: Summary of the main RANS turbulent heat transfer models.

Simple Gradient Diffusion Hypothesis (SGDH): This relates the turbulent heat flux components to the mean temperature gradients using an isotropic turbulent diffusivity (normally assumed proportional to the turbulent viscosity via the turbulent Prandtl number, Pr_t)[14]. Pr_t may be a constant by default, but CFD tools often allow this to be varied by the user (Pr_t is not constant in many buoyancy affected flows). This approach assumes that the turbulent heat fluxes are not directly influenced by buoyancy, and depend directly on the corresponding mean temperature gradient (a constant temperature in one direction implies no turbulent heat transport in that direction), which may well not be the case. This model therefore has limited validity, and while it may work well in some forced convection flows (e.g. ribbed ducts/passages, Manceau *et al.*, 2000) it can cause errors in flows dominated by buoyancy (Hanjalić, 2002).

Generalized Gradient Diffusion Hypothesis (GGDH): Introduced by Daly and Harlow (1970), this generalises the SGDH by introducing an anisotropic turbulent diffusivity (which depends on all components of the Reynolds stress tensor). This model therefore depends on reliable predictions of the Reynolds stresses. It considers all of the mean temperature gradients (rather than just the one aligned with the turbulent heat flux), but if these mean gradients are all zero, it will still return a zero value. It has little computational overhead compared to SGDH, and has demonstrated improvements in natural convection with strong stratification (Ince and Launder, 1989).

[14] An application of the Reynolds analogy, which assumes similarity between the way turbulence affects the transport of momentum and heat. Similar models may be available for mass transfer using the turbulent Schmidt number, Sc_t

Algebraic Heat Flux Model (AHFM): AHFM is based on an algebraic simplification of the full transport equations for the turbulent heat fluxes, and retains all of the major generation terms (mean temperature gradients, mean velocity gradients and direct buoyancy effects). Since the SGDH and GGDH only include contributions due to mean temperature gradients, AHFM can potentially account for a wider range of buoyant interactions. The model requires values of temperature variance, which can be calculated algebraically (similar to GGDH) or, more commonly, by solving a transport equation for it. AHFM has been successfully applied to a range of buoyancy driven flows in enclosures (Hanjalić, 2002; Hanjalić *et al.*, 1996).

Differential Flux Model (DFM): Solves transport equations for each of the turbulent heat fluxes (and normally the temperature variance). This better accounts for the various ways turbulent heat fluxes are generated, transported and dissipated and addresses a number of deficiencies with more primitive models (SGDH, GGDH and AHFM). However, DFM adds significant computational cost, and is not normally available in commercial CFD software at time of writing (Dehoux *et al.*, 2017).

2.3 Fluid Material Properties

Natural convection flow fields are driven by density variations in response to temperature changes, so the material properties of the fluid (density, viscosity, specific heat capacity, thermal conductivity) are particularly important. In general, the properties of fluids vary due to a range of factors that should be considered, including:

Nature of Fluid: The properties of fluids may be altered by a range of factors, including contamination, addition of different species, specific mixture/solution composition and ageing under radioactivity. The key factors to consider, and their impact, are likely to be case specific.

Pressure: There are often two aspects to pressure variations: firstly, the overall pressurisation of a system and secondly, pressure changes occurring in the flow. The impact of both of these on material properties should be considered. For liquids, variations in material properties with *flow* pressure changes are often small, so that the impact of flow pressure changes on material properties may be neglected (from a density perspective this is equivalent to treating the flow as incompressible). In this case, the properties can be evaluated at the appropriate system pressure. For gases, often only the density is significantly affected by flow pressure changes, and these compressibility effects usually only have a significant impact where $Ma \gtrapprox 0.3$ (which is unusual for natural convection).

Temperature: Temperature changes often cause larger variations in properties than pressure changes. For natural convection in particular, it is precisely the variation in density with temperature that provides the buoyancy forces that drive the flow (Section 2.2.2). Other properties such as viscosity, specific heat capacity and thermal conductivity may also exhibit significant variation with temperature. The variations in properties with temperature are therefore a key aspect to consider when performing analysis of buoyancy affected flow fields.

Critical point and phase changes: Near the critical point or phase changes, very large variations in properties may be encountered with small changes in pressure or temperature, and these can have a large impact on flow fields and heat transfer.

The rest of this section identifies some sources of material property data and considers how these might be used. Including properties in modelling work may be challenging where there are strong gradients in properties, such as near the critical point or phase changes as noted above. These challenges may include accuracy of the data itself, the accuracy of the calculation of properties within the model, and the stability of the model.

The properties of solids and the impact of surface modifications on heat transfer are considered in Volume 2 (Section 2).

2.3.1 Sources of Property Data

Possible sources of fluid material properties data for a number of common fluids are presented below. Whatever source is chosen, this is a key input to analysis work, so it is necessary to record the approach taken and consider the accuracy of the data. Uncertainty in property data can have a significant impact on the analysis of natural convection flows; the management of input uncertainty is considered in Volume 4 (Confidence and Uncertainty).

Water and Steam: The International Association for the Properties of Water and Steam (IAPWS) presents formulations for properties of light water, heavy water and sea water at the time of writing, and new formulations may be released periodically[15]. Two of these formulations for the thermodynamic properties of light water (IAPWS-95, Wagner and Pruß, 2002, and the less computationally intensive IAPWS-IF97, Wagner *et al.*, 2000) are considered accurate by IAEA (2006). Properties data based on current formulations, including saturation curves, may be available from NIST (via the Chemistry WebBook or REFPROP tool[16]) or steam tables like Haywood (1990). Saturation curves for light and heavy water (and more general properties for light water) are also presented in IAEA (2009b). It is inappropriate to consider steam as a perfect or ideal gas. While phase change is not considered in this volume, it is noted that condensation can be greatly affected by the presence of non-condensible gases (further detail available in Rohsenow *et al.*, 1998 and Collier and Thome, 1996).

Carbon Dioxide, Nitrogen and Helium: If pressures are not high and temperatures are not low (or if properties are not of great concern, like basic studies, model debugging etc.) it may be appropriate to consider these gases as perfect or ideal[17]. Real gases are more likely to behave like ideal gases than perfect gases; further discussion on the use of perfect or ideal gas assumptions is presented in Rogers and Mayhew (1992). It may well be appropriate to check perfect or ideal gas assumptions against full properties, or full properties data can be used exclusively. Full properties data for these gases may be available from NIST Chemistry Webbook (for pure gases) or NIST REFPROP (for pure or mixed gases). Data for specific conditions may be available in textbooks, such as Incropera *et al.* (2011). Data for helium at low pressure is included in IAEA (2009b). These gases are often used in closed or sealed systems where moisture content is controlled at a low value, but if this is not the case, the impact of moisture on properties can be significant and should be considered.

[15] www.iapws.org
[16] webbook.nist.gov/chemistry and www.nist.gov/srd/refprop respectively
[17] Perfect gases obey the ideal gas law *and* have a constant specific heat capacity; ideal gases only obey the ideal gas law.

Air: Air is a mixture of gases and should generally be considered as such. Like carbon dioxide, nitrogen and helium, it may be appropriate to either use perfect or ideal gas assumptions, or use full properties data (see above). Published sources include Lemmon *et al.* (2000), Lemmon and Jacobsen (2004) and IAEA (2009b). Unlike carbon dioxide, nitrogen and helium, air is often used in open or unsealed systems, where moisture content is likely to vary. The presence of moisture can significantly affect properties and hence the performance of a cooling system (e.g. the impact on density is considered in Picard *et al.*, 2008). Moisture content is also an important aspect of the design of HVAC systems, which can have a role in preservation of mechanical equipment as well as habitability for operators (further detail in Haines and Myers, 2010 and ASHRAE, 2017).

Liquid Metals and Molten Salts: The use of material properties for liquid metals and molten salts requires particular considerations, which are discussed in Volume 5, Volume 6 and (IAEA, 2002a, 2013b). In general, obtaining reliable information about the properties of more advanced but less established coolants may be challenging, as a range of formulations may be available and the accuracy of the data may be difficult to ascertain.

2.3.2 Implementing Property Data

The exact approach taken in a given project will be a judgement specific to the analysis being performed and the programs being used. Sources of data are discussed in Section 2.3.1. Common ways of including this data in analysis are illustrated in Figure 2.11 and discussed below.

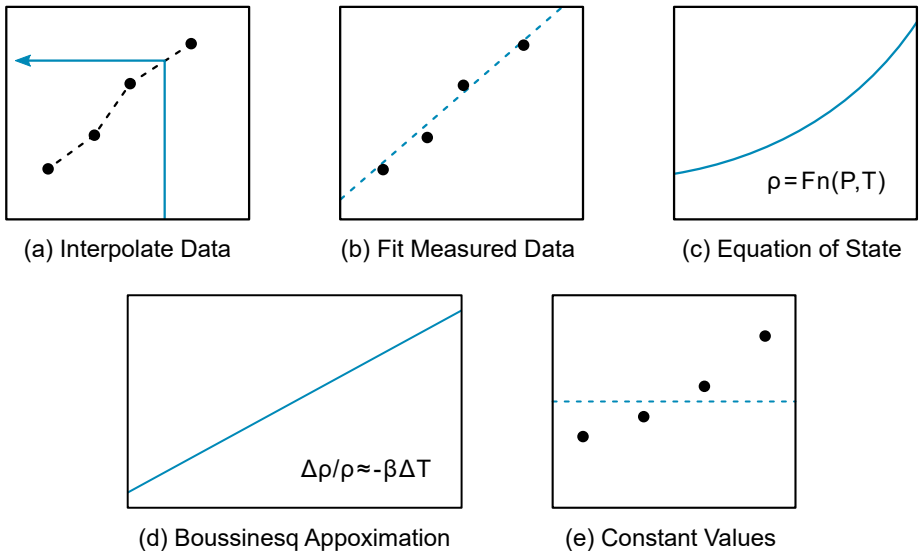

Figure 2.11: Common ways of including material properties data.

Interpolate directly from measured data: This typically involves reading property data into an analysis program and using linear interpolation to provide property values. This gives full control over the values used, but may cause computational overheads and require a large amount of data to be read into the analysis program that has to be checked. Additionally, the user must be confident that they will be alerted when values outside the range of the data are requested, as this may cause errors.

Fit measured data: This typically involves reading property data into a computer program, fitting curves or surfaces to the data, and then entering the constants of these fits into an analysis program. The exact approach is likely to depend on what the analysis program will easily accept (polynomial, exponential fit etc). This may be especially useful if properties are considered only a function of temperature (i.e. the flow is considered incompressible), gives full control over the values used with minimal computational overheads and saves reading a lot of data into an already complex analysis program. However, care must be taken to ensure that the fit closely represents the data and the user must be confident that they will be alerted when values outside the range of the fit are requested, as this may cause errors.

Equation of state: An equation of state uses an algebraic expression to provide properties for given conditions (pressure and temperature). The complexity of equations of state varies from simple (such as the ideal gas law, $\rho = P/RT$) to extremely complex functions. It is important to understand the assumptions underlying these equations and confirm they are relevant to the assessment before using them. It is also important to implement them carefully and check their output, as large errors could result from inaccurate use.

Boussinesq approximation: This approximation[18] is sometimes used in analysis of buoyancy-driven flows. This allows the density to be considered constant in the governing equations, except when multiplied by the acceleration due to gravity in the buoyancy force terms (i.e. ρg). The density variations caused by thermal expansion are included by assuming a linear dependence with temperature (e.g. $\Delta\rho/\rho \approx -\beta\Delta T$). This simplifies the governing equations and may make including density changes easier, particularly for ideal gases where $\beta = 1/T$ (although in general, β and other properties such as viscosity may be set as constant or varying when the Boussinesq approximation is being used).

The Boussinesq approximation is only valid for small density variations ($|\beta\Delta T| \ll 1$, Gebhart *et al.*, 1988) and is therefore a potential source of uncertainty in analysis work. For flows in loops, using this approximation rather then IAPWS-IF97 (Section 2.3.1) has been seen to cause significant changes in predicted system behaviour (Krishnani and Basu, 2016). If this approximation is used, care should be taken to ensure that it is appropriate for all fluid properties across the range of local conditions (pressure, temperature etc) that may be encountered in the flow field. This might be achieved by comparing with measured data or an equation of state, using sensitivity studies, or analytical methods (Gray and Giorgini, 1976).

Constant values: Using fixed values for fluid properties may be useful in some situations, but must be used carefully and is of little use for natural or mixed convection flows, where by definition density changes have a significant impact on the flow.

In summary, using temperature dependent properties appropriate to the average pressure of the flow in the system of interest (or full pressure and temperature dependent properties) should be considered for natural or mixed convection assessments. Using fits to measured data may be an appropriate starting point, as this may give a good balance between accuracy and complexity.

It is important that properties data is provided for the range of conditions that occur in the analysis to avoid unphysical model behaviour. Checks may (or may not) be included in modelling software to generate warnings where conditions are outside of the range for which properties are available. It

[18] This is not to be confused with the Boussinesq eddy-viscosity hypothesis, see Section 2.2.4.

may be necessary to use more than one dataset to obtain properties over the range of conditions, in which case the properties should be carefully combined in a consistent manner. Whatever is done, it is important to record the approach taken, as properties are key inputs to any flow analysis.

2.4 Modelling Challenges

This section introduces the typical challenges that may be encountered in modelling buoyancy affected flows. Addressing these challenges is considered in Section 3.

Local Flow Unsteadiness and Complexity: Like the plume rising from a cup of tea, buoyancy driven flows are often unsteady and complex/three-dimensional, even where the boundary conditions are essentially constant and two-dimensional. Inside these flows, the dynamic field (the local velocities, including turbulence if present) is tightly coupled to the thermal field (the local temperatures) as well as the related shear forces, mixing, changing fluid properties and buoyancy forces. This places particular demands on modelling work that seeks to predict detailed flow fields (such as CFD). Similarly for experimental work, this may impact aspects such as choices of measurement approaches, data logging equipment and probe placement.

System Flow Unsteadiness and Complexity: Just as buoyancy affected flow fields can be unsteady and complex, so can the behaviour of the system as a whole. In particular, systems using natural circulation may exhibit complex oscillatory behaviour with significant sensitivity to initial states and evolving boundary conditions during postulated accident scenarios. Small changes in one area may spread to the whole system, and differences between thermal and dynamic timescales may result in oscillatory and unintuitive flow behaviour. Even simple systems can exhibit complex flow behaviour as the overall system flow develops during start-up, particularly if pressure losses (Section 2.2.2), which can provide a level of damping, are low. The impact of instability on start-up times may be a challenge if these times are safety significant (IAEA, 2005 and Krishnani and Basu, 2016 consider stability of passive cooling systems). An example for a simple natural circulation loop is shown in Figure 2.12, where complex eddying local flows couple with the wider system flow field to cause the bulk flow to reverse repeatedly (Wilson, 2021).

Pressure Losses and Mixing: As noted above and in Section 2.2.2, in buoyancy affected flows, pressure losses and mixing act to resist the movement of fluid via shear forces, and to reduce temperature gradients. Both of these effects can have a large impact on flows both locally and over the whole system. However, the unsteady and complex flow fields that can exist in buoyancy affected flows can challenge the assumptions used in the correlations in system models and the turbulence models often used in CFD (Section 2.2.3) which are often important in predicting these effects.

Characteristic Timescales: As noted in Volume 3 (Section 2.5), there is generally a large disparity between the timescales associated with detailed flow effects (e.g. shedding or plume development, with timescales typically less than a second), system effects (e.g. through-flow duration or flow reversal), solid conduction (e.g. heating of large masses of metal, with timescales typically in hours) and the whole plant (e.g. transients lasting days, weeks, or even months or years for accident scenarios). If the flows during a long plant transient are to be predicted using a CFD

model, it is likely to be expensive to predict the whole plant transient using the smallest timescale characteristic of the flow field.

Confidence: It is important to develop a level of confidence in the predictions of modelling work that is proportionate to its significance in the economic or safety case for the plant, in line with a graded approach (Volume 1, Section 2.2). Since buoyancy driven flows may be challenging to model, developing this confidence can be a particular challenge for these flows. This topic is considered further in Volume 4.

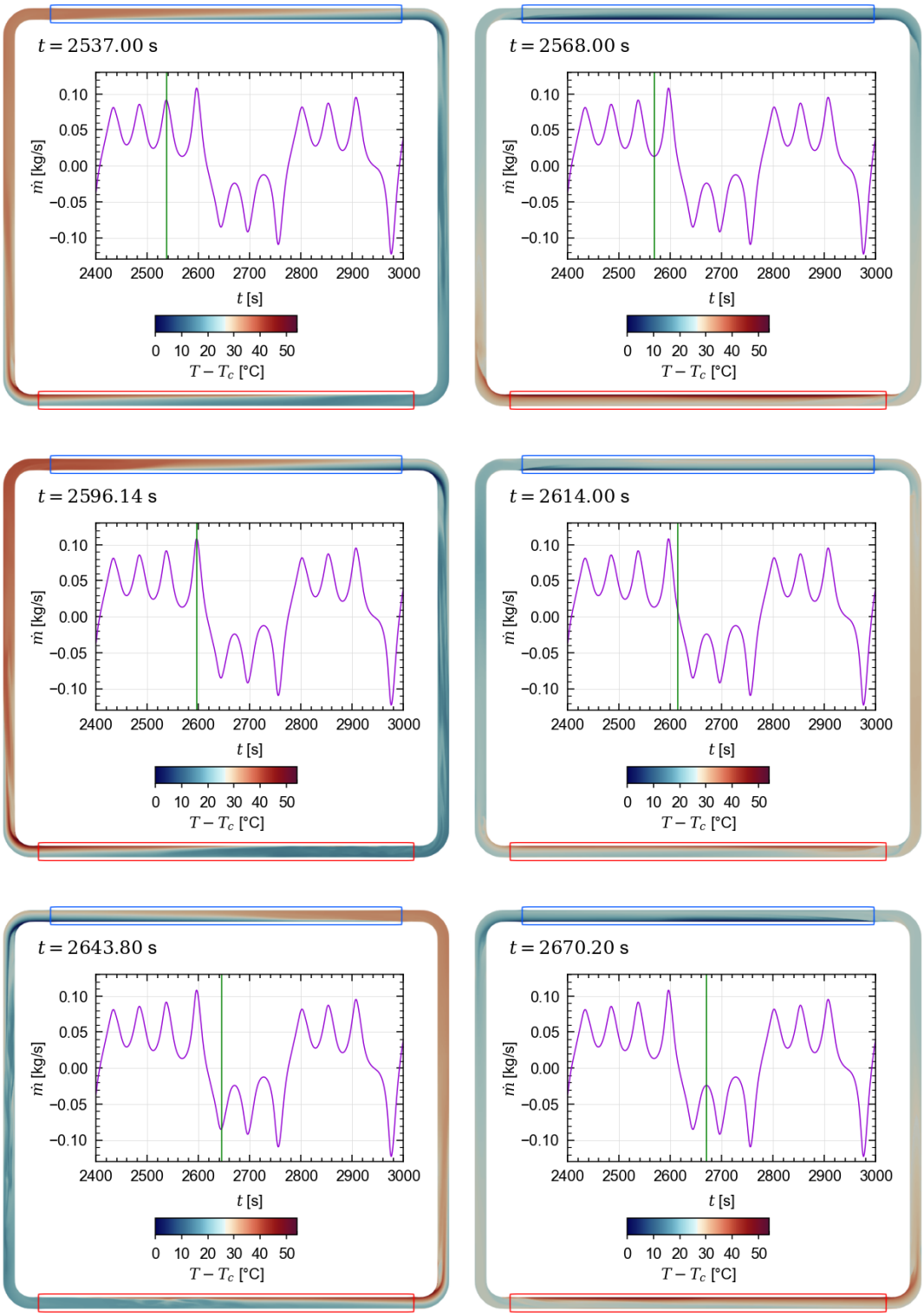

Figure 2.12: Flow unsteadiness and system level instability in a simple natural circulation loop with a horizontal heater and horizontal cooler (Wilson, 2021). The mass flow rate is $\dot{m}$ in this figure.

3 Methodology

This section presents an overview of methods used to predict and understand the performance of passive cooling systems, to assist engineers performing analysis. Typical approaches to NTH analysis are considered, before assessments using system and subchannel analysis, CFD analysis and experimental methods are discussed in more detail.

The overall approach to NTH analysis is introduced and discussed in Volume 1 (Section 4.1). In general:

- System codes are often used to predict the performance of whole systems or groups of sub-systems, while CFD is often used to understand the detailed flow field in specific plant areas.
- Application-specific codes (like subchannel or containment codes) are often used where some flow field modelling is needed, but a full CFD approach is too cumbersome or computationally expensive.
- Experiments are often used to understand the overall behaviour using scaled test facilities, investigate detailed flow effects and provide comparative data to validate analysis work.

As for any NTH analysis, the amount of technical justification required is likely to depend on the safety or economic significance of the system as part of a graded approach (Volume 1). It is also common, and often necessary for passive cooling systems, to employ different methods together, for example using a system code to predict overall performance and a subchannel or CFD code to predict flow fields in specific areas, i.e. multiscale analysis (Volume 2, Section 3.1).

Pools and Plena: Buoyancy affected flows in pools and plena are often complex and three-dimensional because the flow is less constrained by walls. Relevant flow phenomena include plumes, thermal stratification, thermal striping, jet interaction and free surfaces (Section 2.1). In general, this tends to imply more of a role for methods that resolve spatial and temporal variations, particularly CFD and experimental methods, rather than system codes. A notable exception is the system code SAM (Volume 1, Section 4.4.1), which is being developed to model liquid metal pools.

Loops and Channels: System and subchannel codes have been developed and validated for primary circuit flows under a wide range of fault scenarios, particularly for forced circulation conditions. However, the complex flow fields associated with buoyancy driven flows and natural circulation mean that three-dimensional effects become more significant and reduces the suitability of these tools. In particular, complex geometry or flow phenomena, such as flow reversal, cold water injection, thermosyphons (dead legs) and cold traps (Section 2.1.2) need to be carefully considered and may require more detailed CFD analysis to build confidence in the overall modelling approach.

3.1 System and Subchannel Analysis

System and subchannel codes are introduced in Volume 1 (Section 4.4) and their capability and limitations for Conjugate Heat Transfer (CHT) modelling is discussed in Volume 2 (Section 3.2).

System codes in particular are key design tools, allowing the performance of a system (or groups of sub-systems and modules) to be rapidly assessed in a wide range of scenarios. However, buoyancy-driven flows can present particular challenges for analysis using these codes. Subchannel codes or CFD are more commonly used for in-depth analysis of subchannels, where system codes may be used to provide boundary conditions, such as key core inlet parameters.

Some challenges associated with modelling natural circulation scenarios are common to both system and subchannel codes. In general, modelling of natural circulation using these codes depends on a number of constitutive equations including those for friction factor, form loss and heat transfer. Most of these correlations are relatively well-established for fully-developed flow in a circular pipe. However, in natural circulation, the flow may well be complex and uneven or include counter-current flow, even within simple circular pipes. Discrepancies may also occur if one (or more) of the following conditions is involved:

- Non-circular, complex geometries (e.g. tube bundles);
- Complex flow paths (e.g. flow obstructions, orifices);
- Developing flow;
- Multi-dimensional effects;
- Transition between different flow regimes.

The geometry, conditions and flow phenomena within the system being modelled should be reviewed against the Verification and Validation (V&V) database and user documentation for the system/subchannel code. If issues are identified regarding the suitability of the code for the scenario being modelled, then a number of options are available.

- Experimental (or CFD) data could be generated for the expected natural circulation flow conditions to improve the existing correlations in the system/subchannel code, although this may require access to the source code. For example, CFD may be used to generate an array of coefficients to account for pressure loss due to flow obstructions (Avramova *et al.*, 2016). This will require users to carry out additional V&V activities to ensure the code accuracy.
- If sources of errors are identified, users may ‘tune’ user-provided parameters in the input file to remedy discrepancies. For example, users may ‘adjust’ parameters such as junction pressure loss coefficients, hydraulic diameter and heated diameter.
- Users may also couple the system/subchannel code to CFD models in order to properly resolve a portion of the system where complex flow phenomena and/or geometry are expected (Volume 2, Section 3.1).

3.1.1 System Analysis

System codes are generally based on a two-fluid model (solving mass, momentum and energy conservation equations for gas and liquid phases) and use flow regime maps for different flows (such as vertical, horizontal and mixing flows, see Section 2.2.1). The flow regime map is used to select appropriate correlations (or closure relations or constitutive models) for interfacial heat transfer, interfacial drag, wall drag, wall heat transfer and wall friction based on the local flow conditions (Section 3.1.1.2).

System codes have been primarily developed for forced circulation systems, which are dominated by pressure drop and inertial effects, rather than natural or mixed circulation, where buoyancy (density differences) has a significant impact on the flow. While the capability of system codes to predict single-phase and two-phase natural circulation has been studied, these studies are generally not as extensive as for forced circulation. The approach, capability and limitations of system codes to predict natural circulation is discussed in the following sections.

3.1.1.1 Nodalisation and Discretisation

Nodalisation is the representation of plant geometry within a system code. The user is required to construct this nodalisation, which describes the network of plant components. Each component may then be further discretised using hydrodynamic cells. There is considerable scope for variability in nodalisation (as for meshing in CFD) and this is often a source of 'user effects'.

Nodalisation within system codes usually relies on the use of building blocks. These building blocks include pipe, junction, branch and single volume and each building block is equipped with component models. For example, pipe components are a one-dimensional system of volumes and junctions and its geometry is described using flow area, length and hydraulic diameter.

Traditionally, the nodalisation process involves a compromise between accuracy and computational cost, however computational cost is less of a concern for modern studies. It may seem desirable to improve the accuracy of results by refining the discretisation to provide increased spatial resolution, but for most system codes this does not necessarily guarantee improved solution accuracy (Petruzzi and D'Auria, 2008), because:

- A large number of empirical constitutive models have been developed assuming a fixed/coarse nodalisation. For example, in RELAP5, spatial derivative terms in the virtual mass force were neglected as these were inaccurately approximated using relatively coarse nodalisation.
- System codes are often based on the first-order upwind scheme, and so reducing the spatial resolution below a certain threshold may lead to some unphysical instabilities.
- The two-fluid model can become ill-posed, which can lead to numerical instabilities (Dinh *et al.*, 2003). RELAP-7 claims to eliminate this issue by using a seven equation two-phase flow model.

In addition, the complexity of a component or system geometry is often simplified so that it can be represented in a system code. This simplification may inaccurately predict the flow behaviour, particularly in a multi-dimensional flow and a scaled-down facility where system specific effects may become exaggerated. As there is no optimum approach to construct a nodalisation, it is recommended that nodalisation and convergence studies are carried out.

Pools and Plena: In pools, multi-dimensional phenomena such as thermal stratification and mixing are expected. In order to capture these conditions, a pool may be modelled using a multi-dimensional component or parallel (vertical) channels connected by cross-flow junctions (Kumar, 2017). The multi-dimensional components in system codes are based on an orthogonal, three-dimensional grid. In order to represent the actual amount of fluid within a cell or include the local geometry effect, a porosity factor and junction factor are used. This can be another potential source of user effects. It should be noted however that the code manuals claim that TRAC-based codes and RELAP cannot model recirculation flows in a large open region (INL, 2018, Roth and Aydogan, 2014b).

In general, plena are modelled using a branch component or 1D volumes connected by cross-flow junctions. However, under natural circulation flow conditions, multi-dimensional and/or non-uniform flow conditions may be observed in the plena (Salah, 2013). These effects may be captured by employing a multi-dimensional component in the system codes noting that multi-dimensional components are intended to capture large-scale effects only.

If the multi-dimensional flow behaviour in pools and plena cannot be captured adequately by system codes, CFD is recommended and typically system codes are used to define appropriate boundary conditions for the CFD analysis.

Loops and Channels: Modelling loops and channels in system codes is limited to employing a pipe/channel component. It should be noted that the prediction may be sensitive to the choice of nodalisation, and a convergence study is necessary to determine an optimal nodalisation for loops and channels (Hou *et al.*, 2017). In general, it is recommended that the node length be set up such that all volumes have similar material Courant limits. As a starting point, a node length may be set such that the ratio of the node length to diameter is ≥ 1.

In the case of multiple, parallel channels, it is recommended that the distribution of node lengths is the same or similar between the channels, particularly in the case of vertical, parallel channels. This is done to prevent numerical oscillations between parallel channels (INL, 2018). In general, these parallel channels should be connected via a branch component at both the top and bottom. It should be noted that there is a limited amount of validation data for natural circulation in parallel channels (Saikia *et al.*, 2019). It is therefore important that users carry out convergence studies for discretisation to ensure an optimal node length.

Systems operating under natural circulation may be less stable compared to forced circulation systems (Section 2.4) and can exhibit flow instabilities and reversal. One of the more prominent experiments by Welander (1967) demonstrated that flow instabilities could occur in a single-phase natural circulation loop. Some examples of the studies that have been undertaken to test whether system codes can predict these flow instabilities include:

- Ferreri and Ambrosini (1999) showed that RELAP can predict flow instabilities however, the nodalisation and time step choices can lead to significant dampening of the instabilities seen. For the same time step, a different nodalisation scheme can lead to significant differences in the flow rate predicted in the pipework due to numerical errors associated with the solver used in the system code. It also contains advice on how to determine whether the model will predict the flow instability.

- The MTT-1 natural circulation loop (rectangular loop with heating and cooling sections at the University of Genoa) was simulated in both RELAP and CATHARE. Misale *et al.* (1999) found that the CATHARE model could predict the flow and temperature behaviour for heating powers below the stability threshold to a reasonable accuracy, but did not predict the flow instabilities seen in the experiment when the heating power exceeded the minimum threshold, while the RELAP model predicted flow instabilities at all heating powers, even when the heating power was below the threshold. This demonstrates that different codes can show different behaviours for similar scenarios as the instability is related to the solver used by the system code, although as noted previously, the nodalisation and time step can have a significant impact on the solution.
- Vijayan *et al.* (1995) used ATHLET to replicate natural circulation experiments with varying heating power for three different pipework diameters. The analysis involved modelling the experiments with either a coarse or fine nodalisation, and found that the flow instability in the experiments was not always predicted by the coarse nodalisation, and the source of the instability impacted whether finer nodalisation was required.

3.1.1.2 Limitations of Constitutive Models

Constitutive models are a key aspect of system codes, and are used to predict parameters such as interfacial heat transfer, interfacial drag, pressure losses, wall heat transfer and wall friction, based on the local flow conditions. The constitutive models are empirical or semi-empirical in nature and represent relevant interface transfer phenomena using spatial and time-averaged variables. While these models underpin the systems analysis approach, their limitations can have a significant impact on their ability to predict natural circulation (Roth and Aydogan, 2014a, Roth and Aydogan, 2014b and D'Auria, 2017):

- In general, each correlation has been developed to represent a single phenomenon using a limited set of experimental data (Volume 1, Section 4.6) usually under steady-state and fully-developed conditions, and therefore may have a limited range of applicability. Flows associated with natural circulation may deviate from these conditions, which may reduce the accuracy of the predictions and ability to predict the flow behaviour.
- The transition region between different flow regimes may not be well-defined, and each system code uses some form of interpolation technique. For typical forced circulation simulations, the impact will be small as frequent changes in the flow field are not seen. However, during natural circulation, flow oscillations can cause the flow field to change more frequently (and so the flow regime assumed will also change more frequently), and so the interpolation technique could have a larger impact.
- System codes are not extensively validated for advanced reactor designs, such as non-water cooled reactors, and so the correlations may be less developed with a narrower range of applicability.

For example, benchmarking work has indicated that RELAP5 may under-predict sub-cooled boiling at low power and low pressure (Shi *et al.*, 2018). This may affect the code's ability to predict flashing instabilities in natural circulation, and make it difficult to demonstrate that no boiling occurs in the fuel channel under natural circulation. In this case, either subchannel codes could be used

to predict flow conditions in the core, or using conservative limits derived from subchannel and system code studies could be considered.

In summary, code specific documentation should be reviewed to understand the correlations available, any known limitations of the code, and whether any correlation is being used outside its range of applicability. The example above also highlights the benefit of literature review of similar cases, particularly for complex flows such as those that occur in natural circulation.

3.1.1.3 Convergence

System codes often feature automatic procedures to optimise the time step size to provide the best convergence and accuracy. The user usually provides minimum and maximum time step size and the code then determines the optimum value dynamically and adaptively.

The solution methods employed tend to depend on the code, but most system codes employ a semi-implicit method and the choice of time step is limited by the Courant condition. In some cases (e.g. the nearly-implicit method in RELAP5-3D and 1D module in CATHARE), the need to satisfy the Courant condition is eliminated. Prior to advancing the hydrodynamic solution, the Courant limit check is carried out, and the time step size may be reduced. Due to the automatic adaptive selection of the time step size, solutions are in general insensitive to the user's choice of maximum time step size. However, the automatic procedure may not always guarantee numerical stability.

Time step sensitivity studies are recommended to ensure that the solution is not overly sensitive to the time step selection. Oscillations in the transient behaviour may be exaggerated by a finer discretisation. For example, in cases where flow reversal may be predicted within a time step, the user may need to enforce a smaller time step for accuracy.

3.1.1.4 User Effects

There are various user options when creating input files particularly for system codes (Petruzzi and D'Auria, 2008), including:

- Physical model parameters (e.g. flow multipliers for choked flow, pressure loss coefficients and separator characteristics);
- Nodalisation;
- Specific system and components (e.g. scaled facility), specialised components such as pumps, valves and separators;
- Initial conditions and boundary conditions.

While this allows code flexibility to be applied to different reactor scenarios, it can result in large variations in results from different users when applying the same code for the same reactor and postulated accident scenario. These differences are considered as user effects, and are one of the most important sources of uncertainty. Sensitivity Analysis (SA) and Uncertainty Quantification (UQ) methods (as described in Volume 4) can be used to assess and quantify the uncertainty due to user effects.

While the development of more advanced codes is supposed to reduce user effects, International Standard Problem (ISP) exercises initiated by the Committee on the Safety of Nuclear Installations (CSNI) have shown that there are still significant user effects (D'Auria, 2017). Some ways to

minimise user effects have been proposed by CSNI groups, including user training and guidelines based on validation activities and quality assurance.

3.1.2 Subchannel Analysis

Subchannel codes are primarily used to predict the core flow behaviour and the occurrence of Critical Heat Flux (CHF) in order to assess reactor operation against thermal hydraulic safety margins. The COBRA-TF family of codes are based on the two-fluid model with three fields (liquid, vapour and liquid droplets). The three-field model is shown to improve the code's capability to predict entrainment phenomena. However, other subchannel codes may employ different methods, such as the two-fluid model with two fields (i.e. liquid and vapour) and the three-equation approach (Cheng and Rao, 2015).

Similar to system codes, some subchannel codes employ flow regime maps. For example, in COBRA-TF codes, the map is divided into a normal wall region and hot wall region: the normal wall region tends to correspond to pre-CHF region, while hot wall region corresponds to post-dryout region. The flow regime in each mesh cell is determined using its fluid properties and flow conditions, and the appropriate models are selected to determine the closure terms including interfacial heat transfer, interfacial drag, wall heat transfer, wall friction and wall drag.

Subchannel codes also allow the modelling of fuel assemblies such that full-core, pincell-resolved (i.e. one row of meshes/nodes per subchannel) simulations can be carried out. Whilst subchannel codes are, in principle, multi-dimensional there are significant differences between subchannel codes and conventional CFD analysis. These differences include:

- Computational requirements: In general, the number of cells used for subchannel analysis is of the order 10^3 to 10^5. The number of cells used for CFD analysis is typically of the order 10^6 so CFD is likely to be much more computationally expensive.
- Scale: Only component scale is available in subchannel codes while CFD can model different components and scales, if required. The minimum spatial resolution of subchannel codes is fixed by the size of a subchannel (usually order of 10^{-2} m).
- Constitutive models: Subchannel codes are based on a number of empirical correlations, which reduces their accuracy (Section 3.1.2.2) and range of applicability. More complex flow behaviour can be modelled in CFD.
- Turbulence: Numerous turbulence models (e.g. RANS, LES, hybrid) are available in CFD. In subchannel codes, advanced turbulence models are not generally available. Since subchannel codes assume that the flow is axially dominant, a simple turbulent diffusion model is normally used to compute turbulent transfer of axial momentum through channel gaps.

As CFD is capable of analysing flow behaviour in fine detail (at increased computational expense), it becomes more appropriate for targeted analysis (e.g. analysing rod surface temperature for structural analysis and pressure drop for spacer grids).

3.1.2.1 Nodalisation and Discretisation

A subchannel code is often used to model domains, such as a fluid volume between rods, a lumped region of a core or a segment of downcomer. The subchannel can be viewed as a stack of mesh cells. The distribution of mesh cell length along the subchannel length can be uniform or non-uniform. If the subchannel includes a geometrical feature such as a spacer grid, a non-uniform mesh with smaller mesh cell sizes around the grid may be used (Avramova and Cuervo, 2013).

3.1.2.2 Limitations of Constitutive Models

Similar to system codes, some subchannel codes employ flow regime maps. Since subchannel codes are designed for vertical flow, it is common to exclude horizontal flow regime maps.

Some codes allow users to choose between different models, such as the friction factor correlation (including Zigrang-Sylvester, Churchill and McAdams correlations). In this case, sensitivity analyses are recommended to determine an optimal choice of model. Some of the COBRA-TF code limitations (Salko *et al.*, 2016, Avramova *et al.*, 2016) include:

- COBRA-TF based codes tend to over-predict the rate of void generation and two-phase pressure. This may indicate that some improvements are needed in the interfacial, wall friction, sub-cooled heat transfer and turbulent mixing models.
- Most codes experience difficulty in predicting void distribution near unheated regions.
- Some codes have a bias with respect to pressure; there may be a tendency to over-predict critical power at lower pressure and under-predict at higher pressure.
- Most V&V has been limited to single channel and small rod bundle configurations.
- Subchannel codes alone are not equipped to capture all local effects of spacer grids (e.g. grid enhanced heat transfer, pressure loss, vane directed cross-flow and grid-enhanced turbulent mixing). Therefore, use of CFD (or coupling between CFD and subchannel codes) may be necessary if detailed modelling of the spacer grids is required.

3.1.2.3 Convergence

As for system codes, subchannel codes generally have automatic procedures to select the time step size for convergence and accuracy. The user provides the minimum and maximum time step size and the code will determine the time step dynamically and adaptively.

In COBRA-TF based codes, there are two iteration loops per time step; the outer iteration for setting the continuity and energy equations over the entire mesh and the inner iteration for solving the pressure matrix which was created in the outer iteration. The maximum pressure change during the inner iteration is compared to the user-specified convergence criterion. If the convergence criterion is not satisfied, the code changes the time step size by taking into account the Courant limit, pressure change, void fraction change and error. It is noted that convergence issues can arise in low pressure conditions (< 4 bar).

3.2 CFD Analysis

This section considers modelling buoyancy affected flows using CFD. It builds on the more general discussion in Volume 1 (Section 4.5) and complements a number of more general sources of guidance for industrial CFD computations (e.g. industrial guidelines such as ERCOFTAC, 2000, NAFEMS, 2019, CSNI, 2015b and NAFEMS, 2003, and books such as Versteeg and Malalasekera, 2007).

As such, only aspects considered particularly relevant to passive cooling and natural convection are included. After introductory remarks, this section considers:

- The CFD approaches available, aspects of mesh generation and case definition for these approaches (Sections 3.2.2, 3.2.3 and 3.2.4 respectively).
- Specific aspects of using LES, RANS and hybrid approaches to model buoyancy affected flows (Sections 3.2.5, 3.2.6 and 3.2.7 respectively).
- Judging convergence (Section 3.2.8).

It is noted that while much of Section 2.2 is relevant to CFD analysis, Section 2.2.4 in particular discusses key aspects of theory relevant to modelling buoyancy affected flows using CFD. In general, using CFD tools to solve natural convection flow fields is relatively complex, and best performed by experienced users.

3.2.1 Introductory Remarks

As noted in Volume 1, the motivation for the development of CFD methods extends widely beyond the nuclear industry, and CFD tools are well established in the design, analysis and assessment of engineering systems across a wide range of sectors. This greatly increases the pace of development of models relevant to challenging areas (such as buoyancy affected flow) and enables engineers to use the same tools and experience to address challenges in a range of industries.

The computational cost associated with large-scale CFD means routine analysis of full passive cooling systems is likely to remain rare for at least the foreseeable future. System codes are designed for this and are often well validated for their intended use. However, buoyancy driven flows can exhibit complex behaviour even in simple geometries (Section 2.1), and closed passive cooling systems using natural circulation may exhibit unstable and transient behaviour (Section 2.4).

In this context, CFD provides a means of predicting information that could not easily be obtained otherwise (particularly full field information for unsteady or complex flows) and can provide useful comparative data for system-level or experimental analysis (especially where local 3D flow features might be expected to significantly influence overall performance). CFD may have a key role in areas like detailed design and optimisation, exploring concepts, understanding detailed flow phenomena and supporting the planning and interpreting of experimental analysis. CFD is also used to provide information that can drive the development of lower fidelity models used in system codes and can help transfer experimental findings from reduced-scale to reactor conditions. As the cost of performing CFD simulations has fallen relative to the cost of experimental analysis, many industries are doing more CFD and less experimental work.

Whilst the complexity and applicability of CFD tools is vast, CFD predictions remain only as trustworthy as the models they use and the user operating them. The models that CFD tools include for buoyancy effects may differ significantly in complexity and maturity, making the choice of model itself a complex task, requiring users competent both in the tool itself and in the underlying physics of the problem at hand. Volume 1 considers how CFD analysis might be planned, and notes that a staged approach to quality assurance is often beneficial, which is particularly true for technically complex work like the prediction of buoyancy driven flows.

3.2.2 CFD Approaches

A number of CFD approaches are available, primarily resulting from different ways of predicting turbulence, and these are introduced in Volume 1 (Section 4.5.3). The application of these approaches to buoyancy affected flows is introduced briefly below and discussed in more detail in the following sections. There are a range of approaches and plenty of variations; for NTH, engineers must make informed judgements about the complexity and fidelity of their modelling work within the context of a graded approach informed by their safety and economic case. More general NTH guidance is provided in D'Auria (2017) and CSNI (2015b).

DNS: Direct Numerical Simulation (DNS) can resolve all the length and timescales within a flow field. As discussed in Volume 1, it is considered highly accurate, but is very computationally expensive, so is predominantly used to study low Re or Gr flows in simple configurations. For buoyancy affected flows, DNS has been used to study basic scenarios such as fully-developed pipe flow with heat transfer and differentially heated cavities (Sebilleau *et al.*, 2018). The extremely detailed data that DNS can provide has then been used to develop fundamental understanding and refine the models used in other CFD approaches. This is particularly valuable for buoyancy driven flows, where experimental work is often challenging and there is often a lack of sufficiently detailed measured data to use in CFD model development. However, in view of its limited industrial use, DNS is not considered further.

LES: In LES, the Navier-Stokes equations are 'filtered', so that a proportion of the turbulence is resolved using the mesh and the remainder is modelled using a SGS model. As discussed in Volume 1, LES is much less computationally expensive than DNS and potentially more accurate than RANS, but the computational costs (which scale with Re and Gr) are still high. Within the context of a graded approach for NTH, LES is most likely to be used in areas of high safety significance or commercial impact. For passive cooling systems, LES is most likely to be used to provide comparative data to gain confidence in RANS work, or to enable more detailed analysis of particular flow phenomena.

RANS: In RANS, the instantaneous flow variables in the Navier-Stokes equations are decomposed into mean and fluctuating parts, so that the mean flow is resolved and all turbulence is modelled (lower frequency unsteadiness in the mean flow can be captured using Unsteady Reynolds-Averaged Navier-Stokes (URANS), up to a point). As discussed in Volume 1, RANS approaches are used for the vast majority of industrial CFD (including for modelling buoyancy affected flows) and are often used to support more detailed analysis methods like LES or hybrid approaches. Within the context of a graded approach for NTH, RANS is therefore likely to be used in most situations where CFD is needed, with the complexity of the modelling work reflecting the complexity

of the case and the safety significance and commercial impact associated with the work. Despite their well-known shortcomings for modelling buoyancy affected flows (which are discussed in the following sections and Section 2.2.4), RANS models can provide useful results with practical computational expense. For analysis of long plant transients containing buoyant flows, URANS is likely to be the most detailed CFD method that can be used with practical computational expense.

Hybrid Methods: Hybrid methods combine RANS with aspects of LES within the same model, to take advantages of both. As discussed in Volume 1, there are a number of significantly different approaches available (and variants within these approaches). Hybrid methods may well be useful for modelling buoyancy affected flows, which often feature unsteady free-shear or highly separated flows away from walls. Resolving turbulent length scales in some areas of the domain is likely to increase the computational expense compared to RANS, but reduce it compared to LES. Like LES, the use of hybrid approaches is increasing in industry, and their use within a graded approach for NTH sits between the points made above for RANS and LES.

3.2.3 Mesh Generation

The majority of industrial CFD calculations use a computational mesh on which the flow is solved. The mesh determines the computational domain and is fitted to the geometry of interest. Its purpose is to enable gradients in the flow variables to be resolved. The mesh can affect the results of a calculation significantly (particularly for complex buoyancy driven flows) and may be difficult to update once work has started.

Computational Domain and Geometry: These key aspects of CFD analysis are considered in Volume 1 (Section 4.5.2). Additional aspects that may be significant for buoyancy affected flows include:

- Using symmetry planes or periodicity to reduce the size of the computational domain should be approached with care. Buoyancy affected flows are often asymmetric and aperiodic (even in symmetric or periodic geometry) as a result of the intrinsically unsteady and complex flow fields (such as plumes) that may occur. Using periodicity may also not allow enough space in the domain for flow effects to form. For example, in Rayleigh-Bénard convection between two large horizontal plates, the developing convection cells may have a diameter of the order of the domain height. However, if the domain width is insufficient, these convection cells will be unduly restricted and the predicted flow field may be incorrect.
- On simplifying geometry, studies have shown (IAEA, 2014, 2013a; Groetzbach, 2002) that natural convection flow fields can be particularly sensitive to thermal disturbances caused by structures and small geometrical features where flow is locally accelerated (such as the radii of hole edges).

Meshing Background: General background on mesh types and quality is provided in Volume 1 (Section 4.5.2). More detailed guidance on creating meshes is provided in Volume 2 (Section 3.4.2). As noted in Volume 1, when a flow solution is available, the predicted flow should be visualised on top of the mesh and reviewed by an experienced CFD user who can consider whether the mesh is capable of appropriately resolving gradients that may (or perhaps should) exist in the flow.

Natural or mixed convection flows may have complex features such as plumes or areas of recirculation (Section 2.1) which will require sufficient mesh to resolve these regions of the domain. These will be in addition to other flow features which may be impacted by, or entirely unrelated to, buoyancy affects (such as boundary layers or areas of separated flow). Because of this, more mesh cells will generally be required in the interior of the domain than needed for forced convection flows, and mesh quality needs to be considered more carefully across the whole domain.

If the mesh is too coarse, flow features may not be able to develop in the solution, leading to incorrect flow predictions. For example, a plume has a shear layer around its circumference that may vary in space with time, which must be modelled to capture the flow feature. Ideally, enough mesh points are needed to model each resulting shear layer that may occur in the flow (typically at least 10 normal to the shear layer, although software specific guidance should be checked). This may be challenging for industrial geometries, but can be investigated using validation data, sensitivity studies and uncertainty quantification (Volume 1, Section 4.3). Specific aspects of meshing relevant to passive cooling systems are considered further in the following sections.

Meshing Pools and Plena: CFD is used to predict flow temperatures in pools or storage buildings, for example to check cooling flow is appropriately distributed. While pool geometries may be simple, the items stored within them may be geometrically complex. To avoid modelling these complex features, it may be appropriate to use a sub-model to predict the flow rates and temperatures associated with the heat input. Appropriate mesh is then needed both to model the heated flow entering the domain, and the resultant plumes. The resolution needed may be difficult to assess without prior knowledge, so initial calculations using periodic boundary conditions to roughly capture part of the repeating geometry may be useful. A prismatic or hexahedral mesh is likely to be helpful within the volume to avoid dissipating plume flow features.

For plena, the inflow and outflow pipework are often coupled with the plena to some extent, so it is likely to be worth extending the calculation domain down this pipework for some distance. Initial scoping calculations may be helpful to ensure that the boundary conditions are not over constraining the predicted flow. The flow within plena themselves is often complex and three-dimensional, so providing sufficient mesh in the volume and capturing the flow transitioning from the pipework to the volume are likely to be important.

Meshing Loops and Channels: For natural circulation applications, the flow in loops and channels may be as complex as pools and plena, since the flow may not be aligned with the geometry and contain flow features like plumes. Meshes therefore are likely to be finer in the volume and have smaller aspect ratios than would be normal for forced convection, to enable buoyancy-related flow features to be predicted.

3.2.4 Case Definition

Once a computational mesh has been developed, the CFD case can be configured by defining physical information and solver settings. This section focuses on the areas that may be particularly important for buoyancy affected flows and are general across CFD approaches (e.g. setting boundary conditions, fluid material properties and spatial and temporal discretisation). Turbulence and unsteadiness are also significant, and these are discussed separately in following sections. For buoyancy driven flows, the energy equation will need to be solved as well as the Navier-Stokes equations, because flow velocities and temperatures are intrinsically coupled.

Boundary Conditions: Boundary conditions define the problem being solved, so if they contain inaccurate information or are not applied correctly, it is likely the results will also be inaccurate. The application of boundary conditions in CFD tools varies, so software specific documentation should be consulted. This is particularly true for buoyancy driven flows, where flows near boundary conditions can be more complex than for forced convection flows. For buoyancy affected flows, the following aspects are particularly significant:

- Inflow and outflow boundary conditions should ideally be placed sufficiently far from areas of interest to avoid unwanted interactions (as noted in Section 3.2.3). If an inflow is fully developed, suitable profiles for flow variables could be applied from literature sources, or created (e.g. by using a sub-model or extending the domain). Where a system is connected to external or ambient conditions at both inlet and outlet (like the simple example in Figure 2.6), and those boundaries are represented by pressure conditions (rather than a specified velocity) then the solution may be harder to converge and care is needed to specify pressure correctly. The external hydrostatic variation between the two heights drives the flow, and this pressure difference should be applied. However, if the inlet and outlet are vertical planes, then a height varying pressure across the boundary would need to be specified. To avoid this, and to improve numerical convergence, CFD codes often allow an operating density to be specified, ρ_{op} and redefine the pressure field for the solution to be $P' = P - \rho_{op} g z$, where z is the co-ordinate in the direction of gravity. In this case, a zero gauge pressure can be applied to all external boundaries and the hydrostatic contribution will be included. Care should be taken not to 'double count' by applying both an operating density and a prescribed pressure difference (this is a common error).
- Inflow turbulence will need to be specified in an appropriate form for the modelling approach being used. In transitional-Re flow, such as may occur in natural convection, inflow turbulence levels can have a significant impact on results. For RANS, the values being specified can be converted into a turbulence intensity and length scale to check they are consistent with the case. For LES, the velocity specified at the inlet is necessarily unsteady and must include turbulent fluctuations. There are a number of methods to generate this 'synthetic turbulence' (most CFD codes provide at least one), but the resulting boundary conditions should be checked to ensure they have realistic statistics (see Jarrin *et al.*, 2006 and di Mare *et al.*, 2006 for further detail).
- Wall boundary conditions may have a significant impact, because they are often used to introduce heat to buoyancy driven flows. For natural circulation loops, the fluid's ability to exchange heat with solid walls, the thermal mass of these solid walls and changes in ambi-

ent temperature can affect flow stability (Basu *et al.*, 2007). In addition, even well-insulated systems may have important heat losses and axial conduction along pipework may be significant. As such, simply assuming adiabatic walls may result in incorrect behaviour. Either a uniform heat flux or uniform temperature boundary conditions are often applied, but consideration should be given to how appropriate this assumption is. For buoyancy affected flows consideration should be given to using a CHT approach that solves the solid temperatures at the same time as the flow, using a thin wall, shell conduction or fully meshed solid (Craft *et al.*, 2010). This is discussed further in Volume 2. Near-wall treatments for RANS turbulence models are considered in Section 3.2.6.

Fluid Material Properties: Fluid properties are particularly important for natural convection, as the flow is driven by changes in these properties. As such, sourcing and using properties is discussed in some detail in Section 2.3.

In order to simulate buoyancy effects, it is necessary to include gravity and variable density within a CFD model. For closed domains (i.e. there are no inflows or outflows), this needs careful consideration in order to ensure that the CFD solver conserves mass in the computational domain. If the average density in the domain is not calculated correctly each iteration, it can lead to errors in the mass conservation. Two common solutions to prevent this problem are:

1. Providing the domain with at least one inlet/outlet. In a closed natural circulation loop for example, a constant pressure boundary might be added using a small bore T-junction along the top horizontal leg, effectively mimicking a physical thermal expansion vessel (which would be present in a real loop) without having a significant impact on the flow. This boundary then allows small amounts of fluid to enter and leave the domain as needed.
2. Using the Boussinesq approximation for buoyancy. As discussed in Section 2.3.2, this approximation is valid only for small density variations and thus, for most liquids, small temperature differences. For real passive cooling systems this may not hold, so the validity of this approach should be checked before use.

Regardless of the solver, for steady-state situations, the Boussinesq approximation may well be useful in getting CFD calculations to start in a stable manner, before the approach is switched to another method once the flow field has developed from the initial guess.

Spatial and Temporal Discretisation: Discretisation errors arise as a result of replacing the continuous derivatives in the governing equations with discrete numerical approximations that can be solved. Spatial discretisation provides a numerical approximation of the flow variable derivatives, while temporal discretisation provides a numerical approximation of the time derivatives in an unsteady (also called transient or time-resolving) calculation. The magnitude of discretisation errors depend on:

- The nature of the flow.
- The nature and order of the discretisation scheme.
- For spatial discretisation, the size, quality and type of mesh employed (Section 3.2.3).
- For temporal discretisation, the time step used (Section 3.2.5 and 3.2.6.2).

Spatial discretisation errors generally manifest as an additional source of diffusion in the flow

(called 'numerical diffusion'). This can potentially dominate over real molecular or turbulent diffusion, especially where meshes are coarse. Temporal discretisation errors can cause inaccurate prediction of unsteady flows, or prevent unsteadiness from occurring entirely. Mixing and unsteadiness are often significant areas of interest for natural convection.

In general, low order schemes are likely to be more stable but cause more diffusion than higher-order schemes, and so are often used initially to stabilise and converge solutions (Section 3.2.8). For RANS, second-order accuracy is most often used (particularly for pressure and momentum fields) but first-order may be appropriate in some cases (e.g. turbulence fields). For LES, second-order or higher is often recommended (Benhamadouche, 2017). However, CFD solvers may offer a number of numerical schemes and specific documentation should be consulted for recommended settings.

Sensitivity studies considering mesh resolution (and numerical schemes) can be used to assess the impact of spatial discretisation errors if required. Likewise, sensitivity studies considering the time step (and time discretisation scheme) can be used to assess the impact of temporal errors in transient calculations. Ideally, a combined spatial-temporal sensitivity study (considering spatial and temporal aspects together) should be used, but due to the large computational expense of this it is more usual to perform a time step sensitivity study using a mesh that has been determined to provide sufficient spatial resolution. Further guidance on understanding discretisation errors can be found in ERCOFTAC (2000) and CSNI (2015b).

3.2.5 LES Aspects

LES is introduced in Sections 3.2.2 and 2.2.4.1, meshing aspects are considered in Section 3.2.3, and this section presents some advice for conducting LES work. Further details on LES methods are available in Georgiadis *et al.* (2010), Bouffanais (2010) and Meyers *et al.* (2008). Despite computational costs (discussed below) the application of LES to NTH is steadily increasing. Some industrial examples of LES include:

- T-junctions (Smith *et al.*, 2011; Höhne, 2014).
- PWR plena (Simoneau and Champigny, 2008).
- Pressurised Thermal Shock (PTS) (Loginov *et al.*, 2011).
- Rod-bundles (Mikuž and Tiselj, 2016).
- Natural convection in the primary vessel (Merzari *et al.*, 2017).

Some further examples of modelling buoyancy affected flows in the academic literature include:

- Differentially heated cavities (Ammour *et al.*, 2013; Kumar and Dewan, 2016).
- Buoyancy-aided channel flows (Duan and He, 2017; Lau *et al.*, 2012).
- Transition in natural convection (Padilla and Silveira-Neto, 2008).
- Mixed convection around large spent fuel storage cylinders (Champigny *et al.*, 2007).

Computational Cost: As noted in Section 3.2.2, the computational cost of LES is less than DNS but significantly higher than RANS. This is particularly so for high Re or Gr boundary layer flows, and because near-wall turbulence levels are coupled to surface heat transfer, the computational cost also increases as Ra increases. For natural circulation flows, the computational expense of LES is still likely to be prohibitively large for industrial calculations, limiting its use to studies of specific areas of interest.

High Performance Computing (HPC) facilities are typically required to produce LES results within reasonable time frames. Even so, the computational demands of performing properly resolved LES will likely make it unsuitable for routine large scale industrial calculations for some time. Projections in Larsson and Wang (2014) suggest that LES is unlikely to replace RANS for design and optimisation within the next 30 years at least. Hybrid approaches, considered in Section 3.2.7, may offer a useful compromise between more accurate LES and less computationally expensive RANS. In particular, Wall Modeled Large Eddy Simulation (WMLES) is so commonly used to avoid resolving turbulence near walls it is often presented as an option for LES rather than a hybrid approach. However, for long plant transients, even URANS may be impractical in some cases (Section 3.2.6).

Time Step: LES calculations are transient, so a time step is generally used by the solver. It is important that the temporal resolution should match or exceed the spatial resolution (i.e. the time step should be small enough to adequately resolve the flow as it passes through each cell). CFD software may incorporate a number of different tools to apply and vary the time step so specific documentation should be reviewed.

The time step needed (Δt) may be estimated from the mesh size using the Courant-Friedrichs Lewy (CFL) number (CFL $= U\Delta t/\Delta x$, where U is the flow speed and Δx is the cell length in the flow direction). CFL numbers of 1 or less are normally used for LES. Like the mesh size (Volume 2, Section 3.4.2.4), the time step is often estimated using an initial RANS calculation. To ensure that CFL < 1 in each cell of the LES calculation, this is normally achieved by conservatively considering a CFL ≈ 0.5 (i.e. using $\Delta t \approx \Delta x/2U_{RANS}$) to account for any differences between LES instantaneous and RANS averaged velocities, and any effects specific to the RANS solution.

Care is required when starting an unsteady LES simulation from a steady RANS solution (or changing a time step during a calculation) to ensure that a proper transient solution is achieved before starting to average the statistical data. It may take a long time for the solution to reach a statistically averageable state (Section 3.2.8), and could require a large number of residence/through-flow times (usually between 3 to 10). The residence time can be estimated using the bulk flow average velocities or locally generated streamlines (from a point, line or plane).

Sub-Grid Scale Models: A number of SGS models are available for LES, and their purpose and background are introduced in Section 2.2.4.1. As previously mentioned, although the different SGS models have their strengths and weaknesses, the prime benefit of LES arises from its ability to *resolve*, rather than model, a significant proportion of the turbulent spectrum. The main features of the flow are usually well represented and the SGS models are generally less complex and less significant to the accuracy of the simulation than RANS turbulence models. Some common SGS models are introduced in Section 2.2.4.1. To summarise:

- The Smagorinsky model is regarded as simple and robust, but in view of its limitations the

Dynamic Smagorinsky model is generally preferred. However, while this does not require the Smagorinsky coefficient to be specified in advance, it inherits the weaknesses of the more basic model.

- The WALE model is also straightforward, but provides better modelling near walls and in regions of laminar flow. As such, the WALE model is more likely to be used for the wall-bounded or low *Re* flows associated with natural circulation.

Other SGS models may be available in specific CFD software, so software-specific documentation should be consulted for guidance. It is noted that WMLES and similar hybrid approaches (introduced in Volume 1 and discussed in Section 3.2.7) may be presented in a similar manner to an SGS model in software documentation, as these approaches are commonly used in industrial LES calculations to overcome onerous near-wall meshing requirements (discussed in Section 3.2.3), particularly where *Re* is not low.

Transition: It is possible to have fully-turbulent, transitional and laminar regions present within the same buoyancy-driven flow field, and this may or may not have a significant impact on the accuracy of CFD predictions. There are also a number of different transition mechanisms (Section 2.2.3). As a result, predicting laminar-turbulent transition using CFD is important, but complex, and an active research area. LES can be used to predict transition, but is likely to be too expensive to be used for this purpose for most industrial applications for some time. While the cost of LES calculations is lower than DNS, the predicted flow behaviour is likely to be sensitive to the performance of the SGS model and the detailed specification of upstream turbulence (which can be difficult to obtain in industrial contexts).

3.2.6 RANS Aspects

RANS is introduced in Sections 3.2.2 and 2.2.4.2, and meshing aspects are considered in Section 3.2.3. This section presents some advice for conducting RANS modelling work.

3.2.6.1 Steady and Unsteady RANS

One of the key aspects of RANS is the ability to run models as either steady-state (RANS) or unsteady (URANS). While turbulent flows are, strictly, always unsteady (due to turbulent fluctuations in flow quantities), large-scale unsteady motion can also arise from non-turbulence phenomena[1] or be imposed externally by boundary conditions which vary in time. This large-scale 'coherent' unsteadiness is often also present in laminar flows and can be considered distinct from the unsteady small-scale 'incoherent' unsteadiness typically associated with turbulence.

URANS methods exploit the above distinction by solving a form of the RANS equations which retain the time-derivative term. Large-scale low frequency unsteadiness is then resolved, and turbulence is modelled using the same models as steady RANS (for example, moving plume structures may be predicted that provide a mixing mechanism in addition to that provided by turbulence). This approach is well established and has been applied successfully to many flows involving buoyancy (Ammour *et al.*, 2013; Kenjereš and Hanjalić, 1999; Wilson *et al.*, 2015), and has been extensively reviewed (Benhamadouche, 2017; Kenjereš and Hanjalić, 2009; Speziale, 1998).

[1] Such as plumes, periodic vortex shedding behind a bluff body, flows subject to system rotation, or the convective roll cells that develop in Rayleigh-Bénard convection.

Steady-state calculations account for the majority of engineering analysis, but must be used with care for buoyancy affected flows because, like the plume rising from a cup of tea, natural and mixed convection flow fields are often unsteady even with steady boundary conditions (Section 2.4). Obtaining a converged steady solution where flows are unsteady in reality may be possible (Section 3.2.8), but the predicted flow fields may not be meaningful, or depend on the number of iterations and applied under-relaxation parameters. Therefore, **a steady RANS solution may not give the same results as a long-term time-averaged URANS solution.**

Moving from RANS to URANS can result in significantly different flow field predictions (Figure 3.1). If RANS and URANS predicted flow fields are the same, this may suggest that the real flow is broadly steady.

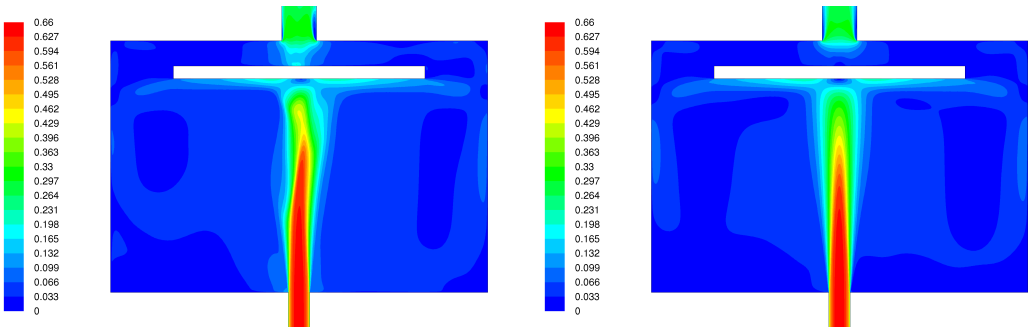

a) Steady RANS b) Time-averaged URANS

Figure 3.1: Example of impinging jet, RANS vs URANS (Contours of velocity magnitude (m/s) in TALL-3D test section from Study A).

URANS provides a statistical representation of the flow as it evolves in time. It will not provide a time-exact reproduction of the flow that might be otherwise obtained with experimental, or even higher fidelity (LES, DNS) numerical, methods. In particular, caution should be used in interpreting coherent structures predicted in URANS (Benhamadouche, 2017). This should be considered if comparing URANS with LES or DNS. Some additional aspects of using URANS are:

- Unlike LES, contributions from the turbulence model are not tied to the mesh-size and thus decreasing the mesh-sizing will not enable additional, turbulent, motions to be captured. This means that it is possible to obtain a truly mesh-independent solution using URANS methods.
- Often, unsteadiness arises from instabilities in the flow which subsequently develop into coherent motion. As turbulence is, however, principally a dissipative phenomenon, a turbulence model which is overly dissipative may prevent these instabilities from developing in the first place, suppressing unsteady motion. Generally, turbulence models which are less dissipative (typically those able to account for some level of anisotropy, so RSMs or non-linear EVMs) will be better at reproducing unsteady behaviour. This point reveals a subtlety with URANS; whilst the turbulence model is only responsible for modelling incoherent turbulent motion, a change in turbulence model may enable previously damped out unsteady coherent motion to be subsequently captured.
- URANS assumes there is scale separation between the turbulent fluctuations and unsteady coherent motions[2]. As the frequency of the coherent motion increases, the distinction be-

[2] This implies an assumption that the temporal average of the turbulent quantities is not affected by the global unsteadiness.

tween what constitutes coherent motion and what constitutes turbulent fluctuations can become more difficult to discern. In such cases it may still be possible to obtain a converged solution, so care is required when interpreting results. In buoyancy driven flows, where plumes and large-scale roll cells may interact with both highly turbulent and laminar regions within the same flow, this distinction can be difficult to ascertain without analysis.

As noted in Volume 1, for many decades URANS is likely to be the only practical CFD method for predicting long duration problems such as reactor shut-down transients (which may extend over several hours and include buoyancy affected flows). Given the points on unsteadiness noted above, URANS may well be the most appropriate method for solving natural convection flow fields. However, it is more complex than using RANS, and this should be considered when the approach to Verification, Validation and Uncertainty Quantification (VVUQ) is developed. Further details surrounding the meaning and interpretation of URANS methods can be found in Spalart (2000).

3.2.6.2 Time Step

If transient data is required from a URANS solution, a time step is normally specified[3]. The choice of time step will depend on the timescales present in the flow, and can have a significant impact on results. Identifying and estimating these timescales normally requires engineering judgement, but the below considerations may be helpful:

- Explicit solvers generally need $\mathrm{CFL}_{max} \approx 1$, while implicit solvers are usually less sensitive to numerical instability and so larger CFL values may be acceptable. Recommended values for CFL numbers are often provided in specific documentation for CFD software (and are particularly important for explicit methods).
- For features or regions within the computational domain, a time step may be derived using $\Delta t = t/N$ where N is an appropriate number of time steps to resolve motions on an estimated characteristic timescale (t). The number of time steps required is likely to depend on the numerical scheme (and number of iterations per physical time step for implicit schemes), so software-specific documentation should be consulted. Methods for estimating a characteristic timescale include:
  - For transient developing flows (e.g. a jet starting across a volume), it may be appropriate to use a characteristic flow velocity (e.g. the jet velocity) and the length over which the flow is expected to develop.
  - For buoyant flows (High Ra number), it may be appropriate to use a buoyancy-driven reference velocity $t = L/U = L/\sqrt{g\beta\Delta T L}$, where g is acceleration due to gravity, β is thermal expansion coefficient, ΔT is a characteristic temperature difference and L is a characteristic length scale consistent with this temperature difference.
  - For unsteady flows, it may be appropriate to estimate the expected flow oscillation frequency using the Strouhal number (Sr), and hence the timescales for vortex shedding.
  - For analysis supporting experimental work, it may be appropriate to estimate a time step based on experimental results.

[3] Some solvers may provide methods of obtaining time-averaged flow fields without a time step, but such results may not be helpful in understanding an unsteady buoyant flow field (for example switching behaviour between two states).

- Where aspects such as the boundary conditions, parameters or geometry are changing through time, a time step might be also be defined by $\Delta t = t/N$ where N is a number of time steps needed to capture the given change occurring over a timescale t.

Ideally, the chosen time step would be the smallest value predicted for the various aspects identified. However, this may not always be possible due to the number of time steps that would be needed (e.g. if the smallest timescales are of the order of tenths of seconds but overall plant transient timescales last for weeks) leading to a judgement about what timescale can be used. In some cases, it may be appropriate to use a system code to predict the plant transient behaviour, with a CFD calculation performed assuming conditions are quasi-steady-state at key points through the transient, or to train a correlation or sub-model using a number of CFD studies to build into the system code directly (Volume 2, Section 3.1).

A time step sensitivity study should be performed to ensure that the chosen time step is appropriate for the case. Unlike LES or DNS, a URANS solution can, in principle, be independent of time step (as well as mesh-size). Starting an unsteady solution or changing the time step during a solution must be done with care, and like LES the time taken for the solution to reach a statistically averageable state should be considered (Section 3.2.8). Other considerations may be needed for solids in CHT cases (Volume 2, Section 3.4.5).

3.2.6.3 Turbulence Models

As introduced in Volume 1, turbulence modelling is a key aspect of the RANS approach. It is generally accepted that a 'universal' turbulence model ideal for all flows does not exist. However, turbulence modelling for single-phase CFD has matured to the point where reasonably reliable and good results can be obtained for a wide range of engineering applications with current computers.

The choice of turbulence model should be made on a case by case basis, and is likely to involve aspects such as common practice, user experience, sensitivity studies, validation data, computational resources, implementations within the CFD tools being used, as well as the technical aspects of the models themselves. A number of common models and their technical background are introduced in Section 2.2.4.3. For buoyancy affected flows, either a two-equation linear EVM (probably a variety of k-ε model or the k-ω SST model) or a variety of RSM is likely to be chosen, although they are likely to be challenged by buoyancy affected flows. More details on using these models are provided in the following sections.

The implementation of turbulence models in CFD tools can vary, so it is always necessary to consult software specific documentation (e.g. user/modelling/theory guides) for detailed information on the configuration and use of the modelling approaches offered. A number model variants are normally offered, and complexity in turbulence modelling is such that a variant that works well in some scenarios may fail in others in ways that can be difficult to predict. This is partly why VVUQ, which is introduced in Volume 1 (Section 4.3) and discussed in Volume 4, is a key part of industrial CFD.

Turbulence models are empirically calibrated to a wide range of flows by the developer, which may or may not be directly applicable to a given case. However, recalibrating turbulence model coefficients needs great care because it is possible to void the original calibration, cause unintended or unphysical behaviour, mask unrelated modelling deficiencies and lose the ability to compare

results with other work. Such recalibration would need detailed validation (e.g. using detailed experiments and/or DNS) and may therefore be very expensive. However, some turbulence models (such as the GEKO model, Section 2.2.4.3) provide additional parameters that enable tuning within controlled bounds. While this may offer benefits in some flow regimes, these parameters should be used with caution as these models are fairly new and have little published application to buoyancy affected flows.

In summary, particularly for buoyancy affected flows, the turbulence modelling approach chosen will be dependent on the individual case, software-specific documents should be consulted, and sensitivity to different modelling approaches may be tested as part of VVUQ.

k-ε and k-ω: These two-equation linear EVMs are by far the most commonly used models in industrial CFD, and are widely used in NTH applications. They are simple to use and computationally affordable. They may be particularly challenged by natural or mixed convection flows (Section 2.2.4.3), but given their well-known limitations it can be surprising how well they perform in complex industrial cases, including mixed and natural convection. Global quantities, such as pressure drops, mass flow rates, bulk temperatures and averaged Nusselt numbers etc., can be reliable (Benhamadouche, 2017), although some turbulence quantities are likely to be less accurate. Whether this is acceptable or not will depend largely on the application. Where more complex models are used (such as RSM or LES), these models are often helpful to gain initial solutions. More advanced EVMs have been proposed (Section 2.2.4.3) but are little used. Example uses of two-equation linear EVMs include:

- Vertical mixed convection flows (Cotton and Jackson, 1990; Keshmiri *et al.*, 2012, 2008).
- Natural convection in enclosures (Altaç and Uğurlubilek, 2016; Hsieh and Lien, 2004; Miroshnichenko and Sheremet, 2018).
- Differentially heated cavities (Omranian *et al.*, 2014; Rathore and Das, 2016).
- Natural circulation loops (Naphade *et al.*, 2013; Wang *et al.*, 2013; Kudariyawar *et al.*, 2016).
- Ribbed passages with heat transfer (Keshmiri *et al.*, 2016).
- Lower core of a PWR (Fournier *et al.*, 2007).
- Reactor cavity of modular HTGR (Zhao *et al.*, 2017).
- Passive residual heat removal heat exchanger (Ge *et al.*, 2018; Zhang *et al.*, 2015).
- Internally heated melt pools (Mao *et al.*, 2018).
- Heat transfer due to impinging jets (Craft *et al.*, 1993; Sharif and Mothe, 2009).
- Buoyant plumes (Kumar and Dewan, 2014; Macpherson and Tunstall, 2020).

k-ε: It can be difficult to choose between the three main variants in this family of models. In principle, RNG or Realizable should be at least as accurate as the standard k-ε model for many applications. However, mixed results have been reported in the literature for buoyancy affected flows and thus neither variant provides a clear and consistent advantage over the standard or low-Re, form of the k-ε model (Chen, 1995; Faheem *et al.*, 2016; Grassi and Testi, 2007). In fact, the low-Re form of the standard model (Launder and Sharma, 1974) has demonstrated reasonably good performance in predicting heat transfer in several buoyancy influenced flows, including vertical mixed convection (Keshmiri *et al.*, 2008) and differentially heated cavities (Ince and Launder, 1989; Omranian *et al.*, 2014). Further comparisons of various low Reynolds k-ε models can be found in Costa *et al.* (1999).

***k*-ω:** The k-ω SST model is the most popular variant of this family of models. It has proved successful in a number of situations, including external aerodynamic and internal wall-bounded flows with adverse pressure gradients. Less attention has been paid to understanding its use and reliability in buoyancy affected flows compared with k-ε models, which might arguably reduce confidence, although good results have been reported for wall-bounded plumes (Macpherson and Tunstall, 2020).

RSM: Despite providing a more sound theoretical basis for modelling than EVMs (Section 2.2.4.3), RSMs have not been as widely used in industrial CFD as once anticipated. A variety of factors are thought to contribute towards this, including the increased number of coupled equations reducing numerical stability and increasing computational cost. Some early studies may have been compromised by low mesh resolution making it hard to differentiate between model performance and numerical errors (Benhamadouche, 2017). However, a number of more recent studies have demonstrated clear improvements:

- PWR primary loops: Bellet and Benhamadouche (2011) showed that even advanced EVMs (such as the v^2-f model) predicted the tangential velocity profile in a confined vortex tube poorly compared with the SSG RSM.
- Inclined heated cavities: In an unstable configuration, Omranian *et al.* (2014) demonstrated many models, including EVMs, could return reasonable results since the flow is dominated by large-scale unsteady roll cells. However, in a stable configuration, a RSM together with advanced wall functions was needed to capture the subtle secondary flows present in the measured flow field.
- Buoyancy driven counter-current flow within a pipe: EBRSM was used by Sebilleau *et al.* (2016) to predict buoyancy driven counter-current flow, demonstrating improvements over both k-ε and k-ω linear EVMs.
- PWR plenum: Martinez and Alvarez (2009) demonstrated that secondary motions are well-captured by a RSM once a fine enough grid is employed to adequately represent the intricate geometric details.

Since RSMs may be less numerically stable than EVMs (especially when starting from relatively unrealistic initial conditions), it is often useful to start the calculation with an EVM before switching to a RSM when the predicted flow is more realistic. RSMs are also more sensitive to discretisation errors than EVMs (Benhamadouche, 2015), so a fine mesh and at least second-order discretisation scheme may be needed (see Section 3.2.4). First-order schemes may, however, improve numerical stability at the start of the calculation.

Code documentation should be checked to ensure buoyancy effects are properly included, as this can be inconsistent[4]. In addition, not all RSMs are valid within the near-wall region, so documentation should be checked to ensure that models are compatible with the near-wall modelling approach chosen.

[4] In one commercial code, buoyancy effects are included with an ε-based RSM but cannot be included with an ω-based RSM.

3.2.6.4 Near Wall Modelling

For natural convection, the modelling of the near-wall region can have a significant impact on model predictions. As introduced in Volume 1 (Section 4.5.3), RANS near-wall modelling approaches typically include wall resolving (low-Re, fine mesh, small y^+), standard wall functions (high-Re, coarser mesh, larger y^+), enhanced wall functions (CFD code tailors approach to local y^+) and advanced wall functions (more complex models catering for non-equilibrium conditions), although the terms used and detailed implementations may vary between CFD software.

A wall resolving approach is likely to provide more accurate solutions than a standard wall function approach for buoyant flows (see below). In addition, natural convection usually results in much lower flow rates than in forced convection, and thus the computational cost of a wall resolving approach may be reduced. However, in many industrial contexts, obtaining a mesh to provide a small enough y^+ across the whole domain for a wall resolving approach is likely to be difficult and lead to unnecessary computational expense. Therefore, an enhanced wall function approach is often used in industry, with the mesh designed to enable near-wall flows to be resolved in key areas and wall functions used elsewhere. Developing a mesh to enable this is considered in Volume 2 (Section 3.4.2), which considers near-wall meshing generally.

If a wall-resolving approach is used (either on its own or through enhanced wall functions), the turbulence model must be valid for use in the near-wall region. ω-based models are valid near walls, but low-Re versions that improve near-wall predictions may be available. Many original ε-based models are not valid near walls, but many low-Re extensions exist (such as Launder and Sharma, 1974) and are widely used. Some low-Re turbulence models may use functions based on wall distance, which may be a problem in complex geometries (wall distances may be hard to define). Other options (e.g. based on turbulent Re) could be considered if available.

Standard wall functions based on the logarithmic law-of-the-wall should be used with care, as they were developed for fully-developed flows subjected to simple shear, with the near-wall region in local equilibrium. This is highly unlikely to be true in buoyancy-driven boundary layers, where turbulence creation and destruction rates are far from balanced and transport effects may be substantial. These limitations are also shared by the corresponding formula for the thermal field. Standard wall functions may therefore cause significant errors in natural or mixed convection flows, especially where transition might be expected.

A number of advanced wall functions have been developed to account for buoyancy effects (see, for example Craft *et al.*, 2002), which have shown good performance in natural and mixed convection flows (Craft *et al.*, 2006; Omranian *et al.*, 2014). Extensions to account for the effects of rough walls have also been published (Suga *et al.*, 2006). However, these are not currently widely available in commercial CFD solvers.

3.2.6.5 Turbulent Heat Transfer Models

The modelling of turbulent heat fluxes can have a large impact on predictions of buoyant turbulent flows because it can directly affect surface heat fluxes and mean temperature profiles[5]. The choice of model will largely depend on the approach used to model the Reynolds stresses, since these

[5] This is analogous to the impact of Reynolds stresses on the mean velocity profile.

appear directly in most advanced turbulent heat flux models[6]. CFD software codes may have limited models/options available, and so the code documentation should be checked. A number of models are introduced in Section 2.2.4.4 and their use is discussed below:

- If a linear EVM is used for the Reynolds stresses, there is generally little benefit in using more advanced models than the SGDH, although a modified version of the GGDH has been used with success in natural convection (Ince and Launder, 1989). SGDH is best suited to simple forced or mixed convection flows (where only the cross-stream component of the turbulent heat fluxes is significant) and is therefore likely to struggle in more complex natural convection flows (Kenjereš and Hanjalić, 1999).
- The GGDH is likely to be the simplest approach used with a turbulence model capable of reliably predicting individual Reynolds stresses (i.e. a non-linear EVM or RSM). Even then, its implementation in CFD codes may be simplified to improve numerical robustness.
- DFMs will normally only be used with RSMs and for specialist work due to the large increase in cost and numerical stiffness (four or five extra transport equations in 3D).

Further guidance is provided in Hanjalić (2002) and Kays (1994).

3.2.6.6 Transition

Turbulent to Laminar: High-*Re* RANS models are calibrated for fully-turbulent flows and thus usually cannot take account of the viscous effects which lead to laminarisation. However, the modifications included in some low-*Re* models mean that these are capable of (and often quite successful in) capturing laminarisation. For the differentially heated cavity discussed in Section 2.2.3, low-*Re* k-ε models may well predict laminarisation as a result of these modifications, although the physical mechanisms are not modelled.

Laminar to Turbulent: This poses a significant challenge for many RANS based methods. Whilst they cannot inherently predict natural transition (since the instabilities which cause it are averaged out), some low-*Re* models have shown limited success in modelling bypass or separated transition (Menter *et al.*, 2006). Transition specific models (such as k-ω SST γ) introduce additional variables (i.e. turbulence intermittency) to improve the accuracy of transition prediction. However, these models are generally developed for predicting transition in classic boundary layers not in other wall-bounded flows, free-shear flows or fully developed pipe flows. Further, they may only be designed to predict certain transition mechanisms (e.g. bypass transition, Section 2.2.3) and may not be calibrated to predict transition in buoyant flows.

These are clearly significant limitations for predicting transition in natural convection flow fields. These models should be approached with caution, particularly if transition is not clearly expected based on local geometry or flow features, or good quality validation data from a well understood system is not available. The existence of transition within a flow should be anticipated through consideration of the governing non-dimensional parameters and examination of any relevant experimental data. Approaches which use standard wall functions will not be able to accurately predict laminar-turbulent transition, and a low-*Re* approach is recommended as a minimum.

[6] More advanced models are unlikely to provide a benefit if the turbulence model cannot provide appropriately reliable Reynolds stresses.

A RANS/URANS simulation that has become fully laminar because of a lack of turbulence production (by mean strain or otherwise), cannot subsequently become turbulent, even if those production mechanisms do later become significant[7]. However, if only part of the flow laminarises, turbulence may be convected from other parts of the domain if the flow field allows. As a result of this, if the velocity field must be initialised at zero when modelling a buoyancy driven flow, the fields representing the turbulence (e.g. k, ε, ω) should be initialised at such levels that turbulence does not completely decay before buoyant motions (i.e. mechanisms that generate turbulence) develop and subsequently sustain the turbulence.

3.2.7 Hybrid Approaches

There are many hybrid approaches available with various names that may require different meshes with different strengths and weaknesses, settings to use and subtleties in results interpretation. Some common approaches are introduced in Volume 1, including WMLES, Zonal or Embedded LES, the many variants of Detached Eddy Simulation (DES) and Scale-Adaptive Simulation (SAS) (Figure 3.2). There is no 'ideal' approach for all situations, and the best approach to use is likely to be application and software specific. It is therefore necessary to obtain a detailed understanding of the approaches available within a given software before using them.

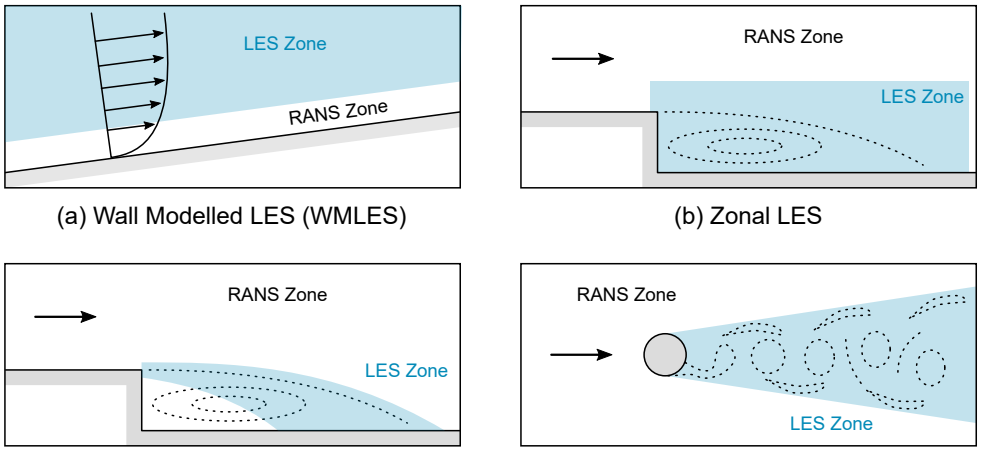

(a) Wall Modelled LES (WMLES)

(b) Zonal LES

(c) Detached Eddy Simulation

(d) Scale Adaptive Simulation

Figure 3.2: The main hybrid methods.

Broadly however, some areas of the computational domain are likely to be solved using a turbulence resolving approach (often LES) and remaining areas solved using RANS, with flow information passed between the two. As such, much of the discussion provided in previous sections can be considered for the relevant part of the domain and flow solution. Specific to hybrid approaches:

- It is necessary to understand where in the domain the scale resolving method is needed, so that the mesh can be tailored appropriately. This can be particularly difficult to assess for buoyancy affected flows without a flow solution, so an initial RANS solution may help identify areas to use scale resolving methods and support mesh sizing (Section 3.2.3) and

[7] Because the mathematical form of the production term, which is exact, contains the Reynolds-stresses themselves. Thus even if the mean velocity gradients later become significant they will be multiplied by the current (zero) value of the Reynolds stresses. Terms representing buoyancy generation are similarly affected, since they contain the turbulent heat fluxes.

selecting an appropriate time step (Section 3.2.5). Tailoring the mesh and time step to the flow is particularly important for LES approaches, such as WMLES, Zonal LES or DES. SAS may offer more flexibility on mesh sizing than more traditional LES-based methods, depending on the level of detailed flow information required. As the details are model dependent, software-specific advice should be consulted. When a flow solution is available, this can be interrogated to check that the solver is being used correctly and consistently with the mesh.

- A key feature of many hybrid approaches is that information is passed between scale-resolving methods (often LES-like) and non-scale resolving methods (often RANS-like). This is particularly significant for turbulence information, and is often a key difference between approaches (particularly for DES variants) so it is necessary to understand how this is managed by consulting software-specific advice. It may be possible to apply synthetic turbulence at the inflow to LES aspects of the flow. This should be considered if the inflow is turbulent and it is appropriate to the models being used (consult software-specific advice). If used, it is normally necessary for the mesh resolution to be of LES quality to ensure this turbulence is transported properly. When a flow solution is available the performance of the solver and mesh around these interfaces can be considered.
- WMLES is commonly used in industrial LES to reduce mesh requirements near walls (Section 3.2.3), and is often necessary unless Re is low. It may be possible to use this for the scale-resolving parts of other hybrid approaches as well; some approaches may need to use WMLES to obtain correct behaviour near walls (consult software-specific advice).

Significant development of hybrid approaches is continuing, partly driven by large-scale projects (such as the European Union DESider project, Haase *et al.*, 2009). Gritskevich *et al.* (2014) applied a number of different approaches to the OECD/NEA Vattenfall T-junction benchmark test case (Smith *et al.*, 2011), including SAS, Delayed Detached Eddy Simulation (DDES) and Embedded LES (ELES). These models were able to accurately predict velocity profiles, although SAS results were more sensitive to settings than for DDES and ELES. However, the application of these methods to buoyancy driven flows is much more limited (Kenjereš and Hanjalić, 2006; Ding *et al.*, 2019; Kocutar *et al.*, 2015) so there is less guidance available.

While hybrid approaches may offer improved predictions, they are still relatively new and thus do not currently have the benefit of decades of extensive use associated with RANS (or pure LES). It is therefore appropriate to be cautious when using these methods, especially for flows strongly affected by buoyancy. Software-specific documentation (such as Menter, 2015) should be reviewed to gain a good understanding of the limitations associated with the specific model chosen. Further general advice can be found in Fröhlich and von Terzi (2008), D'Auria (2017) and a review by Holgate *et al.* (2019) provides details on recent advances.

3.2.8 Convergence

CFD calculations are generally iterated until the predicted flow field is considered converged (i.e. further iterations would give little benefit). There is no universal way of assessing convergence, and it may be particularly difficult to assess for complex flows affected by buoyancy. As such, experienced engineering judgement is often important, based on appropriate metrics. The metrics chosen are usually case-specific, but will typically include monitoring the detailed flow variables and consideration of residuals as well reviewing the predicted flow field itself (including checking

that the mesh is appropriate to resolve gradients in flow variables, Section 3.2.3). For unsteady calculations, locations where significant unsteady flow occurs are often visualised over a number of time steps to check that the time step is sufficient.

Monitors: Relevant flow variables should generally be monitored at key locations in the flow. These point monitors should be placed using engineering judgement (e.g. in locations considered particularly important, or where strong variation in flow variables is expected). Integral monitors are also used to monitor variables such as mass flows or average temperatures across a surface. Both the value and behaviour of the monitored quantities should be considered in the light of engineering judgement and intuitive insight on expected behaviours. For point monitors, this might include comparing the steady-state values with expected behaviour, studying the nature of any oscillations and calculations of moving averages. For integral monitors, this might include checking mass and energy conservation through boundary conditions and within the domain.

For steady-state calculations, the solution should be advanced until values no longer change with further iterations. It is noted that unchanging variables at monitor locations do not provide any indication of solution accuracy or that the solution has necessarily converged, only that further iteration may not change the monitor value (situations where this may be significant include CHT cases, or where under-relaxation is used heavily). In a complex case, it is likely that a large number of monitors will be needed (different flow variables at different points in the flow).

For unsteady calculations, the simulation must be solved for a sufficient number of time steps in order to reach a statistically averageable state before generating any required statistical data. However, areas with relatively slow moving flow (such as are likely to occur in passive cooling systems) may take 3 to 10 residence times through the domain to reach an acceptable solution. This should be confirmed using monitors that should be located where key quantities are expected to vary the most, and may also support judgements on whether the time step used is suitable. For scale-resolving simulations (such as hybrid methods or LES), the mean flow parameters may converge more quickly than fluctuating parameters (such as the Reynolds stresses), which should be considered when choosing monitor variables.

Residuals: Residuals are often scaled or normalised by physical quantities associated with the flow to make them more physically meaningful. Most CFD software does this automatically, but specific documentation should be consulted to ascertain their meaning and presentation before using them to judge convergence. In general, a reduction of at least three or four decimal orders of magnitude is often sought, although this may depend on how good the initial guess of the flow field used to initialise the calculation is (a good initial guess may be associated with smaller residual reductions, while a poor one may be associated with larger residual reductions). The behaviour of the residuals throughout the solution process should be monitored to ensure that they do not start to increase, which may indicate that the calculation is diverging. While residuals are easy to obtain and review, it is very unlikely that simply checking them will enable an adequate judgement on convergence, particularly for buoyancy affected flows. Flow quantities (local, integral or most likely both) should always be monitored in tandem with residuals.

Convergence Problems: Fixing convergence problems is normally case specific. The case should be checked (if not done already) to ensure it has been configured appropriately and consistently. The relationship between the predicted flow field and local aspects of the case such as the geometry, mesh and boundary conditions can be investigated, and many CFD solvers enable the location of maximum residual to be plotted to aid this. Often problems can result from the mesh (perhaps as a result of the relationship between local mesh quality and flow variable gradients) or from inconsistencies in boundary conditions (usually between inlet and outlet). For steady-state RANS calculations, difficulty in obtaining convergence may indicate that the real flow is unsteady[8]. Switching to a URANS approach may allow the numerical method to capture unsteadiness in the mean flow variables and improve convergence (Section 3.2.6.1). For unsteady calculations, using a smaller time step (or solving more iterations per time step in iterative schemes) may be useful.

In addition, first-order schemes and under-relaxation parameters within the CFD software can be used to enable the flow to converge initially, by reducing them from their default values. However, once the flow has stabilised, the flow should ideally be converged using second-order schemes with the under-relaxation parameters set to their default values. This is particularly true for the energy equation as the temperatures may still be changing (just extremely slowly), even though the residuals/monitors appear converged.

3.3 Experimental Methods

The role of experimental methods in NTH analysis and the value of experimental and modelling teams working together closely is introduced in Volume 1 (Section 4). This section builds on this, discussing flow rate and velocity measurements that might be used in passive cooling experiments, while temperature measurements are discussed in Volume 2 (Section 3.5). Flow visualisation and two-phase flow measurement techniques are discussed in Frazer-Nash (2019).

3.3.1 Scaling

As noted in Volume 1 (Section 4.6.5), it is rarely possible to perform experimental analysis of test rigs built to full scale, so some scaling is needed to ensure that the phenomena and performance seen in the experimental rig is representative of the full scale plant. This scaling may be challenging for passive cooling systems, as a result of the potentially large number of parameters that influence the performance of the system. A detailed introduction to scaling is provided by CSNI (2017).

A detailed example of scaling for natural circulation is provided by Reyes and Hochreiter (1998), using a Hierarchical 2-Tiered Scaling (H2TS) approach to design an 'ideally scaled' Integral Effect Test (IET) facility to study natural convection. The Advanced Plant EXperiment (APEX) test facility was designed on the basis of this scaling analysis to provide a geometric representation of the Westinghouse AP600 nuclear steam supply system.

The H2TS scaling approach was developed by Zuber (1991) to provide a comprehensive scaling approach that reduced the reliance on judgement to define scaling requirements, and consists of four stages: system breakdown, scale identification, top-down scaling analysis and bottom-up

[8] Especially if residuals, or monitors, appear to oscillate, although the frequency content of such oscillations may be meaningless as the solver is not necessarily time-accurate.

scaling analysis. It was intended to be widely applicable to engineering tests for the purposes of code validation and aligns the test priorities with the complex applicability structure of analysis codes.

H2TS has been widely adopted for the design of more recent IET facilities and has been considered successful, primarily due to the comprehensive and auditable nature of the approach. As scaling distortions are inevitable for complex systems, the quantification of uncertainties resulting from scaling effects is a key consideration within the United States Nuclear Regulatory Commission (US NRC) Evaluation Methodology Development and Application Process (EMDAP) and as part of a Best Estimate Plus Uncertainty (BEPU) approach.

Another example of scaling for natural circulation is provided by Ishii (2016), using a three-level scaling approach to design an 'ideally scaled' IET facility to study natural convection. This approach considers firstly a global scaling analysis based on dimensionless numbers; secondly a scaling analysis based on the main system components and the interfaces between them; and thirdly analysis based on local phenomena. The 'engineering scaled' facility is then designed to approach the 'ideally scaled' facility as closely as possible, taking into account practical engineering constraints (such as standard sizes of pipework and safety-related pressure limits that might apply to test environments). System codes are also used to predict the overall performance in both facilities under steady-state conditions, to improve confidence in the overall scaling and to demonstrate matching with other facilities considered representative of a real PWR design.

While developing detailed scaling to provide performance data may be complex, the overall qualitative behaviour of the flow in systems may not be greatly affected by the scale of the testing facility. For example, Schultz *et al.* (1987) reviews work on a number of PWR natural circulation rigs and observes similar overall system performance and detailed steam generator flows, despite the tests being at a large range of scales.

3.3.2 Integral Measurements

Integral measurements include the mass flow rate, temperature differences across any heat exchangers and also spot temperature measurements at key locations within the system. These measurements are often used to understand the system performance as a whole and provide data to compare with system analysis (Section 3.1).

Two key measurements required for assessing the performance of a passive cooling system are the mass flow rate and heat transfer rates of the heat exchangers (i.e. heater or cooler):

- Sensitivity of natural circulation flows to disturbances mean that instrumentation should be as non-invasive as possible. This needs particular consideration for measuring the flow rate (Section 3.3.2.1), since conventional flow meters or orifice plates are likely to have a significant impact on the flow. Low impact methods include Doppler shift ultrasonic or electromagnetic flow meters, alternatively the flow rate can be deduced by measuring the pressure drop across particular sections of the loop using pressure transducers (e.g. over a horizontal leg or between the inlet and outlet of a heat exchanger).
- For heat transfer measurements, both the heater and cooler heat flux should be quantified if possible. Probes should be positioned to provide information about both local behaviour (e.g.

inlet and outlet of heater) and the global system behaviour (at enough positions to provide a reasonable measure of, for example, the loop fluid temperature).

3.3.2.1 Flow Rate Measurement Techniques

A number of common measurement methods are summarised below. It is worth noting that many flow measurement techniques, particularly non-intrusive methods, rely on an assumption that the flow is fully developed. This normally requires at least an $L/D > 10$ from an inlet or bend, and may need an $L/D = 100$ for the flow to be really fully developed (Klein, 1981). This may not be met in a real plant situation, increasing the uncertainty of the measurements.

Orifice Plate: An orifice plate is a thin metal disc containing one or more holes, which is inserted into the pipe carrying the flow (LaNasa and Upp, 2014). Flow is restricted by the hole which introduces a differential pressure across the orifice. The upstream and downstream pressures are measured using a differential pressure gauge, and a calibrated pressure loss coefficient is applied to calculate the flow rate. Orifice plates are a simple, cheap and widely used method for measuring volumetric flow rate. However, measurement inaccuracy is typically $\pm 2\,\%$, but can reach as high as $\pm 5\,\%$ (LaNasa and Upp, 2014).

Coriolis Flow Meters: These are typically used to measure the mass flow rate of liquids, but can also be used on some gases and can be applied to indirectly measure volumetric flow rate. A Coriolis flow meter contains a pair of parallel vibrating tubes, or a single vibrating tube formed into two parallel sections (Morris and Langari, 2020). As fluid flows through the vibrating tube(s), a Coriolis force is generated and the tube is deflected further to the existing vibratory motion. This deflection is proportional to the mass flow rate of the fluid, which can be measured using a suitable sensor. Coriolis flow meters may have a high accuracy of $\pm 0.2\,\%$ (Morris and Langari, 2020) and can be used on liquids, gases, slurries and two-phase flows (LaNasa and Upp, 2014). However, they are expensive and can suffer from mechanical problems such as fatigue and corrosion.

Doppler Shift Ultrasonic Flow Meter: A Doppler shift flow meter consists of an ultrasonic transmitter and receiver clamped to the outside of a pipe or fluid carrying vessel (Morris and Langari, 2020). The transmitter emits ultrasonic waves which are deflected by scattering elements in the fluid and received by the receiver. This deflection causes a change in wave frequency, which is used to determine the flow rate. Doppler shift flow meters are typically inexpensive and can be used on gases or liquids; however the measurement accuracy depends on a number of different parameters, and so accurate measurements require careful calibration. These instruments are typically used for flow indications instead of accurate quantification of volumetric flow rate (Morris and Langari, 2020). Variants with higher measurement accuracy have been developed, but these can be significantly more expensive. However, since these flow meters are clamped to the outside of a pipe, no contact is required between the flow meter and fluid.

Electromagnetic Flow Meter: Electromagnetic flow meters use Faraday's Law to determine the flow of liquid in a pipe, as a conductive liquid flowing through a magnetic field generates a voltage. Since the voltage generated is proportional to the velocity of the liquid, the flow rate can be measured from the voltage signal. The main advantages are that it is non-intrusive with no moving parts and a typical accuracy of up to $\pm 0.5\,\%$. However, they can be relatively heavy and only work for conductive fluids, and so gases and deionised water cannot be measured.

3.3.3 Detailed Flow Field Measurements

Passive cooling systems often use natural convection phenomena to drive the flow and thus detailed measurements of such phenomena in isolation, through use of idealised loops or very simple geometries (differentially heated cavities, for example), can advance both physical understanding and the development of numerical models. Models validated in these simple scenarios can then be taken forward into more complex situations with increased confidence. Several benchmark experiments in differentially heated cavities have been conducted, such as Betts and Bokhari (2000) and Cooper *et al.* (2012).

Advanced laser-based techniques for obtaining flow field measurements include Particle Image Velocimetry (PIV) and Laser Doppler Anemometry (LDA). Though such non-invasive techniques seem well suited to the kind of sensitive flows typical of passive cooling systems, they require optical access. This can be impossible for opaque fluids, but also difficult for water, since the pipes in real systems are likely to be made of opaque materials like metal. Transparent materials require optical properties matched to the fluid for best results in complex geometries (Hassan, 2019), and will typically have very different thermal properties to those likely to be used in any real system, which can interfere with the observed system performance, so need to be applied with care.

In addition, the associated equipment can be cumbersome. For these reasons, it may be useful to use CFD modelling to identify areas where flow features of particular interest may occur and then focus the use of these techniques in these areas. CFD may also be used to indicate where additional measurements may be of value, such as using phased measurements in scenarios where the flow in the system is expected to be unstable.

3.3.3.1 Velocity Measurement Techniques

Pitot Tube: A pitot tube consists of two openings; one perpendicular to the flow, sampling local static pressure and one normal to the flow, sampling local total pressure (where the kinetic energy of the flow is converted to a pressure increase). The difference in measured static and total pressure is used to calculate the local fluid flow velocity (Morris and Langari, 2020).

Pitot tubes are a simple, cheap and widely used method for measuring velocity; however they have a low measurement accuracy. In addition, a pitot tube provides a single 1D velocity, although pitot cylinders (3-hole) and pitot spheres (5-hole) can measure 2D and 3D velocities respectively, but require calibration and may be bulky.

Constant Temperature Anemometry: Constant Temperature Anemometry (CTA), also known as Thermal Anemometry, is a technique for the measurement of 1D, 2D or 3D velocity and turbulence in gas and liquid flows, using hot-wire or hot-film probes inserted in the flow. CTA is particularly suitable for the measurement of flows with very fast fluctuations at a point (high turbulence) and the study of flow micro-structures, where there is a need to resolve small flow eddies down to the order of tenths of a millimetre.

Hot-wire anemometers consist of a thin electrically heated wire and the measurement principle is based on the cooling effect of a flow on a heated body, which reduces its resistance. Measurement of this resistance change is used to calculate the fluid velocity. Hot-wire anemometers have a fast response time (20 - 50 kHz); however they are not very robust due to the small diameter of the wire (Morris and Langari, 2020). Multiple wires are required to measure velocity components, which can become bulky and difficult to work with, so a single wire and traverse gear with phase-locking is often a more practical approach.

Application areas include temperature, shear stress, velocity and turbulence measurements in e.g. jets, boundary layers and transitional flows. Wire sensors are used in gases and non-conducting liquids, while film sensors are primarily designed for use in water and other conducting liquids, as well as transition in gases. However, the temperature range for CTAs is limited, and they require careful, regular calibration.

The Thermal Anemometry Grid Sensor is based on the same principle; however it contains multiple temperature resistant resistors arranged in a grid. This enables spatially resolved velocity measurements to be obtained.

Wire Mesh Sensor: Wire mesh sensors (WMSs) are an intrusive technique that allow the investigation of multiphase flows with high spatial and temporal resolution. They can be used to obtain information about fluid velocity, void fraction, droplet/bubble size and distribution, interfacial area, film thickness, thermal distribution and flow regimes (Velasco Peña and Rodriguez, 2015).

Typically, a WMS consists of two parallel planes of wires; one plane containing transmitter wires, and one containing receiver wires. The planes are configured such that the wires on the top and bottom planes cross at an angle of 90°, forming a mesh grid of electrodes. This is placed into the cross-sectional area of the pipe or flow region of interest. The transmitter wires are activated sequentially, while the receiver wires are sampled in parallel. An electrical property (conductivity or permittivity) at each crossing point is evaluated to determine the fluid distribution across the cross-section. Velocity measurements are typically obtained using two WMS in different locations, and high accuracy 3D measurements can be made using two sensors separated by a few centimetres (Velasco Peña and Rodriguez, 2015).

WMS can be used at typical reactor temperatures and pressures, but is intrusive and so can influence the flow field and size/shape of the bubbles. In addition, two phases are required in order to evaluate the conductivity/permittivity variation at each crossing e.g. air-water, steam-water or water with varying dissolved solute concentrations. This limits its applicability to velocity measurements, and therefore it is often used for measurements of mixing and void fraction.

Particle Image Velocimetry: PIV is a non-intrusive optical measurement technique which is used to obtain 2D or 3D fluid velocity measurements. PIV involves introducing small light scattering particles into the fluid flow. These particles are then illuminated by two consecutive pulses of a high intensity laser, and the scattered light across a plane of flow is recorded by a high resolution camera. The fluid velocity is then determined by analysis of the displacement of the particles between the successive frames.

Stereo PIV measures three velocity components in a plane using two cameras, with the second camera at a different orientation such that it can record the third dimension component. Tomographic PIV uses multiple cameras and can measure three velocity components in a volume. Time resolved PIV benefits from the advances in camera technology to acquire high resolution PIV images at tens of thousands of frames per second with full camera resolution.

In air flows, the seeding particles are typically oil drops in the range $1\,\mu m$ to $5\,\mu m$. For water applications, the seeding is typically polystyrene, polyamide, hollow glass spheres or pepper in the range $5\,\mu m$ to $100\,\mu m$. It is worth noting that the seeding particles can affect the bulk fluid properties (Section 2.3), so it is important that the properties of the seeded fluid are understood and reported (and using in scaling assessments where appropriate, Section 3.3.1).

Since PIV uses scattered light, the test fluid and test section walls must be optically transparent, which makes it difficult to use at reactor pressures and temperatures. PIV can be applied to flow regimes ranging from laminar, transitional to fully turbulent flows (Scarano, 2012).

Laser Doppler Velocimetry/Anemometry: Laser Doppler Velocimetry (LDV) or LDA is a non-intrusive, optical technique for 1D, 2D and 3D point measurement of velocity and turbulence distribution in both free flows and internal flows. LDV requires that light scattering particles are present within the flowing fluid. The flow is then illuminated by a known frequency of laser, and the light scattered by the moving particles is detected by a photomultiplier. The difference in frequency between the incident light and light reflected back is measured (i.e. the Doppler frequency), and used to calculate the velocity.

LDV can be used in hostile environments and confined areas and can measure a wide range of velocities (Morris and Langari, 2020) with high spatial and temporal resolution. However, the method tends to be expensive and it can be difficult to collect data in close proximity to walls. Doppler Global Velocimetry is based on the same principles as LDV, but allows measurement of the velocity distribution within a plane. Since LDV uses lasers, the test fluid and test section walls must be optically transparent, which makes it difficult to use at reactor pressures and temperatures.

Ultrasound Doppler Velocimetry: Ultrasound Doppler Velocimetry (UDV) is based on the pulse-echo method with velocity derived from shifts in positions between pulses, rather than shifts in frequency due to the Doppler effect. This requires acoustic inhomogeneities in the fluid to measure, which may be of natural origin as for many metal melts or artificial scattering particles have to be added. This technique is especially useful for opaque fluids or systems without optical access, since established optical flow measurement techniques such as PIV and LDV cannot be used.

2D or 3D UDV can be used to measure two or three velocity components simultaneously along a line. UDV-2D is based on a three transducer system with one transducer as an emitter and two others as receivers. For UDV-3D measurements, a similar arrangement is used with three receivers. In

addition, spatial flow measurements can be achieved using several transducers arranged laterally to each other. However, the spatial and temporal resolution is limited by the number of transducers and sequential excitation required.

3.3.4 Geometry, Boundary and Operating Conditions

Clear and complete geometric information should be recorded, ideally with an 'as-built' Computer Aided Design (CAD) geometry. Where work is reported in a paper, geometric drawings dimensioned with sufficient detail to enable an accurate CAD representation to be extracted are important to enable following researchers to recreate the experiment.

Seemingly minor geometric details that are often overlooked include bend radii and wall thicknesses, which can vary due to flanges and manufacturing methods (e.g. bending pipes to form bends/coils can lead to thinner walls on the outer edge). The former is important since bends contribute to pressure losses within the pipe and inaccurate capture of these can lead to differences in mass flow rate and system performance at the low driving forces produced by natural convection. Wall thicknesses are important because the ability of the walls to absorb or release heat can affect the stability of the flow. For passive cooling systems, small differences can cause systems to switch between stable and unstable flow.

It is equally important to obtain complete information about the boundary and operating conditions. For a passive cooling system, this would include at a minimum, the nature of the heat exchanger (i.e. best represented as a uniform heat flux or uniform temperature), the heat flux (or power) and, if appropriate, flow performance information for the secondary side, such as the mass flow rate and temperature. Values of ambient temperature should also be recorded and the details of any insulation surrounding any apparatus should be reported in detail, since this is often a source of uncertainty. In cases where the transient behaviour is of interest, detailed knowledge of any heater control systems is also important to record and report for future reference.

3.3.5 Post-Processing

There is often more than one way to compute key non-dimensional parameters that are used to characterise the system and, as such, the procedure used to compute the parameter should be recorded clearly, including quantifying the measurement uncertainty. The same procedure should be used for both numerical and experimental studies to ensure comparisons are valid (as discussed in Volume 1, Section 4.6.1). In addition, the temperature at which material properties have been evaluated at, and where or how that temperature was evaluated should also be reported.

Material properties (Section 2.3) are often raised to various powers in non-dimensional parameters, meaning small differences in properties associated with small changes in temperatures can be greatly amplified and have a significant impact on the results. As an example, in a passive cooling system under natural circulation, the steady-state Re is often computed using a steady-state mass flow rate. Many experimental studies use an energy balance to compute this mass flow rate, since direct measurement is difficult. This can create uncertainty when comparing the Re from experimental work to values from numerical analysis.

4 Future Developments

To conclude the present volume, this section considers how the aspects presented on the preceding pages may change in the future.

Over the past two decades, general purpose CFD codes (and particularly the RANS and URANS approaches contained within them) have reached a degree of maturity for the prediction of single-phase buoyant flows, and their use is now as routine as the longer established and very mature system codes. This maturity in development has been facilitated by a combination of extensive industrial use and modelling developments based on simple test cases. It is also expected that the use of coupled CFD and system code analyses will increase to better understand and predict the characteristics of areas of complex flow in parts of systems (Volume 2, Section 4).

Looking further forward, Machine Learning (ML) could be used to drive analysis software in support of the more routine aspects of analysis, for example making decisions about how best to run previously developed and understood system and CFD models in support of a design sequence, or using a digital twin to predict the future performance of operating plant. In the nuclear industry however, the judgement of skilled engineers in understanding and justifying the safety of NPPs, to their own organisations, regulators and the public, is likely to remain of critical importance.

In the short term, research and development is required on natural circulation, hybrid methods and turbulent heat transfer models to support the design of passive cooling systems in advanced reactors.

4.1 Natural Circulation

New reactor designs are making more extensive use of passive cooling systems for both normal operation and fault scenarios. Therefore, it is essential to be able to confidently predict the flow rate within the system loop under natural circulation conditions, and ensure that there is no chance of flow reversal or instability and the time taken for the flow to develop is understood. This challenge is highlighted in Section 2.4 and the current limitations of system codes is discussed in Section 3.1.1.

Although CFD codes are able to more accurately predict the flow rate and onset of instability in natural circulation loops than system codes, the timescales for the flow to develop and extent of passive cooling systems means that using CFD analysis to support the design of reactor scale passive cooling systems is likely to be unfeasible. Therefore, further development is required to understand and develop best practice in this area. This should include:

- A review of existing experimental data for natural circulation loops (Wilson, 2021) has been conducted as part of the Department for Business, Energy and Industrial Strategy (BEIS)

thermal hydraulics Nuclear Innovation Programme (NIP) (Volume 1, Appendix A). This demonstrated that there are very few high-fidelity measurements of natural circulation flows in representative reactor system loops. Therefore, there is a requirement for improved reactor scale natural circulation test facilities with high-fidelity measurements, such as non-intrusive optical techniques providing instantaneous and time-averaged flow and thermal fields for model validation (Section 3.3.2, Section 3.3.3 and Volume 2, Section 3.5.1).

- The capability, limitations and adequacy of system codes to predict natural circulation in system loops needs to be better quantified and understood. This will enable best practice guidance to be developed in order to determine when a system code is suitable, when it should be coupled with a CFD code and when it is necessary to use CFD analysis.
- Though considered relatively mature, RANS and URANS are not well tested in complex passive cooling cases, such as modelling full natural circulation loops. Good progress has been made in Wilson (2021) as part of the BEIS thermal hydraulics NIP (Volume 1, Appendix A) to assess the benefit of using CFD for these applications. However, further work is required to apply and validate it on representative reactor-scale system loops.

4.2 Hybrid methods

As the cost of HPC resource reduces, so judgments on what is practicable for industrial modelling and the design process will also change. However, as outlined in Volumes 1, 2 and 3, the complexity and cost of moving to more detailed modelling approaches in CFD are significant. Therefore, while the use of LES is likely to increase slowly, it is unlikely to replace RANS (Hanjalic, 2005).

The use of hybrid methods, such as WMLES, zonal LES, DES and SAS is also likely to increase. While significantly more computationally expensive than RANS, hybrid methods may offer increased fidelity and improved ability to resolve the flows in complex passive cooling systems, without the likely much greater cost of LES. In particular, this provides an alternative way of providing validation or benchmark data as part of a CFD design optimisation. A typical design/safety justification process might involve the following steps:

- An initial validation exercise involving hybrid methods and experimental data relevant to the application of interest.
- This would provide a benchmark for validating simpler RANS/URANS simulations.
- The design/application could then be optimised through multiple RANS simulations with formal uncertainty quantification.
- Finally, a number of hybrid models could be run of the final solution to confirm the results/conclusions from the RANS modelling.

However, there is a requirement for more high-quality experimental data for detailed validation and performance assessment of hybrid methods for passive cooling systems. Further, more industry application is required in order to better understand the benefits and limitations of the current hybrid methods available (i.e. which method is most suitable for a particular application), and develop clear guidelines for appropriate mesh generation, model set-up and solution strategy.

4.3 Turbulent Heat Transfer Models

Turbulent heat transfer models (Sections 2.2.4.4 and 3.2.6.5) simulate the turbulent heat transport, while RANS turbulence models simulate the turbulent momentum transport. These models have the potential to significantly improve the prediction of temperature gradients and turbulence generation for buoyancy affected flows (i.e. natural and mixed convection) using RANS turbulence models.

This is an active area of research, particularly for low-Prandtl number flows of liquid metal (Volume 5), although the options available in most CFD tools are limited. Examples include the implementation of the SGDH and GGDH models in Fluent using User Defined Functions (UDFs) (Kumar and Dewan, 2013), and development of an explicit AHFM model in OpenFOAM (Manservisi and Menghini, 2014). Much of the recent development has been undertaken on implicit AHFMs within the Simulations and Experiments for the Safety Assessment of MEtal cooled reactors (SESAME) project. This includes the AHFM-2005 version that has been implemented in STAR-CCM+, and Nuclear Research and Consultancy Group (NRG)'s new variant of the model called AHFM-NRG+ (Shams *et al.*, 2019).

It is expected that these models will become more widely available within standard CFD analysis tools over the next few years (Volume 1, Section 4.5.4). Further validation will then be required to understand and assess their potential benefits for buoyancy driven, mixed and natural convection flows.

5 References

Altaç Z, Uğurlubilek N (2016) Assessment of Turbulence Models in Natural Convection from Two- and Three-Dimensional Rectangular Enclosures. *International Journal of Thermal Sciences*, 107, 237–246, dx.doi.org/10.1016/j.ijthermalsci.2016.04.016.

Ammour D, Craft T, Iacovides H (2013) Highly Resolved LES and URANS of Turbulent Buoyancy-Driven Flow Within Inclined Differentially-Heated Enclosures. *Flow, Turbulence and Combustion*, 91(3), 669–696, dx.doi.org/10.1007/s10494-013-9497-1.

ASHRAE (2017) ASHRAE Handbook: Fundamentals. American Society of Heating Refrigerating and Air-Conditioning Engineers.

Avramova M, Blyth T S, Salko R K (2016) CTF User's Manual. CASL-U-2016-1111-000, Oak Ridge National Laboratory, dx.doi.org/10.2172/1342676.

Avramova M, Cuervo D (2013) Assessment of CTF Boiling Transition and Critical Heat Flux Modeling Capabilities Using the OECD/NRC BFBT and PSBT Benchmark Databases. *Science and Technology of Nuclear Installations*, 2013, 1–12, dx.doi.org/10.1155/2013/508485.

Basu D N, Bhattacharyya S, Das P K (2007) Effect of Heat Loss to Ambient on Steady-State Behaviour of a Single-Phase Natural Circulation Loop. *Applied Thermal Engineering*, 27(8), 1432–1444, dx.doi.org/10.1016/j.applthermaleng.2006.10.004.

Behnia M, Parneix S, Shabany Y, Durbin P A (1999) Numerical Study of Turbulent Heat Transfer in Confined and Unconfined Impinging Jets. *International Journal of Heat and Fluid Flow*, 20(1), 1–9, dx.doi.org/10.1016/S0142-727X(98)10040-1.

Bellet S, Benhamadouche S (2011) Swirling and Secondary Flows in PWR Primary Loops: CFD Might Bring Some Light. In *18th International Conference on Nuclear Engineering*, pp. 999–1008, American Society of Mechanical Engineers Digital Collection, dx.doi.org/10.1115/ICONE18-30039.

Benhamadouche S (2015) Pressure Drop Predictions Using Code_Saturne in NESTOR CFD Benchmark. In *Proceedings of the 16th International Topical Meeting on Nuclear Thermal Hydraulics*.

Benhamadouche S (2017) On the Use of (U)RANS and LES Approaches for Turbulent Incompressible Single Phase Flows in Nuclear Engineering Applications. *Nuclear Engineering and Design*, 312, 2–11, dx.doi.org/10.1016/j.nucengdes.2016.11.002.

Betts P, Bokhari I (2000) Experiments on Turbulent Natural Convection in an Enclosed Tall Cavity. *International Journal of Heat and Fluid Flow*, 21(6), 675–683, dx.doi.org/10.1016/S0142-727X(00)00033-3.

Billard F, Revell A, Craft T (2012) Application of Recently Developed Elliptic Blending Based Models to Separated Flows. *International Journal of Heat and Fluid Flow*, 35, 141–151, dx.doi.org/10.1016/j.ijheatfluidflow.2012.04.012.

References

Bouffanais R (2010) Advances and Challenges of Applied Large-Eddy Simulation. *Computers & Fluids*, 39(5), 735–738, dx.doi.org/10.1016/j.compfluid.2009.12.003.

Champigny J, Simoneau J P, Duret B (2007) A LES-Experiment Comparison of Mixed-Convection Around a Large Vertical Cylinder. In *12th International Topical Meeting on Nuclear Reactor Thermal Hydraulics*, p. 21.

Chen Q (1995) Comparison of Different K-e Models for Indoor Air Flow Computations. *Numerical Heat Transfer, Part B: Fundamentals*, 28(3), 353–369, dx.doi.org/10.1080/10407799508928838.

Cheng Z, Rao Y (2015) Strategies for Developing Subchannel Capability in an Advanced System Thermalhydraulic Code: A Literature Review. *AECL Nuclear Review*, 4(1), 23–41, dx.doi.org/10.12943/ANR.2015.00039.

Chien K (1982) Predictions of Channel and Boundary-Layer Flows with a Low-Reynolds-Number Turbulence Model. *AIAA Journal*, 20(1), 33–38, dx.doi.org/10.2514/3.51043.

Ciofalo M (1994) Large-Eddy Simulation: A Critical Survey of Models and Applications. In **Hartnett J P, Irvine T F, Cho Y I, Greene G A** (editors) *Advances in Heat Transfer*, volume 25, pp. 321–419, Elsevier, dx.doi.org/10.1016/S0065-2717(08)70196-5.

Collier J G, Thome J R (1996) Convective Boiling and Condensation. Third edition, Clarendon Press.

Cooper D, Craft T, Esteifi K, Iacovides H (2012) Experimental Investigation of Buoyant Flows in Inclined Differentially Heated Cavities. *International Journal of Heat and Mass Transfer*, 55(23-24), 6321–6339, dx.doi.org/10.1016/j.ijheatmasstransfer.2012.05.082.

Costa J J, Oliveira L A, Blay D (1999) Test of Several Versions for the k–ϵ Type Turbulence Modelling of Internal Mixed Convection Flows. *International Journal of Heat and Mass Transfer*, 42(23), 4391–4409, dx.doi.org/10.1016/S0017-9310(99)00075-7.

Cotton M A, Jackson J D (1990) Vertical Tube Air Flows in the Turbulent Mixed Convection Regime Calculated Using a Low-Reynolds-Number k-ϵ Model. *International Journal of Heat and Mass Transfer*, 33(2), 275–286, dx.doi.org/10.1016/0017-9310(90)90098-F.

Craft T, Iacovides H, Yoon J (2000) Progress in the Use of Non-Linear Two-Equation Models in the Computation of Convective Heat-Transfer in Impinging and Separated Flows. *Flow, Turbulence and Combustion*, 63(1), 59–80, dx.doi.org/10.1023/A:1009973923473.

Craft T, Ince N, Launder B (1996) Recent Developments in Second-Moment Closure for Buoyancy-Affected Flows. *Dynamics of Atmospheres and Oceans*, 23(1-4), 99–114, dx.doi.org/10.1016/0377-0265(95)00424-6.

Craft T J (1998) Developments in a Low-Reynolds-Number Second-Moment Closure and Its Application to Separating and Reattaching Flows. *International Journal of Heat and Fluid Flow*, 19(5), 541–548, dx.doi.org/10.1016/S0142-727X(98)10020-6.

Craft T J, Gant S E, Gerasimov A V, Iacovides H, Launder B E (2006) Development and Application of Wall-Function Treatments for Turbulent Forced and Mixed Convection Flows. *Fluid Dynamics Research*, 38(2-3), 127–144, dx.doi.org/10.1016/j.fluiddyn.2004.11.002.

References

Craft T J, Gerasimov A V, Iacovides H, Launder B E (2002) Progress in the Generalization of Wall-Function Treatments. *International Journal of Heat and Fluid Flow*, 23(2), 148–160, dx.doi.org/10.1016/S0142-727X(01)00143-6.

Craft T J, Graham L J W, Launder B E (1993) Impinging Jet Studies for Turbulence Model Assessment—II. An Examination of the Performance of Four Turbulence Models. *International Journal of Heat and Mass Transfer*, 36(10), 2685–2697, dx.doi.org/10.1016/S0017-9310(05)80205-4.

Craft T J, Iacovides H, Uapipatanakul S (2010) Towards the Development of RANS Models for Conjugate Heat Transfer. *Journal of Turbulence*, 11, N26, dx.doi.org/10.1080/14685248.2010.494608.

CSNI (1994) Proceedings of the Workshop on Large Molten Pool Heat Transfer (1994 : Grenoble, France). NEA/CSNI/R(1994)11, OECD NEA Committee on the Safety of Nuclear Installations.

CSNI (2015a) Assessment of CFD Codes for Nuclear Reactor Safety Problems - Revision 2. NEA/CSNI/R(2014)12, OECD NEA Committee on the Safety of Nuclear Installations.

CSNI (2015b) Best Practice Guidelines for the Use of CFD in Nuclear Reactor Safety Applications - Revision. NEA/CSNI/R(2014)11, OECD NEA Committee on the Safety of Nuclear Installations.

CSNI (2017) A State-of-the-Art Report on Scaling in System Thermal-Hydraulics Applications to Nuclear Reactor Safety and Design. NEA/CSNI/R(2016)14, OECD NEA Committee on the Safety of Nuclear Installations.

Daly B J, Harlow F H (1970) Transport Equations in Turbulence. *Physics of Fluids*, 13(11), 2634–2649, dx.doi.org/doi:10.1063/1.1692845.

D'Auria F (2017) Thermal-Hydraulics of Water Cooled Nuclear Reactors. Woodhead.

Dehoux F, Benhamadouche S, Manceau R (2017) An Elliptic Blending Differential Flux Model for Natural, Mixed and Forced Convection. *International Journal of Heat and Fluid Flow*, 63, 190–204, dx.doi.org/10.1016/j.ijheatfluidflow.2016.09.003.

Denton J D (1993) The 1993 IGTI Scholar Lecture: Loss Mechanisms in Turbomachines. *Journal of Turbomachinery*, 115(4), 621–656, dx.doi.org/10.1115/1.2929299.

di Mare L, Klein M, Jones W P, Janicka J (2006) Synthetic Turbulence Inflow Conditions for Large-Eddy Simulation. *Physics of Fluids*, 18(2), 025107, dx.doi.org/10.1063/1.2130744.

Ding P, Wang S, Chen K (2019) Numerical Study on Turbulent Mixed Convection in a Vertical Plane Channel Using Hybrid RANS/LES and LES Models. *Chinese Journal of Chemical Engineering*, dx.doi.org/10.1016/j.cjche.2019.04.007.

Dinh T N, Nourgaliev R R, Theofanous T G (2003) Understanding of the Ill-Posed Two-Fluid Model. In *Proceedings of the Tenth International Topical Meeting on Nuclear Reactor Thermal Hydraulics (NURETH 10)*, KNS.

Duan Y, He S (2017) Large Eddy Simulation of a Buoyancy-Aided Flow in a Non-Uniform Channel – Buoyancy Effects on Large Flow Structures. *Nuclear Engineering and Design*, 312, 191–204, dx.doi.org/10.1016/j.nucengdes.2016.05.007.

References

Durbin P A (1991) Near-Wall Turbulence Closure Modeling without “Damping Functions”. *Theoretical and Computational Fluid Dynamics*, 3(1), 1–13, dx.doi.org/10.1007/BF00271513.

Durbin P A (2018) Some Recent Developments in Turbulence Closure Modeling. *Annual Review of Fluid Mechanics*, 50(1), 77–103, dx.doi.org/10.1146/annurev-fluid-122316-045020.

Dzodzo M B (2018) Natural and Mixed Convection in Enclosures Containing Liquid Metals and Partition Walls. In *Proceedings of THMT-18. Ninth International Symposium On Turbulence Heat and Mass Transfer*, pp. 461–469, Begellhouse, dx.doi.org/10.1615/THMT-18.460.

Eidson T M (1985) Numerical Simulation of the Turbulent Rayleigh–Bénard Problem Using Subgrid Modelling. *Journal of Fluid Mechanics*, 158, 245–268, dx.doi.org/10.1017/S0022112085002634.

EPRI (2014) Computational Fluid Dynamics Benchmark of High Fidelity Rod Bundle Experiments. Technical Report 3002000504, Electric Power Research Institute.

ERCOFTAC (2000) Industrial Computational Fluid Dynamics of Single-Phase Flows ERCOFTAC Best Practice Guidelines. Version 1, Turbulence and Combustion European Research Community on Flow.

Faheem A, Ranzi G, Fiorito F, Lei C (2016) A Numerical Study of Turbulent Mixed Convection in a Smooth Horizontal Pipe. *Journal of Heat Transfer*, 138(1), dx.doi.org/10.1115/1.4031112.

Ferreri J C, Ambrosini W (1999) Verification of RELAP5/MOD 3 with Theoretical and Numerical Stability Results on Single-Phase, Natural Circulation in a Simple Loop. NUREG/IA-0151, U.S. Nuclear Regulatory Commission.

Fournier Y, Vurpillot C, Béchaud C (2007) Evaluation of Fluid Flow in the Lower Core of a PWR with Code_Saturne. *Nuclear Engineering and Design*, 237(15), 1729–1744, dx.doi.org/10.1016/j.nucengdes.2007.02.025.

Frazer-Nash (2019) Project FORTE - Nuclear Thermal Hydraulics Research & Development Review of Thermal Hydraulic Test Facilities. FNC 53798/46969R Issue 1, Frazer-Nash Consultancy.

Fröhlich J, von Terzi D (2008) Hybrid LES/RANS Methods for the Simulation of Turbulent Flows. *Progress in Aerospace Sciences*, 44(5), 349–377, dx.doi.org/10.1016/j.paerosci.2008.05.001.

Gatski T, Rumsey C (2002) Linear and Nonlinear Eddy Viscosity Models. In **Launder B E, Sandham N D** (editors) *Closure Strategies for Turbulent and Transitional Flows*, pp. 9–46, Cambridge University Press, dx.doi.org/10.1017/CBO9780511755385.003.

Ge J, Tian W, Qiu S, Su G H (2018) CFD Investigation on Thermal Hydraulics of the Passive Residual Heat Removal Heat Exchanger (PRHR HX). *Nuclear Engineering and Design*, 327, 139–149, dx.doi.org/10.1016/j.nucengdes.2017.11.029.

Gebhart B, Jaluria Y, Mahajan R L, Sammakia B G (1988) Buoyancy-Induced Flows and Transport. Hemisphere.

Georgiadis N J, Rizzetta D P, Fureby C (2010) Large-Eddy Simulation: Current Capabilities, Recommended Practices, and Future Research. *AIAA Journal*, 48(8), 1772–1784, dx.doi.org/10.2514/1.J050232.

References

Germano M, Piomelli U, Moin P, Cabot W H (1991) A Dynamic Subgrid-scale Eddy Viscosity Model. *Physics of Fluids A: Fluid Dynamics*, 3(7), 1760–1765, dx.doi.org/10.1063/1.857955.

Grassi W, Testi D (2007) Evaluation of Two RANS Turbulence Models in Predicting Developing Mixed Convection within a Heated Horizontal Pipe. *International Journal of Computational Fluid Dynamics*, 21(7-8), 267–276, dx.doi.org/10.1080/10618560701684470.

Gray D D, Giorgini A (1976) The Validity of the Boussinesq Approximation for Liquids and Gases. *International Journal of Heat and Mass Transfer*, 19(5), 545–551, dx.doi.org/10.1016/0017-9310(76)90168-X.

Gritskevich M S, Garbaruk A V, Frank T, Menter F R (2014) Investigation of the Thermal Mixing in a T-Junction Flow with Different SRS Approaches. *Nuclear Engineering and Design*, 279, 83–90, dx.doi.org/10.1016/j.nucengdes.2014.03.010.

Groetzbach G (2002) Peculiarities of Natural Convective Heat Removal from Complex Pools. In *Advances in Fluid Modeling and Turbulence Measurements*, pp. 587–594, World Scientific, dx.doi.org/10.1142/9789812777591_0071.

Haase W, Braza M, Revell A (2009) DESider – A European Effort on Hybrid RANS-LES Modelling, volume 103 of *Notes on Numerical Fluid Mechanics and Multidisciplinary Design*. Springer Berlin Heidelberg, dx.doi.org/10.1007/978-3-540-92773-0.

Haines R W, Myers M E (2010) HVAC Systems Design Handbook. Fifth edition, McGraw-Hill.

Hanjalić K (2002) One-Point Closure Models for Buoyancy-Driven Turbulent Flows. *Annual Review of Fluid Mechanics*, 34(1), 321–347, dx.doi.org/10.1146/annurev.fluid.34.082801.161035.

Hanjalic K (2005) Will RANS Survive LES? A View of Perspectives. *Journal of Fluids Engineering*, 127(5), 831–839, dx.doi.org/10.1115/1.2037084.

Hanjalić K, Jakirlić S (1998) Contribution towards the Second-Moment Closure Modelling of Separating Turbulent Flows. *Computers & Fluids*, 27(2), 137–156, dx.doi.org/10.1016/S0045-7930(97)00036-4.

Hanjalić K, Kenjereš S, Durst F (1996) Natural Convection in Partitioned Two-Dimensional Enclosures at Higher Rayleigh Numbers. *International Journal of Heat and Mass Transfer*, 39(7), 1407–1427, dx.doi.org/10.1016/0017-9310(95)00219-7.

Hanjalić K, Launder B (2011) Modelling Turbulence in Engineering and the Environment: Second-Moment Routes to Closure. Cambridge university press.

Hassan Y (2019) High-Fidelity Experimental Measurements for Modeling and Simulation of Nuclear Engineering Applications. *Nuclear Engineering and Design*, 354, 110181, dx.doi.org/10.1016/j.nucengdes.2019.110181.

Haywood R W (1990) Thermodynamic Tables in SI (Metric) Units. Third edition, Cambridge University Press.

Höhne T (2014) Scale Resolved Simulations of the OECD/NEA–Vattenfall T-Junction Benchmark. *Nuclear Engineering and Design*, 269, 149–154, dx.doi.org/10.1016/j.nucengdes.2013.08.021.

References

Holgate J, Skillen A, Craft T, Revell A (2019) A Review of Embedded Large Eddy Simulation for Internal Flows. *Archives of Computational Methods in Engineering*, 26(4), 865–882, dx.doi.org/10.1007/s11831-018-9272-5.

Hou X, Sun Z, Lei W (2017) Capability of RELAP5 Code to Simulate the Thermal-Hydraulic Characteristics of Open Natural Circulation. *Annals of Nuclear Energy*, 109, 612–625, dx.doi.org/10.1016/j.anucene.2017.06.010.

Hsieh K J, Lien F S (2004) Numerical Modeling of Buoyancy-Driven Turbulent Flows in Enclosures. *International Journal of Heat and Fluid Flow*, 25(4), 659–670, dx.doi.org/10.1016/j.ijheatfluidflow.2003.11.023.

IAEA (1991) Safety Related Terms for Advanced Nuclear Plants (Report of a Technical Committee Meeting, Vaesteras, Sweden, 30 May - 2 June 1988). IAEA-TECDOC-626, International Atomic Energy Agency.

IAEA (1996) Technical Feasibility and Reliability of Passive Safety Systems for Nuclear Power Plants. IAEA-TECDOC-920, International Atomic Energy Agency.

IAEA (2001) Thermohydraulic Relationships for Advanced Water Cooled Reactors. IAEA-TECDOC-1203, International Atomic Energy Agency.

IAEA (2002a) Comparative Assessment of Thermophysical and Thermohydraulic Characteristics of Lead, Lead-Bismuth and Sodium Coolants for Fast Reactors. IAEA-TECDOC-1289, International Atomic Energy Agency.

IAEA (2002b) Natural Circulation Data and Methods for Advanced Water Cooled Nuclear Power Plant Designs. IAEA-TECDOC-1281, International Atomic Energy Agency.

IAEA (2005) Natural Circulation in Water Cooled Nuclear Power Plants. IAEA-TECDOC-1474, International Atomic Energy Agency.

IAEA (2006) Thermophysical Properties Database of Materials for Light Water Reactors and Heavy Water Reactors. IAEA-TECDOC-1496, International Atomic Energy Agency.

IAEA (2009a) Passive Safety Systems and Natural Circulation in Water Cooled Nuclear Power Plants. IAEA-TECDOC-1624, International Atomic Energy Agency.

IAEA (2009b) Thermophysical Properties of Materials for Nuclear Engineering: A Tutorial and Collection of Data. IAEA-THPH, International Atomic Energy Agency.

IAEA (2012) Natural Circulation Phenomena and Modelling for Advanced Water Cooled Reactors. IAEA-TECDOC-1677, International Atomic Energy Agency.

IAEA (2013a) Benchmark Analyses on the Natural Circulation Test Performed during the PHENIX End-of-Life Experiments. IAEA-TECDOC-1703, International Atomic Energy Agency.

IAEA (2013b) Challenges Related to the Use of Liquid Metal and Molten Salt Coolants in Advanced Reactors. IAEA-TECDOC-1696, International Atomic Energy Agency.

IAEA (2013c) Passive Safety Systems in Advanced Water Cooled Reactors (AWCRs): Case Studies. IAEA-TECDOC-1705, International Atomic Energy Agency.

References

IAEA (2014) Benchmark Analyses of Sodium Natural Convection in the Upper Plenum of the Monju Reactor Vessel. IAEA-TECDOC-1754, International Atomic Energy Agency.

IAEA (2018) Lessons Learned from the Deferred Dismantling of Nuclear Facilities. Nuclear Energy Series NW-T-2.11, International Atomic Energy Agency.

Idelčik I E, Ginevskiĭ A S (2007) Handbook of Hydraulic Resistance. Fourth edition, Begell House.

Ince N Z, Launder B E (1989) On the Computation of Buoyancy-Driven Turbulent Flows in Rectangular Enclosures. *International Journal of Heat and Fluid Flow*, 10(2), 110–117, dx.doi.org/10.1016/0142-727X(89)90003-9.

Incropera F P, DeWitt D P, Bergman T L, Lavine A S (2011) Fundamentals of Heat and Mass Transfer. Seventh edition, John Wiley & Sons.

INL (2018) RELAP5-3D Code Manual Volume V: User's Guidelines. INL-EXT-98-00834, Idaho National Laboratory.

Ishii M (2016) Investigation of Natural Circulation Instability and Transients in Passively Safe Small Modular Reactors. DOE/NEUP 12-3496, Purdue University, dx.doi.org/10.2172/1346153.

Jackson J (1983) Turbulent Mixed Convection Heat Transfer to Liquid Sodium. *International Journal of Heat and Fluid Flow*, 4(2), 107–111, dx.doi.org/10.1016/0142-727X(83)90011-5.

Jackson J D (2018) Applications of Fluids at Supercritical Pressure in the Area of Power Generation – Movements towards Economically-Viable Clean Energy. Chapter 21 in Supercritical and Other High-Pressure Solvent Systems: For Extraction, Reaction and Material Processing. Royal Society of Chemistry.

Jackson J D, Axcell B P, Walton A (1994) Mixed-Convection Heat Transfer to Sodium in a Vertical Pipe. *Experimental Heat Transfer*, 7(1), 71–90, dx.doi.org/10.1080/08916159408946473.

Jackson J D, Cotton M A, Axcell B P (1989) Studies of Mixed Convection in Vertical Tubes. *International Journal of Heat and Fluid Flow*, 10(1), 2–15, dx.doi.org/10.1016/0142-727X(89)90049-0.

Jaramillo J E, Pérez-Segarra C D, Rodriguez I, Oliva A (2008) Numerical Study of Plane and Round Impinging Jets Using RANS Models. *Numerical Heat Transfer, Part B: Fundamentals*, 54(3), 213–237, dx.doi.org/10.1080/10407790802289938.

Jarrin N, Benhamadouche S, Laurence D, Prosser R (2006) A Synthetic-Eddy-Method for Generating Inflow Conditions for Large-Eddy Simulations. *International Journal of Heat and Fluid Flow*, 27(4), 585–593, dx.doi.org/10.1016/j.ijheatfluidflow.2006.02.006.

Jones W, Launder B (1972) The Prediction of Laminarization with a Two-Equation Model of Turbulence. *International Journal of Heat and Mass Transfer*, 15(2), 301–314, dx.doi.org/10.1016/0017-9310(72)90076-2.

Kakaç S, Shah R K, Aung W (1987) Handbook of Single-Phase Convective Heat Transfer. Wiley.

Kang S K, Hassan Y A (2016) Computational Fluid Dynamics (CFD) Round Robin Benchmark for a Pressurized Water Reactor (PWR) Rod Bundle. *Nuclear Engineering and Design*, 301, 204–231, dx.doi.org/10.1016/j.nucengdes.2016.03.007.

References

Kays W M (1994) Turbulent Prandtl Number—Where Are We? *Journal of Heat Transfer*, 116(2), 284–295, dx.doi.org/10.1115/1.2911398.

Kenjereš S, Gunarjo S, Hanjalić K (2005) Contribution to Elliptic Relaxation Modelling of Turbulent Natural and Mixed Convection. *International Journal of Heat and Fluid Flow*, 26(4), 569–586, dx.doi.org/10.1016/j.ijheatfluidflow.2005.03.007.

Kenjereš S, Hanjalić K (1999) Transient Analysis of Rayleigh–Bénard Convection with a RANS Model. *International Journal of Heat and Fluid Flow*, 20(3), 329–340, dx.doi.org/10.1016/S0142-727X(99)00007-7.

Kenjereš S, Hanjalić K (2006) LES, T-RANS and Hybrid Simulations of Thermal Convection at High Ra Numbers. *International Journal of Heat and Fluid Flow*, 27(5), 800–810, dx.doi.org/10.1016/j.ijheatfluidflow.2006.03.008.

Kenjereš S, Hanjalić K (2009) Tackling Complex Turbulent Flows with Transient RANS. *Fluid Dynamics Research*, 41, 012201, dx.doi.org/10.1088/0169-5983/41/1/012201.

Keshmiri A, Addad Y, Cotton M A, Laurence D R, Billard F (2008) Refined Eddy Viscosity Schemes and Large Eddy Simulations for Ascending Mixed Convection Flows. In *Proceedings of CHT-08*, Begellhouse, dx.doi.org/10.1615/ICHMT.2008.CHT.2410.

Keshmiri A, Cotton M A, Addad Y, Laurence D (2012) Turbulence Models and Large Eddy Simulations Applied to Ascending Mixed Convection Flows. *Flow, Turbulence and Combustion*, 89(3), 407–434, dx.doi.org/10.1007/s10494-012-9401-4.

Keshmiri A, Osman K, Benhamadouche S, Shokri N (2016) Assessment of Advanced RANS Models against Large Eddy Simulation and Experimental Data in the Investigation of Ribbed Passages with Passive Heat Transfer. *Numerical Heat Transfer, Part B: Fundamentals*, 69(2), 96–110, dx.doi.org/10.1080/10407790.2015.1096641.

Klein A (1981) Review: Turbulent Developing Pipe Flow. *Journal of Fluids Engineering*, 103(2), 243–249, dx.doi.org/10.1115/1.3241726.

Kocutar P, Škerget L, Ravnik J (2015) Hybrid LES/URANS Simulation of Turbulent Natural Convection by BEM. *Engineering Analysis with Boundary Elements*, 61, 16–26, dx.doi.org/10.1016/j.enganabound.2015.06.005.

Krishnani M, Basu D N (2016) On the Validity of Boussinesq Approximation in Transient Simulation of Single-Phase Natural Circulation Loops. *International Journal of Thermal Sciences*, 105, 224–232, dx.doi.org/10.1016/j.ijthermalsci.2016.03.004.

Kudariyawar J Y, Vaidya A M, Maheshwari N K, Satyamurthy P (2016) Computational Study of Instabilities in a Rectangular Natural Circulation Loop Using 3D CFD Simulation. *International Journal of Thermal Sciences*, 101, 193–206, dx.doi.org/10.1016/j.ijthermalsci.2015.11.003.

Kumar R, Dewan A (2013) Assessment of Buoyancy-Corrected Turbulence Models for Thermal Plumes. *Engineering Applications of Computational Fluid Mechanics*, 7(2), 239–249, dx.doi.org/10.1080/19942060.2013.11015467.

Kumar R, Dewan A (2014) URANS Computations with Buoyancy Corrected Turbulence Models

for Turbulent Thermal Plume. *International Journal of Heat and Mass Transfer*, 72, 680–689, dx.doi.org/10.1016/j.ijheatmasstransfer.2014.01.066.

Kumar R, Dewan A (2016) A Study of LES–SGS Closure Models Applied to a Square Buoyant Cavity. *International Journal of Heat and Mass Transfer*, 98, 164–175, dx.doi.org/10.1016/j.ijheatmasstransfer.2016.02.057.

Kumar S (2017) Experimental and Computational Simulation of Thermal Stratification in Large Pools with Immersed Condenser. *Applied Thermal Engineering*, p. 17.

LaNasa P J, Upp E L (2014) Fluid Flow Measurement. Elsevier, dx.doi.org/10.1016/C2011-0-07523-3.

Larsson J, Wang Q (2014) The Prospect of Using Large Eddy and Detached Eddy Simulations in Engineering Design, and the Research Required to Get There. *Philosophical Transactions of the Royal Society A: Mathematical, Physical and Engineering Sciences*, 372(2022), 20130329, dx.doi.org/10.1098/rsta.2013.0329.

Lau G E, Yeoh G H, Timchenko V, Reizes J A (2012) Large-Eddy Simulation of Natural Convection in an Asymmetrically-Heated Vertical Parallel-Plate Channel: Assessment of Subgrid-Scale Models. *Computers & Fluids*, 59, 101–116, dx.doi.org/10.1016/j.compfluid.2012.01.006.

Launder B, Reece G J, Rodi W (1975) Progress in the Development of a Reynolds-Stress Turbulence Closure. *Journal of Fluid Mechanics*, 68(03), 537–566, dx.doi.org/10.1017/S0022112075001814.

Launder B, Sharma B (1974) Application of the Energy-Dissipation Model of Turbulence to the Calculation of Flow near a Spinning Disc. *Letters in Heat and Mass Transfer*, 1(2), 131–137, dx.doi.org/10.1016/0094-4548(74)90150-7.

Lemmon E W, Jacobsen R T (2004) Viscosity and Thermal Conductivity Equations for Nitrogen, Oxygen, Argon, and Air. *International Journal of Thermophysics*, 25(1), 21–69, dx.doi.org/10.1023/B:IJOT.0000022327.04529.f3.

Lemmon E W, Jacobsen R T, Penoncello S G, Friend D G (2000) Thermodynamic Properties of Air and Mixtures of Nitrogen, Argon, and Oxygen from 60 to 2000 K at Pressures to 2000 MPa. *Journal of Physical and Chemical Reference Data*, 29(3), 331–385, dx.doi.org/10.1063/1.1285884.

Lilly D K (1992) A Proposed Modification of the Germano Subgrid-scale Closure Method. *Physics of Fluids A: Fluid Dynamics*, 4(3), 633–635, dx.doi.org/10.1063/1.858280.

Loginov M S, Komen E M J, Höhne T (2011) Application of Large-Eddy Simulation to Pressurized Thermal Shock: Assessment of the Accuracy. *Nuclear Engineering and Design*, 241(8), 3097–3110, dx.doi.org/10.1016/j.nucengdes.2011.05.027.

Macpherson G, Tunstall R (2020) CFD Validation of Buoyancy Driven Jet Spreading, Mixing and Wall Interaction. *Nuclear Engineering and Design*, 365, 110703, dx.doi.org/10.1016/j.nucengdes.2020.110703.

Manceau R, Hanjalić K (2002) Elliptic Blending Model: A New near-Wall Reynolds-Stress Turbulence Closure. *Physics of Fluids*, 14(2), 744–754, dx.doi.org/10.1063/1.1432693.

References

Manceau R, Parneix S, Laurence D (2000) Turbulent Heat Transfer Predictions Using the v2–f Model on Unstructured Meshes. *International Journal of Heat and Fluid Flow*, 21(3), 320–328, dx.doi.org/10.1016/S0142-727X(00)00016-3.

Manservisi S, Menghini F (2014) A CFD Four Parameter Heat Transfer Turbulence Model for Engineering Applications in Heavy Liquid Metals. *International Journal of Heat and Mass Transfer*, 69, 312–326, dx.doi.org/10.1016/j.ijheatmasstransfer.2013.10.017.

Mao J, Song L, Liu Y, Lin J, Huang S, Zou Y (2018) CFD Analysis of the Passive Decay Heat Removal System of an LBE-Cooled Fast Reactor. *Science and Technology of Nuclear Installations*, 2018, 1–11, dx.doi.org/10.1155/2018/4821746.

Martinez P, Alvarez D (2009) CFD Pour La Conception et La Sûreté Des Réacteurs. In *Société Française d'Energie Nucléaire ST6*.

Martynenko O G, Khramtsov P P (2005) Free-Convective Heat Transfer. Springer-Verlag, dx.doi.org/10.1007/3-540-28498-2.

Menter F R (1994) Two-Equation Eddy-Viscosity Turbulence Models for Engineering Applications. *AIAA Journal*, 32(8), 1598–1605, dx.doi.org/10.2514/3.12149.

Menter F R (2015) Best Practice: Scale-Resolving Simulations in ANSYS CFD. Version 2.0, ANSYS Germany.

Menter F R, Langtry R, Völker S (2006) Transition Modelling for General Purpose CFD Codes. *Flow, Turbulence and Combustion*, 77(1), 277–303, dx.doi.org/10.1007/s10494-006-9047-1.

Menter F R, Matyushenko A, Lechner R (2020) Development of a Generalized K-ω Two-Equation Turbulence Model. In **Dillmann A, Heller G, Krämer E, Wagner C, Tropea C, Jakirlić S** (editors) *New Results in Numerical and Experimental Fluid Mechanics XII*, volume 142, pp. 101–109, Springer International Publishing, dx.doi.org/10.1007/978-3-030-25253-3_10.

Merzari E, Obabko A, Fischer P, Halford N, Walker J, Siegel A, Yu Y (2017) Large-Scale Large Eddy Simulation of Nuclear Reactor Flows: Issues and Perspectives. *Nuclear Engineering and Design*, 312, 86–98.

Metais B, Eckert E R G (1964) Forced, Mixed, and Free Convection Regimes. *Journal of Heat Transfer*, 86(2), 295–296, dx.doi.org/10.1115/1.3687128.

Meyers J, Geurts B, Sagaut P (editors) (2008) Quality and Reliability of Large-Eddy Simulations. ERCOFTAC Series, Springer Netherlands.

Mikuž B, Tiselj I (2016) Wall-Resolved Large Eddy Simulation in Grid-Free 5×5 Rod Bundle of MATiS-H Experiment. *Nuclear Engineering and Design*, 298(Supplement C), 64–77, dx.doi.org/10.1016/j.nucengdes.2015.12.021.

Miller D S (2009) Internal Flow Systems. Second edition, Mentor Graphics.

Miroshnichenko I V, Sheremet M A (2018) Turbulent Natural Convection Heat Transfer in Rectangular Enclosures Using Experimental and Numerical Approaches: A Review. *Renewable and Sustainable Energy Reviews*, 82, 40–59, dx.doi.org/10.1016/j.rser.2017.09.005.

References

Misale M, Frogheri M, D'Auria F, Fontani E, Garcia A (1999) Analysis of Single-Phase Natural Circulation Experiments by System Codes. *International Journal of Thermal Sciences*, 38(11), 977–983, dx.doi.org/10.1016/S1290-0729(99)00106-4.

Morris A, Langari R (2020) Measurement and Instrumentation. Third edition, Elsevier, Inc.

NAFEMS (2003) How to Plan a CFD Analysis. HT24, NAFEMS.

NAFEMS (2019) General Guidelines for Good Convergence in Computational Fluid Dynamics. https://www.nafems.org/publications/guidelines-for-good-convergence-in-cfd/.

Naphade P, Borgohain A, Raj R T, Maheshwari N K (2013) Experimental and CFD Study on Natural Circulation Phenomenon in Lead Bismuth Eutectic Loop. *Procedia Engineering*, 64, 936–945, dx.doi.org/10.1016/j.proeng.2013.09.170.

Nicoud F, Ducros F (1999) Subgrid-Scale Stress Modelling Based on the Square of the Velocity Gradient Tensor. *Flow, Turbulence and Combustion*, 62(3), 183–200, dx.doi.org/10.1023/A:1009995426001.

Ninokata H, Merzari E, Khakim A (2009) Analysis of Low Reynolds Number Turbulent Flow Phenomena in Nuclear Fuel Pin Subassemblies of Tight Lattice Configuration. *Nuclear Engineering and Design*, 239(5), 855–866, dx.doi.org/10.1016/j.nucengdes.2008.10.030.

NSC (2018) Benchmarking of Thermal-Hydraulic Loop Models for Lead-Alloy-Cooled Advanced Nuclear Energy Systems. Phase II: Natural Convection. NEA/NSC/R(2018)1, OECD NEA Nuclear Science Committee.

Omranian A, Craft T, Iacovides H (2014) The Computation of Buoyant Flows in Differentially Heated Inclined Cavities. *International Journal of Heat and Mass Transfer*, 77, 1–16, dx.doi.org/10.1016/j.ijheatmasstransfer.2014.04.068.

Padilla E L M, Silveira-Neto A (2008) Large-Eddy Simulation of Transition to Turbulence in Natural Convection in a Horizontal Annular Cavity. *International Journal of Heat and Mass Transfer*, 51(13), 3656–3668, dx.doi.org/10.1016/j.ijheatmasstransfer.2007.07.025.

Petruzzi A, D'Auria F (2008) Thermal-Hydraulic System Codes in Nulcear Reactor Safety and Qualification Procedures. *Science and Technology of Nuclear Installations*, 2008, 1–16, dx.doi.org/10.1155/2008/460795.

Picard A, Davis R S, Gläser M, Fujii K (2008) Revised Formula for the Density of Moist Air (CIPM-2007). *Metrologia*, 45(2), 149–155, dx.doi.org/10.1088/0026-1394/45/2/004.

Pope S B (2000) Turbulent Flows. Cambridge University Press.

Rathore S K, Das M K (2016) Investigation on the Relative Performance of Various Low-Reynolds Number Turbulence Models for Buoyancy-Driven Flow in a Tall Cavity. *Heat and Mass Transfer*, 52(3), 437–457, dx.doi.org/10.1007/s00231-015-1557-8.

Reay D A, Kew P A, McGlen R J (2014) Heat Pipes. Elsevier, dx.doi.org/10.1016/C2011-0-08979-2.

Reyes J N, Hochreiter L (1998) Scaling Analysis for the OSU AP600 Test Facility (APEX). *Nuclear Engineering and Design*, 186(1-2), 53–109, dx.doi.org/10.1016/S0029-5493(98)00218-0.

References

Rodi W (editor) (1982) Turbulent Buoyant Jets and Plumes. Number 6 in HMT–the Science & Applications of Heat and Mass Transfer, first edition, Pergamon Press.

Rogers G F C, Mayhew Y (1992) Engineering Thermodynamics: Work and Heat Transfer. Fourth edition, Prentice Hall.

Rohsenow W M, Hartnett J P, Cho Y I (1998) Handbook of Heat Transfer. Third edition, McGraw-Hill.

Roth G A, Aydogan F (2014a) Theory and Implementation of Nuclear Safety System Codes – Part I: Conservation Equations, Flow Regimes, Numerics and Significant Assumptions. *Progress in Nuclear Energy*, 76, 160–182, dx.doi.org/10.1016/j.pnucene.2014.05.011.

Roth G A, Aydogan F (2014b) Theory and Implementation of Nuclear Safety System Codes – Part II: System Code Closure Relations, Validation, and Limitations. *Progress in Nuclear Energy*, 76, 55–72, dx.doi.org/10.1016/j.pnucene.2014.05.003.

Runchal A (editor) (2020) 50 Years of CFD in Engineering Sciences: A Commemorative Volume in Memory of D. Brian Spalding. Springer, dx.doi.org/10.1007/978-981-15-2670-1.

Saikia K, Pandey M, Basu D N (2019) Numerical Investigation of the Effect of Inlet Subcooling on Flow Instabilities in a Parallel Channel Natural Circulation Boiling System. *Progress in Nuclear Energy*, 114, 13–21, dx.doi.org/10.1016/j.pnucene.2019.01.028.

Salah A B (2013) Assessment of the CATHARE 3D Capabilities in Predicting the Temperature Mixing under Asymmetric Buoyant Driven Flow Conditions. *Nuclear Engineering and Design*, p. 15.

Salko R K, Blyth T S, Dances C A, Magedanz J W, Jernigan C, Kelly J, Toptan A, Gergar M, et al. (2016) CTF Validation and Verification. CASL-U-2016-1113-000, U.S. Department of Energy.

Scarano F (2012) Tomographic PIV: Principles and Practice. *Measurement Science and Technology*, 24(1), 012001, dx.doi.org/10.1088/0957-0233/24/1/012001.

Schlichting H, Gersten K (2017) Boundary-Layer Theory. Ninth edition, Springer, dx.doi.org/10.1007/978-3-662-52919-5.

Schultz R R, Chapman J C, Kukita Y, Motley F E, Stumpf H, Chen Y S, Tasaka K (1987) Single and Two-Phase Natural Circulation in Westinghouse Pressurized Water Reactor Simulators: Phenomena, Analysis and Scaling. EGG-M–39286, EG and G Idaho.

Sebilleau F, Issa R, Lardeau S, Walker S P (2018) Direct Numerical Simulation of an Air-Filled Differentially Heated Square Cavity with Rayleigh Numbers up to 10^{11}. *International Journal of Heat and Mass Transfer*, 123, 297–319, dx.doi.org/10.1016/j.ijheatmasstransfer.2018.02.042.

Sebilleau F, Issa R I, Walker S P (2016) Analysis of Turbulence Modelling Approaches to Simulate Single-Phase Buoyancy Driven Counter-Current Flow in a Tilted Tube. *Flow, Turbulence and Combustion*, 96(1), 95–132, dx.doi.org/10.1007/s10494-015-9653-x.

Shabbir A, George W K (1994) Experiments on a Round Turbulent Buoyant Plume. *Journal of Fluid Mechanics*, 275, 1–32, dx.doi.org/10.1017/S0022112094002260.

References

Shams A, De Santis A, Koloszar L, Villa Ortiz A, Narayanan C (2019) Status and Perspectives of Turbulent Heat Transfer Modelling in Low-Prandtl Number Fluids. *Nuclear Engineering and Design*, 353, 110220, dx.doi.org/10.1016/j.nucengdes.2019.110220.

Sharif M A R, Mothe K K (2009) Evaluation of Turbulence Models in the Prediction of Heat Transfer Due to Slot Jet Impingement on Plane and Concave Surfaces. *Numerical Heat Transfer, Part B: Fundamentals*, 55(4), 273–294, dx.doi.org/10.1080/10407790902724602.

Shi S, Zhu Q, Sun X, Ishii M (2018) Assessment of RELAP5/MOD3.2 for Startup Transients in a Natural Circulation Test Facility. *Annals of Nuclear Energy*, 112, 257–266, dx.doi.org/10.1016/j.anucene.2017.10.012.

Shih T H, Liou W W, Shabbir A, Yang Z, Zhu J (1995) A New K-ϵ Eddy Viscosity Model for High Reynolds Number Turbulent Flows. *Computers & Fluids*, 24(3), 227–238, dx.doi.org/10.1016/0045-7930(94)00032-T.

Shima N (1998) Low-Reynolds-Number Second-Moment Closure without Wall-Reflection Redistribution Terms. *International Journal of Heat and Fluid Flow*, 19(5), 549–555, dx.doi.org/10.1016/S0142-727X(98)10012-7.

Simoneau J P, Champigny J (2008) Large Eddy Simulation of Mixing in the Outlet Plenum of a High Temperature Reactor: A Benchmark Exercise. In *12th International Conference on Nuclear Engineering*, pp. 503–513, American Society of Mechanical Engineers Digital Collection, dx.doi.org/10.1115/ICONE12-49446.

Smagorinsky J (1963) General Circulation Experiments with the Primitive Equations. *Monthly Weather Review*, 91(3), 99–164, dx.doi.org/10.1175/1520-0493(1963)091<0099:GCEWTP>2.3.CO;2.

Smith B L, Mahaffy J H, Angele K, Westin J (2011) OECD/NEA—Vattenfall T-Junction Benchmark Specifications. Technical Report NEA/CSNI/R(2011)5, OECD-NEA.

Spalart P, Allmaras S (1992) A One-Equation Turbulence Model for Aerodynamic Flows. In *30th Aerospace Sciences Meeting and Exhibit*, Aerospace Sciences Meetings, American Institute of Aeronautics and Astronautics, dx.doi.org/10.2514/6.1992-439.

Spalart P R (2000) Strategies for Turbulence Modelling and Simulations. *International Journal of Heat and Fluid Flow*, 21(3), 252–263, dx.doi.org/10.1016/S0142-727X(00)00007-2.

Speziale C, Sarkar S, Gatski T (1991) Modelling the Pressure–Strain Correlation of Turbulence: An Invariant Dynamical Systems Approach. *Journal of Fluid Mechanics*, 227, 245–272, dx.doi.org/10.1017/S0022112091000101.

Speziale C G (1998) Turbulence Modeling for Time-Dependent RANS and VLES: A Review. *AIAA Journal*, 36(2), 173–184, dx.doi.org/10.2514/2.7499.

Suga K, Craft T J, Iacovides H (2006) An Analytical Wall-Function for Turbulent Flows and Heat Transfer over Rough Walls. *International Journal of Heat and Fluid Flow*, 27(5), 852–866, dx.doi.org/10.1016/j.ijheatfluidflow.2006.03.011.

Turner J S (1973) Buoyancy Effects in Fluids. Cambridge University Press, dx.doi.org/10.1017/CBO9780511608827.

References

Velasco Peña H, Rodriguez O (2015) Applications of Wire-Mesh Sensors in Multiphase Flows. *Flow Measurement and Instrumentation*, 45, 255–273, dx.doi.org/10.1016/j.flowmeasinst.2015.06.024.

Versteeg H K, Malalasekera W (2007) An Introduction to Computational Fluid Dynamics: The Finite Volume Method. Second edition, Pearson Education.

Vijayan P K, Austregesilo H, Teschendorff V (1995) Simulation of the Unstable Oscillatory Behavior of Single-Phase Natural Circulation with Repetitive Flow Reversals in a Rectangular Loop Using the Computer Code Athlet. *Nuclear Engineering and Design*, 155(3), 623–641, dx.doi.org/10.1016/0029-5493(94)00972-2.

Wagner W, Cooper J R, Dittmann A, Kijima J, Kretzschmar H J, Kruse A, Mareš R, Oguchi K, et al. (2000) The IAPWS Industrial Formulation 1997 for the Thermodynamic Properties of Water and Steam. *Journal of Engineering for Gas Turbines and Power*, 122(1), 150–184, dx.doi.org/10.1115/1.483186.

Wagner W, Pruß A (2002) The IAPWS Formulation 1995 for the Thermodynamic Properties of Ordinary Water Substance for General and Scientific Use. *Journal of Physical and Chemical Reference Data*, 31(2), 387–535, dx.doi.org/10.1063/1.1461829.

Wang J Y, Chuang T J, Ferng Y M (2013) CFD Investigating Flow and Heat Transfer Characteristics in a Natural Circulation Loop. *Annals of Nuclear Energy*, 58, 65–71, dx.doi.org/10.1016/j.anucene.2013.01.015.

Welander P (1967) On the Oscillatory Instability of a Differentially Heated Fluid Loop. *Journal of Fluid Mechanics*, 29(1), 17–30, dx.doi.org/10.1017/S0022112067000606.

Wilcox D (1988) Reassessment of the Scale-Determining Equation for Advanced Turbulence Models. *AIAA Journal*, 26(11), 1299–1310, dx.doi.org/10.2514/3.10041.

Wilcox D C (2006) Turbulence Modeling for CFD. Third edition, DCW Industries.

Wilson D (2021) Project FORTE - Nuclear Thermal Hydraulics Research & Development: Natural and Mixed Convection in Passive Cooling Systems. FNC 60148/51219R, Frazer-Nash Consultancy.

Wilson D R, Craft T J, Iacovides H (2015) Application of Reynolds Stress Transport Turbulence Closure Models to Flows Affected by Lorentz and Buoyancy Forces. *International Journal of Heat and Fluid Flow*, 55, 180–197, dx.doi.org/10.1016/j.ijheatfluidflow.2015.06.007.

Woodcock J, Dzodzo M B (2000) Application of Large Scale Containment Database to AP600 Loss-of-Coolant-Accident Internal Circulation and Stratification Evaluations. In *Proceedings of ICONE 8*.

Woods A W (2010) Turbulent Plumes in Nature. *Annual Review of Fluid Mechanics*, 42(1), 391–412, dx.doi.org/10.1146/annurev-fluid-121108-145430.

Yakhot V, Orszag S, Thangam S, Gatski T, Speziale C (1992) Development of Turbulence Models for Shear Flows by a Double Expansion Technique. *Physics of Fluids A: Fluid Dynamics*, 4(7), 1510–1520, dx.doi.org/doi:10.1063/1.858424.

References

Yang Z, Shih T H (1993) A Galilean and Tensorial Invariant K-Epsilon Model for near Wall Turbulence. In *24th Fluid Dynamics Conference*, AIAA.

Yap C R (1987) Turbulent Heat and Momentum Transfer in Recirculating and Impinging Flows. Ph.D. thesis, University of Manchester Institute of Science and Technology (UMIST).

Zhang Y, Lu D, Du Z, Fu X, Wu G (2015) Numerical and Experimental Investigation on the Transient Heat Transfer Characteristics of C-Shape Rod Bundles Used in Passive Residual Heat Removal Heat Exchangers. *Annals of Nuclear Energy*, 83, 147–160, dx.doi.org/10.1016/j.anucene.2015.04.022.

Zhao H, Dong Y, Zheng Y, Ma T, Chen X (2017) Numerical Simulation on Heat Transfer Process in the Reactor Cavity of Modular High Temperature Gas-Cooled Reactor. *Applied Thermal Engineering*, 125, 1015–1024, dx.doi.org/10.1016/j.applthermaleng.2017.05.205.

Zohuri B, Fathi N (2015) Thermal-Hydraulic Analysis of Nuclear Reactors. Springer International Publishing, dx.doi.org/10.1007/978-3-319-17434-1.

Zuber N (1991) Appendix D. A Hierarchical, Two-Tiered Scaling Analysis. An Integrated Structure and Scaling Methodology for Severe Accident Technical Issue Resolution. NUREG/CR-5809, U.S. Nuclear Regulatory Commission.

6 Nomenclature

Latin Symbols

A	Area, m^2
At	Atwood number ($At = (\rho_1 - \rho_2)/(\rho_1 + \rho_2)$)
Bi	Biot number ($Bi = hL/k_s$)
c_p, c_v	Specific heat at constant pressure or volume, $J\,kg^{-1}\,K^{-1}$
d or D	Diameter ($D_h = 4A_{cs}/p_{cs}$ for hydraulic diameter), m
f	Darcy-Weisbach friction factor
Fo	Fourier number ($Fo = \alpha_s t/L^2$)
Gr	Grashof number ($Gr = gL^3\Delta\rho/\nu^2\rho = gL^3\beta\Delta T/\nu^2$, using the Boussinesq approximation $\Delta\rho/\rho \approx -\beta\Delta T$, where ΔT is often taken as $T_w - T_{s,\infty}$)
g	Acceleration due to gravity, $m\,s^{-2}$
h	Specific enthalpy, $J\,kg^{-1}$, Heat Transfer Coefficient (HTC), $W\,m^{-2}\,K^{-1}$ or height, m
I	Radiative intensity, $W\,m^{-2}\,sr^{-1}$ or $W\,m^{-2}\,sr^{-1}\,\mu m^{-1}$ for a spectral density, where sr (steradian) is solid angle
J	Radiosity, $W\,m^{-2}$
k	Thermal conductivity, $W\,m^{-1}\,K^{-1}$
L	Length or wall thickness, m
M	Molar mass of a species, $kg\,kmol^{-1}$
Ma	Mach number ($Ma = U/a$, where a is the speed of sound)
n	Refractive index
Nu	Nusselt Number ($Nu = hL/k_f$)
p	Perimeter, m
P	Pressure (P_s = static pressure, P_T = total pressure), $N\,m^{-2}$ or Pa
Pe	Péclet number ($Pe = RePr$)
Pr	Prandtl number ($Pr = c_p\mu/k_f$)
q	Heat flux (rate of heat transfer per unit area, $q = Q/A$), $W\,m^{-2}$
Q	Rate of heat transfer, W
r	Radius, m
R	Gas constant (for a particular gas, $R = \tilde{R}/M$), $J\,kg^{-1}\,K^{-1}$
$\tilde{R}$	Universal gas constant, $8314.5\,J\,kmol^{-1}\,K^{-1}$
R_{th}	Thermal resistance, $K\,W^{-1}$
Ra	Rayleigh number ($Ra = GrPr$)
Re	Reynolds number ($Re = \rho UL/\mu$, or for an internal flow $Re = WD_h/A_{cs}\mu$)
Ri	Richardson number ($Ri = Gr/Re^2$)
Sr	Strouhal number ($Sr = fL/U$, where f is frequency)

St	Stanton number ($St = Nu/RePr$)
t	Time, s
T	Temperature (T_s = static temperature, T_T = total temperature), K
u_τ	Wall friction velocity ($u_\tau = \sqrt{\overline{\tau_w}/\rho}$), $\mathrm{m\,s^{-1}}$
U	Velocity, $\mathrm{m\,s^{-1}}$ or thermal transmittance, $\mathrm{W\,m^{-2}\,K^{-1}}$
v	Specific volume, $\mathrm{m^3\,kg^{-1}}$
V	Volume, $\mathrm{m^3}$
W	Mass flow rate, $\mathrm{kg\,s^{-1}}$
y	Wall distance, m
y^+	Non-dimensional wall distance ($y^+ = y u_\tau/\nu$)

Greek Symbols

α	Thermal diffusivity ($\alpha = k/\rho c_p$), $\mathrm{m^2\,s^{-1}}$
β	Volumetric thermal expansion coefficient ($\beta = -(1/\rho)(\partial\rho/\partial T)$), $\mathrm{K^{-1}}$
γ	Ratio of specific heats ($\gamma = c_p/c_v$)
ϵ	Emissivity or surface roughness height, m
κ	Absorption coefficient, $\mathrm{m^{-1}}$
λ	Wavelength, m
μ	Viscosity, $\mathrm{kg\,m^{-1}\,s^{-1}}$
ν	Kinematic viscosity and momentum diffusivity ($\nu = \mu/\rho$), $\mathrm{m^2\,s^{-1}}$
ρ	Density, $\mathrm{kg\,m^{-3}}$
σ	Stefan Boltzmann constant, $5.67 \times 10^{-8}\,\mathrm{W\,m^{-2}\,K^{-4}}$
τ	Shear stress, $\mathrm{N\,m^{-2}}$
ϕ	Porosity or void fraction

Subscripts and Modifications

b	Bulk (mass-averaged) quantity
cs	Cross-sectional quantity
f	Quantity relating to a fluid
i	Quantity relating to a particular species
T	Total (stagnation) quantity
t	Turbulent quantity
s	Static quantity or quantity relating to a solid
w	Quantity relating to a wall or surface
∞	Quantity far from a wall or in free-stream
$\overline{\square}$	Average quantity
$\tilde{\square}$	Molar quantity
$\square'$	Varying quantity

7 Abbreviations

AHFM	Algebraic Heat Flux Model
ANT	Advanced Nuclear Technology
BEIS	Department for Business, Energy and Industrial Strategy
BEPU	Best Estimate Plus Uncertainty
CAD	Computer Aided Design
CFD	Computational Fluid Dynamics
CFL	Courant-Friedrichs Lewy
CHF	Critical Heat Flux
CHT	Conjugate Heat Transfer
CRP	Coordinated Research Project
CSNI	Committee on the Safety of Nuclear Installations
CTA	Constant Temperature Anemometry
DDES	Delayed Detached Eddy Simulation
DES	Detached Eddy Simulation
DFM	Differential Flux Model
DNS	Direct Numerical Simulation
EBRSM	Elliptic-Blending RSM
ELES	Embedded LES
EMDAP	Evaluation Methodology Development and Application Process
EVM	Eddy Viscosity Model
GEKO	Generalized k-ω
GGDH	Generalized Gradient Diffusion Hypothesis
H2TS	Hierarchical 2-Tiered Scaling
HPC	High Performance Computing
HTC	Heat Transfer Coefficient
HTGR	High Temperature Gas-cooled Reactor
HVAC	Heating, Ventilation, and Air Conditioning
IAEA	International Atomic Energy Agency
IAPWS	International Association for the Properties of Water and Steam
IET	Integral Effect Test
ISP	International Standard Problem
LCO	Limits and Conditions for Operation
LDA	Laser Doppler Anemometry
LDV	Laser Doppler Velocimetry
LES	Large Eddy Simulation
LRR	Launder-Reece-Rodi
LWR	Light Water Reactor
ML	Machine Learning
NEA	Nuclear Energy Agency
NIP	Nuclear Innovation Programme

Abbreviations

NPP	Nuclear Power Plant
NRG	Nuclear Research and Consultancy Group
NTH	Nuclear Thermal Hydraulics
O&M	Operation and Maintenance
OECD	Organisation for Economic Co-operation and Development
PIRT	Phenomena Identification and Ranking Table
PIV	Particle Image Velocimetry
PTS	Pressurised Thermal Shock
PWR	Pressurised Water Reactor
RANS	Reynolds-Averaged Navier-Stokes
RNG	Re-Normalisation Group
RPV	Reactor Pressure Vessel
RSM	Reynolds Stress Model
RVACS	Reactor Vessel Auxiliary Cooling System
SA	Sensitivity Analysis
SAS	Scale-Adaptive Simulation
SESAME	Simulations and Experiments for the Safety Assessment of MEtal cooled reactors
SGDH	Simple Gradient Diffusion Hypothesis
SGS	Sub-Grid-Scale
SSG	Speziale-Sarkar-Gatski
SST	Shear Stress Transport
TCL	Two-Component Limit
UDF	User Defined Function
UDV	Ultrasound Doppler Velocimetry
UQ	Uncertainty Quantification
URANS	Unsteady Reynolds-Averaged Navier-Stokes
US NRC	United States Nuclear Regulatory Commission
V&V	Verification and Validation
VVUQ	Verification, Validation and Uncertainty Quantification
WALE	Wall-Adapting Local Eddy-Viscosity
WMLES	Wall Modeled Large Eddy Simulation
WMS	Wire mesh sensor

Volume 3